NOTE TO USERS

EFFECT OF INDIVIDUAL CARBOHYDRATE CHAINS ON THE *IN VITRO* AND *IN VIVO* BIOLOGICAL FUNCTION OF RABBIT ANTITHROMBIN

By

HONGYU NI, MD, M.Sc.

A Thesis

Submitted to the School of Graduate Studies

In Partial Fulfillment of the Requirements

For the Degree

Doctor of Philosophy

McMaster University

BIOLOGICAL FUNCTION OF RABBIT ANTITHROMBIN

Doctor of Philosophy (2004) McMaster University
(Science) Hamilton, Ontario

TITLE: Effect of Individual Carbohydrate Chains on the *in Vitro* and in *Vivo* Biological Function of Rabbit Antithrombin

AUTHOR: Hongyu Ni, M.D. (West China University of Medical Sciences, Chengdu, P.R.China), M.Sc. (Queen's University at Kingston)

SUPERVISOR: Professor M.A. Blajchman

NUMBER OF PAGES: xxi, 204

ABSTRACT

Antithrombin (AT) is the principal anticoagulant protein that inhibits thrombin and factor Xa in plasma. AT is a glycoprotein with a molecular weight of 58 KDa and contains four consensus sequences for N-linked glycosylation, located at Asn 96, Asn 135, Asn 155, and Asn192. To investigate the effect of individual glycan side chain on the biological function of AT, each of the four Asn residue sites of glycosylation was mutated to Gln to block glycosylation at these sites. The resulting constructs were initially expressed in COS cells. Permanent cell lines were generated by transfecting CHO cells with the constructs, encoding either the wild-type rabbit AT (AT-WT) or one of the four underglycosylated mutant variants (AT-N96Q, AT-N135Q, AT-N155Q, and AT-N155Q).

The results demonstrated that neither the amount of AT secreted nor the kinetics of secretion differed significantly between cell lines expressing AT-WT and any of the mutant AT variants. Purification and radioiodination of AT-WT and each of the four mutant variants permitted pharmacokinetic analysis of their individual catabolism in rabbits. The rate constants for protein catabolism were significantly higher for underglycosylated mutant variants than that of AT-WT. However, no significant difference was identified among the catabolic half-lives of the underglycosylated mutant variants. These results suggest that the extent of glycosylation is more important than its location for determining AT catabolism in vivo. Further *in vivo* studies of double and triple underglycosylated forms of AT as well as totally deglycosylated AT are needed before a final conclusion can be made

The AT-WT and all forms of mutant variants were capable of forming complexes with thrombin. However, compared with AT-WT, the second order rate constant was significantly reduced for the AT-N155Q variant, by 2 and 20 fold in the absence and presence of heparin, respectively. No statistically significant differences in second order rate constant were observed between AT-WT and other three underglycosylated variants, AT-N96Q, AT-N135Q, and AT-N192Q. These results suggest that a failure to glycosylate Asn 155 in AT results in reduction of its ability to inhibit thrombin.

In comparison with AT-WT, AT-N135Q and AT-N192Q appeared to have slightly higher heparin affinity, but no statistically significant difference was identified. The AT-N96Q showed a small increase in Kd. Compared with AT-WT, however, there was significant reduction in heparin affinity for AT-N155Q (6-fold increase in Kd). These results suggest that a failure to glycosylate Asn 155 in AT results in significant reduction of its ability to bind to heparin.

ACKNOWLEDGMENTS

I would like to thank my supervisor Dr. Morris Blajchman for his guidance, patience, and encouragement throughout the course of my Ph.D. studies. Dr. Blajchman's support and help during the past several years have made this work very enjoyable. I am also very grateful to Dr. Blajchman for his encouragement and advice for my future research

I am very grateful to Dr. Mark Hatton, David Andrews, and Erwin Rogeci for their invaluable suggestion and advice during my studies. I would like to offer my sincere thanks to Dr. William Sheffield for his guidance, encouragement, and advice during the course of my research program.

In addition, I would like to thank Myron Kulczyky and Leslie Bardossy for their technical assistance and management of the experiments with rabbits.

Lastly, I would like to thank my wife Jianli, for her moral support and encouragement throughout this work. I am very grateful to my sons, Jeffrey and Richard for their understanding. I would also like to thank my parents Dr. Zongzan Ni and Dr. Keqin Ou for their support and understanding throughout my medical and graduate training.

PREFACE

During the course of my Ph.D. studies, I completed two research projects related to antithrombin biology.

The first research project entitled "Effect of individual carbohydrate chains on the *in vivo* and *in vitro* biological function of rabbit antithrombin", systemically investigated the role of each individual glycan in the *in vivo* and *in vitro* biological function of antithrombin. The first four chapters of the thesis summarize the studies related to this project.

The second project is entitled "Identification and characterization of a highly polymorphic trinucleotide short tandem repeat (STR) within the human antithrombin gene". This study described and characterized a highly polymorphic short tandem repeat in an intron of the human antithrombin gene. The findings from this project are summarized in the chapter five of the thesis.

TABLE OF CONTENTS

EFFECT OF INDIVIDUAL CARBOHYDRATE CHAINS ON THE *IN VIVO* AND *IN VITRO* BIOLOGICAL FUNCTION OF RABBIT ANTITHROMBIN

LIST OF FIGURES

LIST OF TABLES

LIST OF ABBREVIATIONS

ANOVA	a two-way analysis of variance
APS	ammonium persulfate
AT	Antithrombin
AT-WT	wild-type rabbit AT
ATP	triphosphate
BCIP	5-bromo-4-chloro-3-indolyl phosphate
BHK	baby hamster kidney cell
BIS	N, N'-methylene-bis-acrylamide
CHO	Chinese hamster Ovary cells
COS	African green monkey kidney cells
DMSO	dimethyl sulphoxide
DTT	Dithiothreitol
EDTA	ethylene-diamine-tetraacetic acid
ELISA	Enzyme-Linked Immunosorbent Assay
ER	endoplasmic reticulum
EtBr	Ethidium bromide
FBS	heat-inactivated fetal bovine serum
Factor IIa	thrombin
G-418	Geneticin
Gal	Galactose
GlcNAc	N-acetylglucosamine
HBS	heparin binding site
IPTG	β-D-isopropyl-thiogalactopyranoside
K_2	second order rate constants
K_d	Dissociation constants
KOAc	potassium acetate
LRP	low density lipoprotein receptor-related protein
MEF	mouse embryonic fibroblasts
α-MEM	minimum essential α-medium
MOPS	3-(N-morpholino) propanesulfonic acid
NaOAc	sodium acetate
NBT	nitro blue tetrazolium
NeuAc	N-acetylneuraminic acid
NH_4OAc	Ammonium acetate
NP-40	Nonidet P-40
OD	optical density
PAGE	polyacrylamide gel electrophoresis
PAI-1	plasminogen activator inhibitor I
PBS	phosphate-buffered saline
PCR	Polymerase chain reaction
pd-AT	plasma-derived Antithrombin

PE	pleiotropic effect
PEG	polyethylene glycol
PL	phospholipids
PMSF	phenylmethanesulfonyl fluoride
PNGase F	Glycosidase F
PNPP	p-nitrophenyl phosphate
PPACK	D-phenylalanyl-L-propyl-arginine chloromethyl ketone
RAP	receptor-associated protein
RCL	reactive center loop
RFLP	fragment length polymorphism
RIPA	radioimmune precipitation buffer
RS	reactive site
SCCA1	squamous cell carcinoma Antigen
SDS	sodium dodecyl sulphate
Serpins	serine protease inhibitors
STR	short tandem repeat
TAT	thrombin-AT complex
TBS	Tris-buffered saline
TEMED	N,N,N',N'-tetramethylethylenediamine hydrochloride
TF	tissue factor.
tPA	tissue plasminogen activator
TRIS	Tris(hydroxymethyl) aminomethane
UV	ultraviolet
X-gal	5-bromo-4-chloro-3-indolyl-β-D-galactoside

1. INTRODUCTION

The physiological response to vascular injury leads to the localized formation of an occlusive hemostatic plug, which arrests the loss of blood from an injured vessel. This host defense mechanism is so effective and efficient that it has been a subject of medical research for more than a century (Tulin, 1972). Blood coagulation plays an essential role in this defense mechanism by establishing the hemostatic plug through the generation of thrombin (Jackson *et al.*, 1980). However, without natural plasma clotting inhibitors, excessive and untimely thrombin generation would result in an intravascular clot or thrombus formation, which could have potential life-threatening consequences. Fortunately, under physiological conditions, naturally occurring plasma coagulation inhibitors are capable of limiting coagulation to preserve the fluidity of circulating blood within the vascular tree. The most abundant of these plasma coagulation inhibitors is a plasma glycoprotein known as antithrombin (AT) (Egeberg, 1965). The physiological importance of AT in the maintenance of a hemostatic balance can be demonstrated in AT deficient patients who have the increased risk for venous thromboembolic events (Blajchman *et al.* 1992).

1.1 Historical Background

The existence of a circulating coagulation inhibitor that could lower the action of thrombin was first proposed by Morawitz in 1905 (Morawitz, 1905; Beck, 1977). This substance was designated "antithrombin" (Howell and Holt, 1918). With the isolation, purification and subsequent clinical use of heparin in the late 1930s, the presence of a substance in plasma and serum which was required for the anticoagulation action of

heparin was identified (Brinkhous *et al.*, 1939). This substance was variously called antithrombin III, antithrombin, and heparin cofactor (Seegers *et al.*, 1954; Loeliger and Hers, 1957; Niewiarowski and Kowalski, 1958). In 1955, Monkhouse isolated a component from normal plasma that had both heparin cofactor and antithrombin activities (Monkhouse *et al.,* 1955). This observation suggested that the heparin cofactor and antithrombin activities might be functions of the same protein. In 1973, Rosenberg and Damus successfully isolated large quantities of this protein and thus, were able to provide convincing physicochemical evidence that plasma antithrombin activity and plasma heparin cofactor activity indeed reside in the same molecule (Rosenberg and Damus, 1973, Rosenberg 1975a, Anderson *et al.*, 1976). Recently, the Nomenclature Committee of the International Society of Thrombosis and Hemostasis has recommended to designate this protein as antithrombin (AT) (Lane, *et al.,* 1993, Blomback, *et al*, 1994). It is recognized now, whether in the presence or absence of heparin, antithrombin is the most important physiological protease inhibitor of coagulation.

1.2 Biochemistry of AT

1.2.1 Primary Structure

AT is a single chain glycoprotein with a molecular weight of 58kDa, and isoelectric point ranging from 4.9 to 5.3. Human plasma-derived AT comprises 432 amino acid residues (shown in Fig. 1.1). Its six Cys residues are all linked in disulphide bonds located between residues 8 and 128, 21 and 95, and 247 and 430, respectively (Nordenman *et al.*, 1977). AT contains four biantennary asparagine-linked

Figure 1.1 Structure of human antithrombin protein. A schematic diagram showing the four N-glycosylation sites and the six Cys residues that are linked in three disulphide bonds (Reprinted from Lane et al., 1997; copyright permission obtained.).

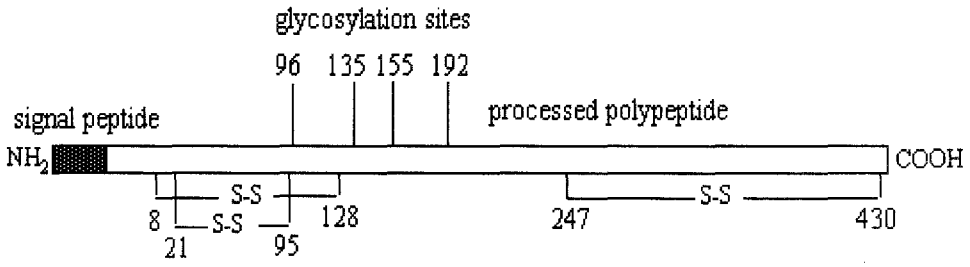
glycosylation sites
96
135
155
192
signal peptide
processed polypeptide
NH2
COOH
S-S
S-S
S-S
8
21
95
128
247
430

oligosaccharides in its fully N-glycosylated form at the amino acid positions 96, 135, 155 and 192 (Franzen *et al.*, 1980).

1.2.2 Biosynthesis of AT

AT has been shown to be synthesized and secreted primarily from liver, although its biosynthesis may also occur in the kidney and endothelial cells (Watada *et al.*, 1981; Leon *et al.*, 1982, 1983; Lee *et al.*, 1979; Chan and Chan, 1979;1981). This conclusion is strongly supported by the observation that the AT levels are remarkably reduced in individuals with liver disorders (Lechner *et al.*, 1977; Ratnoff, 1982). It has also been shown that a human hepatoma cell line, Hep G2, was capable of synthesizing and secreting biologically active AT (Fair and Bahnak, 1984). In addition, the results of perfusion studies have shown that the rat liver and rabbit liver were able to synthesize and secrete AT (Koj *et al.*, 1978; Owens and Miller, 1980; Hatton *et al.*, 1997). Further studies have demonstrated the presence of AT in the Golgi apparatus of rat hepatocytes (Girot *et al.*, 1983).

1.3. Distribution and Catabolism of AT

AT is normally present in human plasma at a concentration of 150 to 200 μg/ml, equivalent to 2-3 μM (Conard *et al.*, 1983). It has also been found to be present in the storage granules of platelets, at a level corresponding to approximately 0.01% of the total AT in normal plasma (Alhenc-Gelas *et al.*, 1985). The physiological significance of this platelet granule associated AT is not yet clear. Its contribution, however, should not be underestimated since platelets are highly concentrated within the hemostatic plug.

The distribution of AT in the rabbit and human can be divided into the plasma compartment and extra-vascular compartment. AT is moving from the plasma through the rapidly-equilibrating compartment to the extravascular space where catabolism occurs. Based on the study of radiolabeled AT in rabbits, Carlson *et al.* suggested that there was a vascular endothelium-associated AT compartment present. They proposed a three-compartment model, including plasma, noncirculating vascular-associated, and extravascular compartments (Carlson *et al.*, 1984). In humans, the fraction of the total-body AT in the plasma, noncirculating vascular-associated, and extravascular pools were calculated to be 0.393±0.015, 0.109±0.016, and 0.496±0.0014, respectively, while in the rabbit were 0.337±0.031, 0.178±0.056, and 0.485±0.069, respectively (Carlson *et al.*, 1985; Regoeczi, 1987; Witmer and Hatton, 1991).

The clearance of AT has been studied in mice, rabbits, and humans (Fuchs *et al.*, 1982; Reeve, 1980; Carlson 1985). After the administration of radioiodinated AT, there is an initial rapid binding phase of AT to the blood vessel wall followed by a slower phase in which AT exits the vessel and enters the extravascular compartment. The half-life of AT has been reported to be 2.8±0.3 days in human (Collen *et al.*, 1977), 2.27±0.11 days in rabbits (Carlson, 1985), 2.14±0.09 days in male dogs and 1.97± 0.05 days in female dogs (Kobayashi and Takeda, 1977).

When AT forms a complex with thrombin and other serine proteases, there is a dramatic change in the clearance rate. The protease-bound AT is much more rapidly cleared from the circulation than its native moiety. This has been demonstrated in humans and in animals including mice, rabbits, and dogs, where the half-life of thrombin-

AT (TAT) complex was found to be a few minutes (Shifman and Pizzo, 1982; Fuchs *et al.*, 1982; Leonard *et al.*, 1983). In rabbits, the half-life of TAT complex ranged from 2 to 11 hours when AT-thrombin binary complex was studied (Vogel *et al.*, 1979). However, this AT-thrombin binary complex may not represent the form of complex that engages *in vivo* clearance, since TAT found in plasma exists predominantly as a covalent ternary complex with vitronectin (Liang *et al.*, 1997; de Boer *et al.*, 1995). Indeed, a recent study of TAT clearance in rabbit by using ternary vitronectin-TAT complex demonstrated that the half-life of this complex was 42 minutes (Wells *et al.*, 1998). The removal of the complex from the circulation is specific and saturable, suggesting a receptor-mediated process located on hepatocytes (Wells *et al.*, 1999). A putative receptor protein called the serpin-enzyme complex receptor (SECR) that may be involved in TAT complex clearance has recently been identified biochemically. However, this receptor was only partially characterized and has not been cloned (Perlmutter *et al.*, 1990). Another candidate receptor that might be involved in TAT clearance is the low density lipoprotein receptor-related protein (LRP) (Strickland *et al.*, 1990). Kounnas *et al.* demonstrated that efficient uptake and degradation of radiolabeled TAT was found to occur in mouse embryonic fibroblasts (MEF) expressing LRP, but to be abolished in the LRP-deficient cell line PEA13 (Kounnas *et al.*, 1996). In addition, uptake and degradation of TAT by HepG2 cells was blocked by anti-LRP antibodies or a receptor-associated protein (RAP). RAP is a 39 kDa protein that has been shown to block LRP and its ligand binding (Strickland *et al.*, 1990; Kristensen *et al.*, 1990). More interestingly, injection of

recombinant RAP fusion protein was found to prolong the clearance of radiolabeled TAT in rats (Kounnas *et al.*, 1996).

It has been proposed that receptor recognition depends on conformational changes induced in both serpin and protease. Such conformational change presumably expresses or properly orients receptor recognition sites (Wells *et al.*, 1999). It has been demonstrated that neither the protease, the native AT, nor the uncomplexed cleaved AT could compete for removal of the complex (Mast *et al.*, 1991; Shifman and Pizzo, 1982). The maximal acceleration of serpin clearance requires formation of covalently associated AT-thrombin complex. Recently, Wells *et al.* proposed a model of TAT clearance that incorporated vitronectin, heparan sulfate proteoglycans, cytokeratin 18, and LRP (Wells *et al.*, 1999). In this model, TAT is associated with vitronectin either in the plasma phase or on the hepatocyte plasma membrane surface. This ternary complex binds to heparan sulfate proteoglycans, and then is transferred to cytokeratin 18 (CK18) on the hepatocyte surface. Subsequently, Vitronectin-TAT-CK18 complex binds to LRP. This multicomponent complex is then internalized into cells and degraded (Wells *et al.*, 1999).

1.4 AT and the Serine Protease Inhibitors

AT shares structural and functional homology with other members of a superfamily of serine protease inhibitors (Silverman *et al.*, 2001). Based on a similarity between the primary structure of ovalbumin, α1-antitrypsin, and AT, Hunt and Dayhoff (1980) proposed the existence of a new superfamily of proteins. Since then, other members of this superfamily have been identified. In 1985, Carrell and Travis (1985) coined the term serpin, an acronym for serine protease inhibitor, as a name for these

proteins to describe the serine protease inhibitory properties of the most members of this superfamily. Serpins are widely distributed in nature, including in mammals, birds, amphibians, insects, plants, and pox virus. Recent studies have shown an expanded distribution of serpins within the kingdoms of metazoa and plantae (Irving *et al.*, 2000). There are at present more than 500 members in this superfamily. Most serpins inhibit serine proteases of the chymotrypsin family. However, cross-class inhibitors have been identified such as PI9 which inhibits the cysteine proteinase, caspase 1, and the squamous cell carcinoma antigen (SCCA1) which neutralizes the potent papain-like cysteine proteinases, cathepsins L, K, and S. In addition, several members no longer function as proteinase inhibitors but perform other roles such as hormone transport (thyroxin-binding globulin, corticosteroid-binding globulin), and blood pressure regulation (angiotensinogen) (Silverman *et al.*, 2001, Irving *et al.*, 2000).

The presence of serpin genes in plants and metazoa, and their absence from the genomes of several eubacterial species, have led to the notion that serpins appeared sometime before the divergence of plants and animals which was approximately 2.7 billion years ago (Irving *et al.*, 2000). The best characterized members of this family are those in human plasma in which these serpins have evolved in parallel with their cognate proteases. These serpins are involved in the regulation of such crucial physiological processes as coagulation, fibrinolysis, inflammation, and the immune response (Carrell and Lomas, 1997a). The most extensively studied serpin member is α1-antitrypsin, the major inhibitor of neutrophil elastase (Carrell and Travis, 1985). It was the first of the serpins to be crystallized and has been used as a model for many of the other serpins

(Huber and Carrell, 1989). Subsequent crystallisation of other serpins including ovalbumin, plasminogen activator inhibitor I (PAI-I), cleaved bovine AT and intact human AT has confirmed the validity of this early model (Wright *et al.*, 1990; Mottonen *et al.*, 1992; Carrell *et al.*, 1994; Schreuder *et al.*, 1994). Analyses of these crystal structures show that 80% of the amino acids are arranged in nine well-defined α-helices (designated A through I) and three large β-sheets (designated A.B.C) of which the A sheet is a dominant feature (Shown in figure 1.2) (Carrell *et al.*, 1994; Schreuder *at al.*, 1994; Larsson et al. 2001).

1.5 Mechanism of Action of AT

The function of AT is the irreversible inactivation and binding of various serine proteases in the blood coagulation cascade (Rosenberg and Damus. 1973). The coagulation cascade consists of a series of proteolytic reactions, culminating in the generation of thrombin. Thrombin, in turn, converts fibrinogen to fibrin (Jackson and Nemerson, 1980). The currently accepted model of blood coagulation involves a cascade of coagulation factor activations that follow one of two pathways, termed intrinsic and extrinsic, which converge at a common pathway (Figure 1.3).

In the intrinsic pathway, factor XII is activated to factor XIIa, which in turn activates factor XI. The activated factor XI then activates factor IX. The activated factor IX with co-factor VIII and calcium then activate factor X. In the extrinsic pathway, tissue factor (TF) works in association with factor VII to activate factor X. In addition, activated factor VII can activate factor IX to factor IXa which can then activate factor X (Mann, 1999). Factor Xa catalyzes the conversion of prothrombin to thrombin, which in

Figure 1.2 The structure of human antithrombin determined by X-ray crystallography. The reactive center loop, with the Arg-393-Ser-394 reactive bond, is at the top of the molecule. A β-sheet is at the front of the molecule. D-helix is involved in the region of proposed heparin-binding sites (Modified from Larsson et al. 2001; copyright permission obtained.).

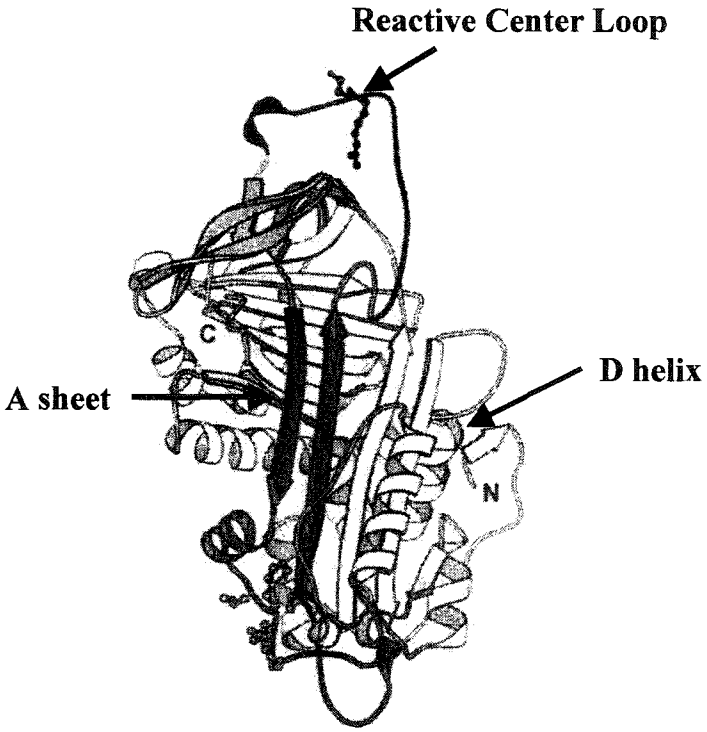
Reactive Center Loop
A sheet
D helix
C
N

Figure 1.3 Reactions in blood coagulation. The activated forms of the nonenzymatic protein cofactors V and VIII are designated Va and VIIIa, respective. TF means tissue factor. PL means phospholipid. PK means prekallikrein and HK represents high molecular weight kininogen.

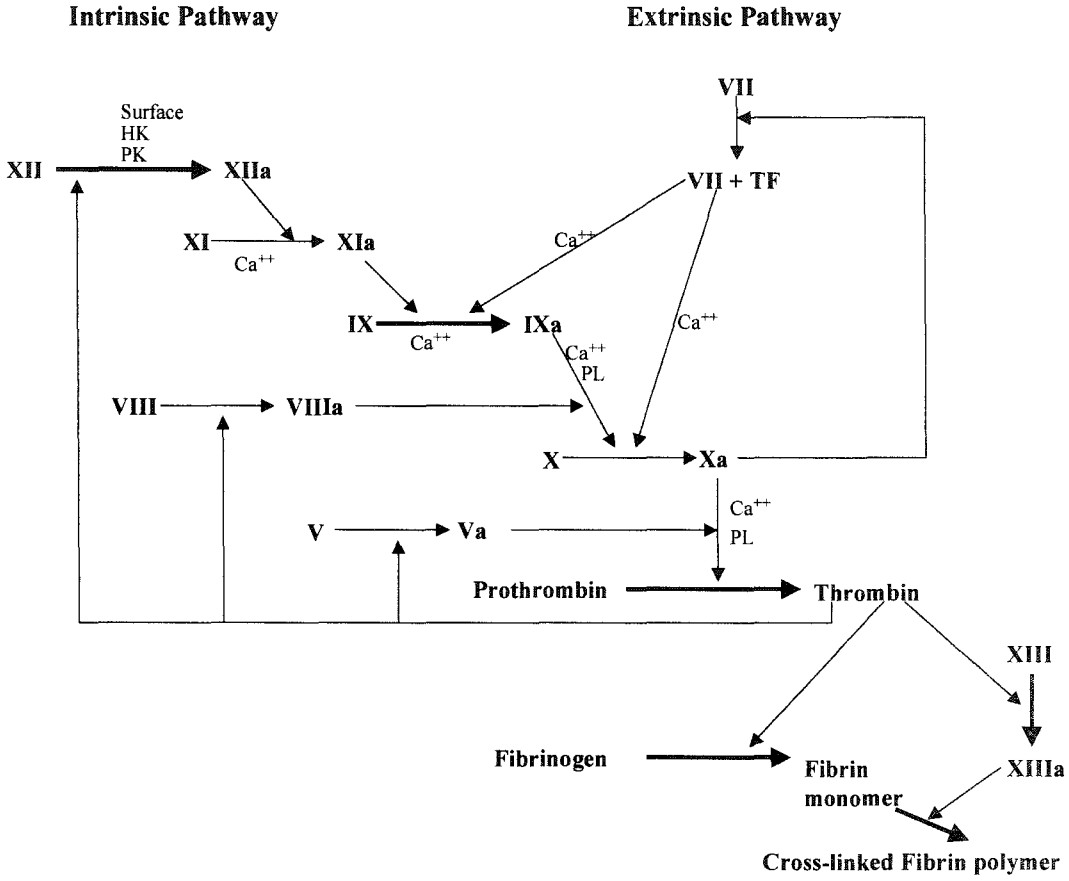
Intrinsic Pathway
Extrinsic Pathway
VII
Surface
HK
PK
XII
XIIa
VII + TF
XI
XIa
Ca++
Ca++
IX
IXa
Ca++
Ca++
PL
Ca++
VIII
VIIIa
X
Xa
Ca++
PL
V
Va
Prothrombin
Thrombin
XIII
Fibrinogen
Fibrin
monomer
XIIIa
Cross-linked Fibrin polymer

turn converts fibrinogen to fibrin. Fibrin monomers are further strengthened by covalent cross-linking catalysed by factor XIIIa (Figure 1.3).

AT has been shown to be the primary inhibitor of the activated clotting factors including thrombin and factor Xa (Jesty, 1986; Fuchs and Pizzo, 1983). To a lesser extent, AT has also been shown to inactivate FIXa, FXIa, FXIIa, FVIIa associated with tissue factor as well as kallikrein, plasmin, urokinase, and trypsin (Fuchs *et al.*, 1984; Gitel *et al.*, 1984; Lawson *et al.*, 1993; Olson *et al.*, 1993a; Rosenberg *et al.*, 1975b; Kurachi *et al.*, 1976; Stead *et al.*, 1976). The most important function of AT in coagulation is the inhibition of thrombin and factor Xa which is relatively slow under physiologic conditions, but greatly accelerated in the presence of heparin (Rosenberg and Damus, 1973; Scott and Colman, 1989).

1.5.1 Interaction Between AT and Thrombin

The inhibitory action of AT depends upon the formation of a stable 1:1 stoichiometric covalent complex through its P1 residue and the active site serine of the cognate protease (Bjork, 1982a). The reactive center of AT is located at amino acid residues 393(arginine) and 394 (serine) towards the carboxyl terminus of the molecule and is commonly designated P1-P1' (Jornvall *et al.*, 1979). Residues which are located N-terminal to the reactive site are numbered P1, P2, P3 *etc.* while those which are located C-terminally from the reactive site are numbered P1', P2', P3' *etc* (Kress and Cataness, 1981). The formation of AT-protease complex is dependent on the presence of an exposed peptide loop containing a reactive-center bond that acts as a preferred substrate for the protease (Owen, 1975; Longas and Finlay, 1980; Fish *et al*, 1979a). In AT, the

reactive center loop (RCL) extends towards the amino terminus from P17 at the top of strand 5 of the A-sheet (s5A) to P1 at the commencement of strand 1 of the C-sheet (s1C) to give an overall length of 17 residues (Zhou *et al.*, 2001; Huber and Carrell 1989).

The P1 residue is important in the defining the substrate specificity of a serpin. This is elegantly demonstrated by a natural variant of α1-antitrypsin, α1-antitrypsin$_{Pittsburgh}$, in which the P1 methionine has been mutated to an arginine. This substitution completely alters the specificity of the α1-antitrypsin and converts it from an inhibitor of leukocyte elastase to a potent inhibitor of thrombin (Owen *et al.*, 1983; Schapira *et al.*, 1986; Scott *et al.*, 1986; Wachtfogel *et al.*, 1994). However, the P1 residue is not the sole determinant of inhibitory specificity. Amino acid substitutions in the RCL beyond the P1 residue also change the specificity of the serpins, suggesting the importance of the P1, P1' and other flanking residues in determining the specificity (Theunissen *et al.*, 1993; Hopkins *et al.*, 1995; Olson *et al.*, 1995; Djie *et al.*, 1996; Zhou *et al.*, 2001).

When crystallographic structural information became available, it was evident that the RCL of AT was mobile in term of its relationship with the main body of the molecule (Carrell *et al.*, 1991; Carrell and Travis, 1985). In contrast to the fixed structure of the smaller inhibitors, the RCL of AT can vary in its conformation by partial or even total incorporation into the A-sheet of the molecule (Whisstock *et al.*, 1998). Three conformational states of antithrombin have been described which include native state, cleaved state and uncleaved latent state (Carrell and Evans, 1992). They differ primarily in the structure of the RCL. In the native state, the RCL is exposed and

accessible for interaction with a proteinase. In the cleaved state, the scissile bond in the reactive site is cleaved, and the RCL forms an additional strand inserted into the A β-sheet. The native to cleaved change is called the "stressed to relaxed" (S to R) transition. The latent state is an alternative R state in which the RCL is inserted into the A β-sheet with the polypeptide chain intact. The ability to incorporate the RCL into the A β-sheet of the molecule must serve a functional purpose as it has been conserved in all the inhibitory serpins including AT, but not in non-inhibitory serpins such as ovalbumin (Carrell and Evans, 1992; Carrell and Travis, 1985). There is evidence to suggest that the partial insertion of the RCL into the A-sheet is required for initial inhibitory activity of AT (Whisstock *et al.*, 2000; Zhou *et al.*, 2001). The mobility of the RCL of AT allows it to conform to that of the active center of the protease to give a docking of the two molecules and so form a complex (Carrell *et al.*, 1991). There is a body of evidence which suggests that following docking there is a further reinsertion of the RCL into the A sheet which serves to lock the inhibitor-protease complex (Huntington and Carrell, 2001). The prevention of this insertion, by use of synthetic peptides homologous to the P2-P14 or P7-P14 region or by the naturally occurring variants of AT involving substitutions at P10 or P12 renders the AT inactive (Molho-Sabatier *et al.*, 1989; Caso *et al.*, 1991; Austin *et al.*, 1991; Skriver *et al.*, 1991; Hopkins *et al.*, 1993; Bjork *et al.*, 1993; Shore *et al.*, 1995).

When AT interacts with thrombin, the two molecules form a stable covalent 1:1 stoichiometric complex. The mechanism of the formation of stable AT-thrombin complex is not completely understood. Kinetics studies have suggested that the formation

of the stable AT-proteinase complex involves at least two steps (Olson and Shore, 1982; Bruch and Bieth, 1989; Longstaff and Gaffney, 1991; Stone and Hermans, 1995). The initial step involves the cleavage of the P1-P1' peptide bond of AT by the reactive site of thrombin. This relatively weak association between cleaved AT and thrombin is then strengthened by the formation of an ester bond between the active site serine residue of thrombin and the carboxyl group of Arg393. Thus a covalent complex between two molecules is formed (Owen, 1975; Fish and Bjork, 1979; Jesty, 1979; Jornvall *et al.*, 1979; Longas and Finlay, 1980; Bjork *et al.*, 1982b; Lawrence *et al.*, 1995).

Recently, based on the crystallographic structure of α_1-antitrypsin-trypsin complex, Huntington *et al.* proposed a model to illustrate the mechanism of antithrombin-thrombin interaction (Huntington *et al.*, 2000a). Following the initial docking of thrombin and antithrombin, the conformational change is induced by reaction between the active serine of thrombin with the reactive center of the antithrombin. The cleavage of the reactive center allows RCL insertion into the A β sheet. This insertion transports thrombin to the opposite pole of the serpin as shown in Figure 1.4. The tight linkage of antithrombin and thrombin molecules and resulting overlap of their structures causes a 37% loss of structure in the thrombin. The disruption of the catalytic site prevents the release of the thrombin from the complex (Huntington and Carrell, 2001, Huntington *et al.*, 2000b). This mechanism of inhibition is critically dependent on a limited reactive center loop length to ensure the kinetic stability of the serpin-protease complex. The loop in almost all the serpins is formed by 17 residues, from the glutamate

Figure 1.4 Proposed model for the serpin-protease complex formation. Following the initial docking of the protease and serpin, the reactive center of serpin is cleaved by protease and covalently bound to the active site of the protease. Cleavage of the reactive center allows reactive center loop insertion into the A β sheet. This insertion transports thrombin to the opposite pole of the serpin. RL indicates reactive center loop (Reprinted from Huntington et al 2000a; copyright permission obtained).

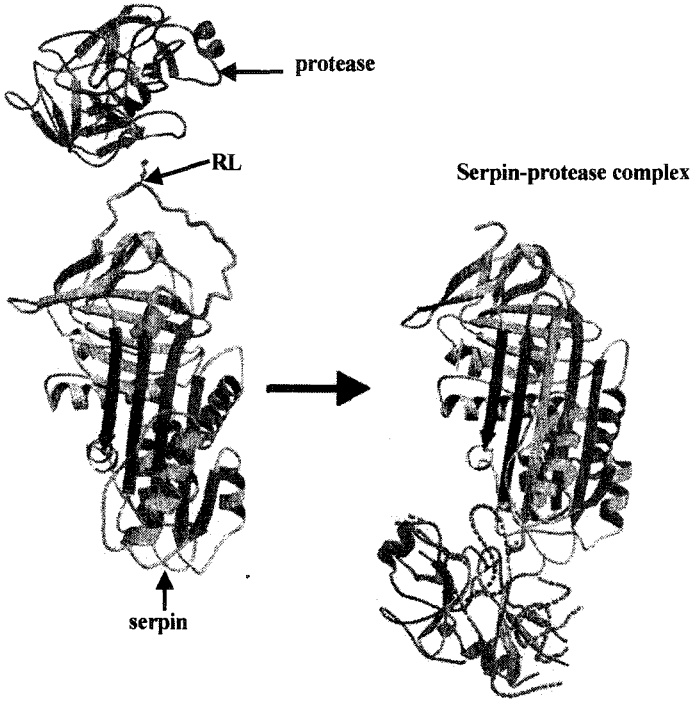
protease
RL
serpin
Serpin-protease complex

(P17) at the base of the proximal hinge of the loop to the reactive center (P1) residue (Zhou *et al*, 2001).

1.5.2 Interaction Between AT and Heparin

The inhibition of serine proteinases by AT alone under physiologic conditions is relatively slow, but can be accelerated by more than 1000-fold in the presence of the polysulphated glycosaminoglycans, heparin and heparan sulphate (Rosenberg and Damus, 1973; Jordan *et al*, 1980; Griffith, 1982; Olson and Bjork, 1991; Olson *et al.*, 1992).

Early studies on the binding of heparin to AT used commercial heparin that was heterogeneous in size. A major breakthrough in our understanding of the AT-heparin interaction resulted from the observation that only approximately one-third of the heparin molecules present in commercial, unfractionated preparation binds to AT with high affinity (Hook *et al.*, 1976). Subsequent study has identified a unique pentasaccharide sequence within the glycosaminoglycan chain of AT-binding heparin which constitutes the specific AT-binding region (Choay *et al.*, 1983).

Our understanding of the heparin binding domains of AT has come from several areas of diverse research, which includes the structural and functional analysis of both naturally-occurring low affinity variants of AT and various chemical modifications of AT associated with reduced heparin affinity (Peterson *et al.*, 1987; Chang, 1989; Chang and Tran, 1986; Olds *et al.* 1992). Relevant information has also been derived from studies involving site-directed mutagenesis, H ^{1}NMR, molecular modeling, as well as computer sequence alignments of the heparin activatable serpins (Borg *et al.*, 1988; Borg *et al.*,

1990; Gandrille *et al.*, 1990; Najjam, *et al.*, 1994; Fan *et al.*, 1994a; Liu and Chang, 1987; Chang, 1989; Sun and Chang, 1990; Peterson et al., 1987). Two putative heparin-binding domains in AT have been proposed that encompass amino acids 41 to 49 and 107 to 156. These regions mainly consist of positively charged amino acids, namely, arginines and lysines (Wu *et al.*, 1994; Stein and Carrell, 1995). When these residues are modeled on the structure of intact AT, they are seen to form a region of positive charge which extends from the D-helix and the base of the A-helix around the molecule towards the reactive center pole (shown in Figure 1.5) (Mourey *et al.*, 1993; Carrell *et al.*, 1994).

1.5.3 Mechanism of Heparin Acceleration of Proteinase Inactivation by AT

The binding of heparin to AT is known to be mediated primarily through the interaction of specific sulphate groups on the pentasaccharide sequence of heparin with basic amino acids (Arg and Lys residues) of AT. This binding alters ultraviolet absorption, circular dichroism and tryptophan fluorescence of AT, suggesting a conformational change (Gettins, 1987b; Gettins and Wooten, 1987a; Horne and Gettins, 1992; Nordenman and Bjork, 1978a; Einarsson and Anderson, 1977; Villanueva and Danishefsky, 1977; Jordan *et al*, 1979). This observation led to a hypothesis that the conformational change is responsible for activating AT to become a potent inhibitor of its cognate proteinases by making it more reactive toward the proteinase. This conformational activation is thought to cause the reactive bond of AT to be more accessible or complementary to the active site of the proteinase (Carrell *et al.*, 1991; Olson *et al*, 1992). Based on this hypothesis, one would expect that heparin and pentasaccharide should produce the same rate enhancing effect on AT in the proteinase-

Figure 1.5 The proposed heparin binding site of antithrombin. A schematic outline of the amino-terminal extension showing its relationship to the proposed heparin binding site spanning from Arg (R) 24 to Arg129 (R). The reactive center loop with Arg-393-Ser-394 reactive bond is to the right of the molecule. The side chains of basic residues proposed to be involved in heparin binding are shown and labeled (Reprinted from Bjork and Olson, 1997; copyright permission obtained.).

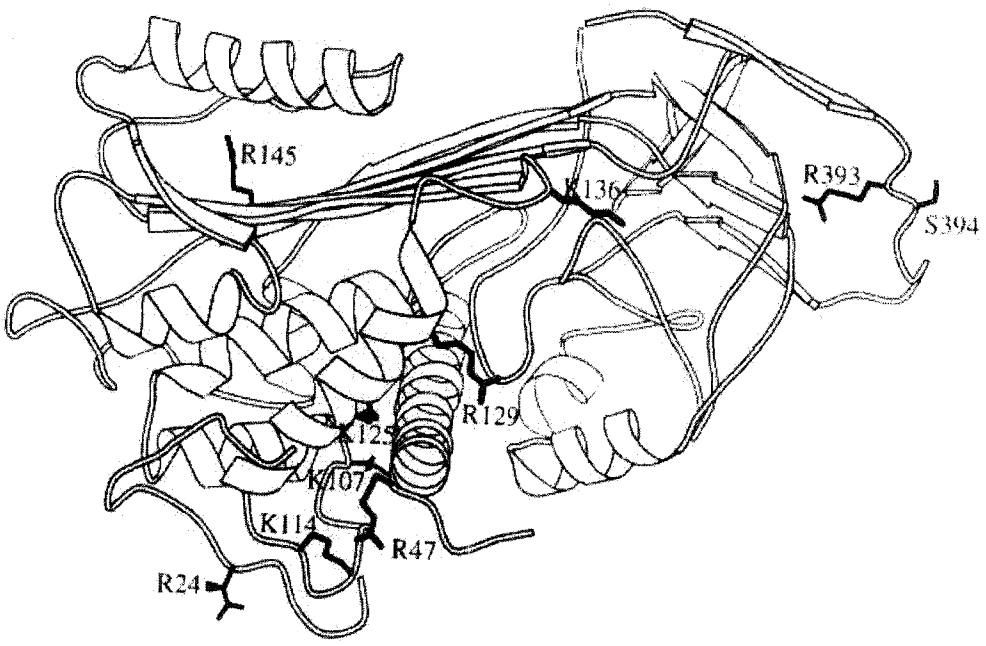
R145
R136
R393
S394
R129
K125
K107
K114
R47
R24

AT reaction, since it has been demonstrated that they both induce similar conformational changes in AT. However, this theory is challenged by the facts that the pentasaccharide enhanced AT reaction with factor Xa by 270-fold, but only by 1.7-fold with thrombin (Holmer *et al*, 1981; Choay *et al*., 1983; Olson *et al*., 1992). In order to attain maximal thrombin inhibitory activity of AT, longer chain heparins containing at least 18 saccharide units are required, the smallest polysaccharide chain that is able to bind AT and thrombin simultaneously (Lane *et al*., 1984; Danielsson *et al*., 1986, Bary *et al*., 1989). This observation led to the second hypothesis which proposed that the longer than 18 saccharide units heparin chain required to accelerate thrombin inhibition by AT is necessary to accommodate both the inhibitor and the proteinase on the same polysaccharide chain (Griffith, 1982; Nesheim, 1983). In this model, a longer heparin chain is able to form a bridge between AT and thrombin, and therefore, enhancing the AT-thrombin reaction rate (Holmer *et al*.,1979; Griffith, 1982; Olson and Bjork, 1991).

Base on the above-mentioned evidence, the current working hypothesis proposes that the accelerating effect of heparin on factor Xa inhibition by AT is mainly due to the conformational activation of AT upon binding of the pentasaccharide, while the major contribution to the rate enhancing effect of heparin on thrombin inactivation, results from the bridging by heparin of thrombin and AT to form a ternary complex (shown in figure 1.6) (Olson *et al*,1992). Recent analyses of crystal structure and kinetics of heparin pentasaccharide binding to AT showed that the binding of heparin pentasaccharide to the D helix of AT induced a series of main conformational changes. These conformational changes include an interdomain rotation of the bottom half of the serpin relative to the

Figure 1.6 Comparison of the proposed mechanism of heparin acceleration of AT inhibition of thrombin (IIa) and factor Xa. AT first binds to the pentasaccharide region of heparin. This binding induces a conformational change of AT that increases the affinity for heparin and alters the structure of the reactive-bond loop. The latter change enhances Factor Xa recognition of the loop, leading to rate enhancement, but minimally affects thrombin (T) recognition. The rate of thrombin inactivation is instead primarily enhanced by the enzyme binding to same heparin chain as AT, so that the interaction between the two reactants is greatly facilitated through a ternary-complex bridging or approximation effect (Reprinted from Bjork and Olson, 1997; copyright permission obtained).

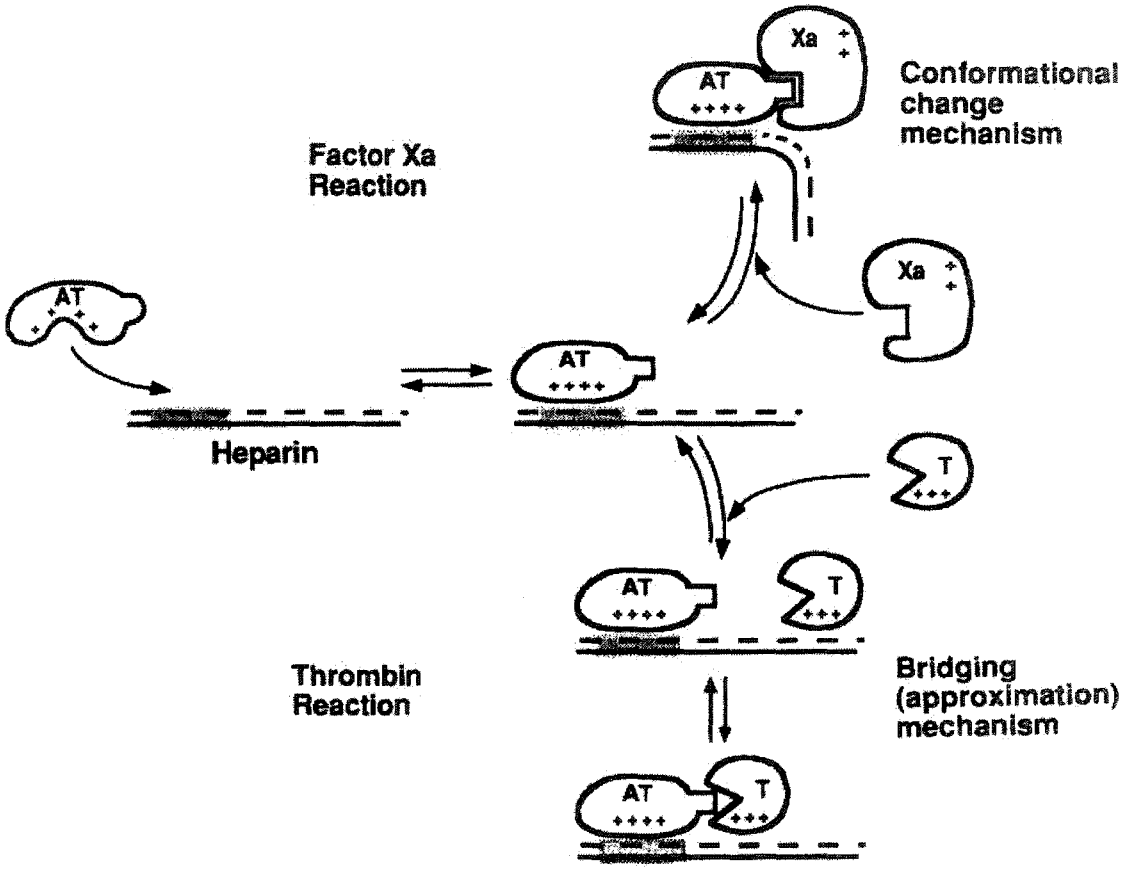
Xa
AT
Conformational change mechanism
Factor Xa Reaction
Xa
AT
AT
Heparin
T
AT
T
Thrombin Reaction
Bridging (approximation) mechanism
AT
T

top half, which leads to RCL expulsion from the A sheet and exposure of the P1 arginine residue (Belzar *et al*, 2000; Huntington *et al*, 2000). These conformational changes allow unhindered access of the proteinase to the loop and permit optimal proteinase interaction (Belzar *et al*., 2002a; Huntington *et al*., 2000b).

1.6 Glycosylation of AT

AT is synthesized in the liver and secreted into the circulation. During the course of its synthesis in the endoplasmic reticulum (ER), AT is modified at four locations of Asn-X-Ser/Thr N-glycosylation consensus sequences with high mannose glycans (Peterson *et al*., 1979). After trimming reactions and the addition of terminal glycosyl residues by sequential glycosylation in the ER and Golgi apparatus, the mature AT contains four identical N-glycosidically linked complex oligosaccharides, which contribute about 15% of the weight of AT (Franzen *et al*., 1980; Mizuochi *et al*., 1980; Brennan *et al*., 1987). In the human molecule, the four glycosylation sites correspond to Asn 96, 135, 155, and 192. Analysis of the structures of the carbohydrate chains showed that human AT has biantennary sugar chains (Franzen and Svensson *et al*., 1980; Danishefsky *et al*., 1977).

The majority of human and rabbit AT found in plasma is fully glycosylated (designated α-AT), while approximately 10% of the AT is not glycosylated at Asn 135 (designated β-AT). Consensus sequences of the AT N-glycosylation sites are Asn-X-Ser for 135 and Asn-X-Thr for 96, 155, and 192. It has been demonstrated that Asn-X-Ser consensus sequences are used less efficiently than Asn-X-Thr consensus sequences during glycosylation (Bause and Legler, 1981). Recently, Picard *et al*. demonstrated that

the presence of a serine rather than a threonine at amino acid position 137 is responsible for the partial glycosylation of asparagine 135 and the consequent production of β-AT. Their results showed that the pattern of glycoform production was changed from a mixture of α and β forms to exclusively fully glycosylated α form by substituting serine to threonine at amino acid position 137 (Picard *et al.*, 1995).

Compared with α-AT isoform, the partially deglycosylated β-AT isoform binds to immobilized heparin with greater avidity and inactivated thrombin faster in the presence of either heparin or heparan sulphate (Turk *et al.*, 1997; Witmer and Hatton, 1991). Moreover, the β-AT isoform has been shown to associate more readily than the α-AT isoform with both uninjured and de-endothelialized rabbit aortic vessel walls and is the major isoform observed in immunoblots of detergent extracts of intima-media from balloon injured rabbit aortas (Witmer *et al.*, 1992). These observations suggested that the ratio of extravascular/intravascular distribution for β-AT was substantially greater than that measured for α-AT. The β-AT isoform has been shown to have a shorter *in vivo* half-life (1.42±0.11 days) than α-AT form (2.27±0.11 days) in small rabbits (2 kilograms) (Carlson *et al*, 1985). This observation was subsequently confirmed by Witmer *et al.* who demonstrated that the *in vivo* half-life for β-isoform (2.39 ± 0.31 days) was shorter than α-isoform (2.63 ± 0.38 days) (Witmer *et al.*, 1992) in rabbits weighed approximately 5 kilograms.

On the other hand, the introduction of a new glycosylation site as in AT Rouen III (7 Ile-Asn substitution) which creates an additional fifth glycosylation site, results in the overglycosylation of AT. This overglycosylated AT isolated from a patient with

pulmonary embolism appears to have a reduced heparin affinity, which is likely due to the blockage of the heparin binding domains by an additional glycosidic side chain (Brennan *et al.*, 1988).

The effect on biological function of other partial deglycosylations is not known. The enzymatic removal of all but one N-acetyl glucosamine sugar subunit from the four oligosaccharide chains of AT has little or no effect on either progressive or heparin-catalyzed thrombin or FXa inhibition *in vitro* (Rosenfeld and Danishefsky, 1984). However, the *in vivo* half-life of the de-sialylated AT in rabbits was found to be drastically shortened (Zettlmeissl *et al.*, 1989).

1.7 Rabbit AT Gene

Rabbit AT cDNA containing the complete open-reading frame has been isolated. The cloned rabbit AT cDNA sequence displays greater than 80% identity to its human counterpart at both the nucleotide and deduced amino acid sequence levels (Sheffield *et al.*, 1992; Bock *et al.*, 1982). The four potential N-linked glycosylation sites are all conserved. However, due to the presence of a single additional amino acid, Glu7, in rabbit AT, the N-linked glycosylation Asn residues are located at Asn residues 97, 136, 156, and 193 (Sheffield *et al.*, 1992). Expression of the cDNA in a cell-free system has shown that the rabbit AT protein is capable of binding heparin and forming SDS-stable complexes with both rabbit and human α-thrombin (Sheffield *et al.*, 1992).

1.8 Expression of Recombinant AT

The availability of AT cDNA clones has allowed the expression of recombinant AT *in vitro*. A number of groups have expressed the AT gene in bacteria (Bock *et al.*,

1982), a reticulocyte cell-free system (Austin *et al.*, 1990), yeast (Broker *et al.*, 1987), slime mold (Dingermann *et al.*, 1991), insect cells (Gillespie *et al.*, 1991; Kridel *et al.*, 1996), and cultured mammalian cells (Stephens *et al.*, 1987; Wasley *et al.*, 1987; Zettlmeissl *et al.*, 1989). In contrast to the bacteria and cell-free systems which produce a nonglycosylated form of AT, all other cells give rise to glycosylated products. However, while glycoproteins produced in yeast or insect cells may be properly folded and exhibit bioactivity *in vivo*, the fact that both types of cells produce AT containing N-linked carbohydrate groups with terminal mannose residues is the reason that AT was rapidly degraded *in vivo* (Broker *et al.*, 1987; Bock *et al.*, 1982). Such considerations demand the use of mammalian cell lines for production of glycoproteins, which represents a system to produce AT in a near natural environment. Transient expression of AT in SV40 transformed African green monkey kidney cells (COS) has provided a convenient tool to study the function and structure of AT when only a small amount of recombinant AT is required (Stephens *et al.*, 1987; 1988). The ability to establish permanent cell lines and express functionally active glycosylated AT in CHO cells represents a significant advance in AT gene expression. The CHO cell has been used to express a number of therapeutically useful proteins, including erythropoietin and tissue plasminogen activator (Spellman *et al.*, 1989; Wasley *et al.*, 1991; Sasaki *et al.*, 1989). The glycosylation potential in CHO cells has been well characterized (Spellman *et al.*, 1989; Dwek *et al.*, 1993). CHO cells allow processing of multi-antennary and poly-N-acetylgalactosamine oligosaccharides. It has also been demonstrated that CHO cells do not incorporate sialic acid in α2-6 linkage, nor do they make the galα3 linkage. Like other recombinant

proteins, recombinant AT from CHO cells showed a heterogeneity of glycosylation (Zettlmeissl *et al.*, 1989; Bjork *et al.*, 1992). Oligosaccharides present in recombinant human AT from CHO cells contain a considerable proportion of tri- and tetra-antennary chains which are not detected in human plasma-derived AT (Zettlmeissl *et al.*, 1989). Additionally, the oligosaccharides of recombinant AT differ from those of natural plasma AT in their NeuAc linkage. While α2-3 is present in the recombinant AT, an α2-6 is detected in natural human plasma-derived AT. Furthermore, the presence of fucose on the proximal GlcNAc is not detected in human plasma derived AT carbohydrate chains. Despite these differences, the *in vivo* pharmacokinetic properties, such as half-life, of the recombinant AT was very similar to that of its plasma counterpart, when injected into rabbits (Zettlmeissl et al., 1989). The CHO-derived AT and plasma AT did not differ significantly when analyzed by circular dichroism, ultraviolet absorbance, fluorescence spectroscope, heparin binding, or kinetics of thrombin inhibition (Zettlmeissl *et al.*, 1989).

Permanent expression of AT in baby hamster kidney (BHK) cells has also produced functionally active AT (Fan *et al.*, 1993). Three forms of AT were isolated from BHK cells, which differed in affinity for heparin. Form I had the lowest affinity and contained a high proportion of highly branched complex carbohydrate. Form II had higher affinity and contained both complex and high mannose-type chains. Form III had the highest affinity and was similar to form II in the type of carbohydrate present, but had a lower level of glycosylation, consistent with the absence of carbohydrate at one of the four glycosylation sites. This carbohydrate heterogeneity did not alter the structure of the

recombinant AT polypeptide or the heparin-induced conformational change. In addition, two patterns of glycosylation at position 155 were identified with the form with lower heparin affinity being 97% fucosylated at this position, whereas the form with higher affinity for heparin was not fucosylated (Fan *et al.*, 1993; Bjork *et al.*, 1992).

1.9 Protein Glycosylation

1.9.1 The Primary Peptide Structure and Potential Glycosylation Sites

There are two main classes of carbohydrate linkages in mammalian glycoproteins which are designated as O-linked glycan and N-linked glycan (Paulson, 1989). While O-linked glycosidic linkages involve oxygen in the side chain of serine, threonine, or hydroxylysine, N-linked glycans involve nitrogen in the side chain of asparagine. In order to have N-linked glycosylation, an asparagine residue must form part of the tripeptide Asn-X-Ser/Thr/Cys, where X is any amino acid except proline. However, the presence of this sequon is not in itself sufficient to ensure glycosylation (Kornfeld and Kornfeld, 1985). The role of the peptide sequence in directing O-linked glycosylation to Ser or Thr is less clear, but a Pro-residue, at -1 and +3, may make it favorable (Lis and Sharon, 1993).

1.9.2 Factors That Control Protein Glycosylation

1.9.2.1 Cell Type and Protein Glycosylation: It is well established that the type of cell has a major role in determining the extent and structure of glycosylation, which is both species and tissue specific. It has been shown that the terminal glycosylation sequences differ from tissue to tissue and also differ from cell types within each tissue (Parekh *et al.* 1987). The ultimate structures of carbohydrates are determined

largely by the glycosyltransferases that synthesize them (Sharon and Lis 1982). Many different enzymatic reactions are involved in the processing pathways. The profiles of the enzyme arrays, which include their type, concentration, kinetic characteristics and compartmentalization, reflect both the external and internal environment of the individual cell in which the protein is glycosylated.

The glycosylation of recombinant glycoproteins can be exquisitely sensitive to changes in physiological conditions used in culture, such as the glucose concentration of the culture medium (Goochee and Monica, 1990). The glycosylation pattern basically reflects the type of cell used in the expression system and the conditions of culture. The use of different cell lines can result in significant differences in glycosylation.

1.9.2.2 The Three-Dimensional Structure of Protein and the Extent and Type of Glycosylation: Although the same glycosylation machinery is available to all the proteins which are translated in a particular cell, it has been estimated that between 10% to 30% of potential glycosylation sites are not occupied (Gavel and von Heijne, 1990). Moreover, site analysis has shown that the distribution of different classes of N-linked oligosaccharide structures is also specific for each site on a protein (Parekh *et al.*, 1987). These observations suggested that the 3-dimensional structure of the individual protein may play a role in determining the type and extent of its glycosylation. This notion is supported by the observation that the position of the glycosylation site in the protein can affect the likelihood of its being glycosylated. N-linked sites at the exposed turns of β-pleated sheets, which are sometimes close to proline residues, are normally occupied by glycans while those near the C-terminus are more often vacant. It has been

suggested that the potential glycosylation sites may be sterically hindered by the local protein structure or by protein folding which may compete with the initiation of N-glycosylation (Dwek *et al*, 1995). In addition, glycosylation at one site in a multi-glycosylated protein may affect glycosylation at other sites (Dwek *et al*, 1995). This may be due to sterically hindering events at a second site on the same molecule.

1.9.3 The Role of N-linked Glycosylation in the Structural and Functional Activities of Protein:

Biologically active glycoproteins are widely distributed in nature and present on all cell surfaces. Both N-linked and O-linked glycans have diverse biological roles in the structural and functional activities. Given the fact that glycoproteins are present on the surface of all cells, they are advantageously positioned to serve as biological recognition determinants which provide signals for protein targeting and cell-cell interaction. In addition, the specific carbohydrates of a particular glycoprotein on the surface of erythrocytes also provide the immunodeterminants for particular ABO blood types (Feizi and Childs, 1987). This section will focus on the role of the N-linked glycan in the biological function of plasma glycoproteins.

1.9.3.1 Modulation of Physicochemical Properties: Carbohydrates may modify the physicochemical properties of plasma proteins by changing their hydrophobicity, electrical charge, mass, and size. The negative charges of sialic acid residues and sulphate group increase the solubility, and affect the conformation of glycoproteins (Springer, 1990). Glycans may also rigidify the protein by forming hydrogen bonds with the polypeptide backbone. In addition, carbohydrate moieties may

influence protein heat stability and susceptibility to proteolysis. Indeed, it has been demonstrated that glycoproteins, especially if they are carbohydrate rich, are more resistant to proteolysis *in vivo* than are nonglycosylated proteins (Montreuil, 1984).

The general function of N-glycosylation is to aid in the folding of the nascent polypeptide chain and in the stabilization of the particular conformation of the mature glycoprotein. As a consequence, glycosylation may affect the protein functionality that depends on conformation. However, the relative requirement for N-linked oligosaccharides varies between glycoproteins. Following exposure of cells to inhibitors of N-linked glycosylation such as tunicamycin, some glycoproteins are found to aggregate in the ER and are then degraded intracellularly. Others are less affected and are secreted, but have compromised biological activities, while some appear to be totally unaffected (Lis and Sharon, 1993; Rademacher *et al.*, 1988). Using site-directed mutagenesis and expression experiments, systematic analyses of individual N-linked sugar chains showed that some glycans can be completely eliminated, while others are critically important for normal biosynthesis (Gallager *et al.*, 1988; Dube *et al.*, 1988). This effect is well demonstrated in the site-directed mutagenesis study of protein C, an anti-thrombotic serine protease that circulates in blood as a mixture of an inactive single-chain zymogen and an active two-chain enzyme. It has been demonstrated that glycosylation at different sites affects distinct properties of this complex two-chain protein. Glycosylation at Asn 97 in one of the enzyme chains is critical for efficient secretion and influences the degree of glycosylation at Asn329 in the other chain. Glycosylation at Asn248, on the other hand, affects the intramolecular cleavage and

removal of the dipeptide Lys-Arg which is required for the activation of the zymogen (Grinnell *et al.*, 1991).

1.9.3.2 Modulation of Biological Activity: The ability of N-linked carbohydrates to modulate the activities of biologically functional molecules has been established unequivocally during the last decade, even though for most glycoproteins the role of the carbohydrates is still obscure. For some glycoproteins, such as ovine submaxillary glycoprotein, a definite function has been attributed to the carbohydrate units (Lis and Sharon, 1993).

1.9.3.2.1 Glycosylation and Biological Activity of Enzymes: In the majority of cases investigated, glycosylation has no effect on the biological activity of enzymes. The first clue that this could be the case was provided by nature itself, when it was found that the enzyme ribonuclease occurs both in non-glycosylated and variously glycosylated forms, all of which exhibited the same catalytic activity (Lis and Sharon, 1993). Recently, however, there has been an increasing number of glycoprotein enzymes whose activity and stability was shown to be modulated by their carbohydrate units (Cumming *et al.* 1991). Perhaps the best documented illustration of the effect of carbohydrate on enzymatic activity is that of tPA, a serine protease which converts plasminogen to plasmin. tPA has a peptide backbone of 527 amino acids, with four potential glycosylation sites, only three of which may be occupied. While Asn117 is occupied by an oligomannose unit, Asn184 and Asn448 are occupied by complex glycans (Patthy, 1985). Two major molecular species of tPA have been isolated from plasma, type I (glycosylated at all three sites) and type II (glycosylated at Asn117 and Asn448 only).

Further, each of these species can exist as single-chain and double-chain forms. It has been found that the rate of conversion of the single-chain into the double-chain form, the enzymatic activity of the different forms and their susceptibility to plasma protease inhibitors are affected by the presence of the glycan at Asn184 (Wittwer *et al.*, 1989; Wittwer and Howard 1990). In a study, in which recombinant type I and type II tPA with modified glycans were produced in CHO cells grown in the presence of the glycosylation processing inhibitor, deoxymannojirimycin, it was shown that the structure of the carbohydrate at Asn448 also affects the catalytic activity of tPA (Howard *et al.*, 1991).

1.9.3.2.2 Glycosylation and Biological Activity of Hormones: Earlier work has shown that while the chemically or enzymatically deglycosylated glycoprotein hormones bind to their receptors on target cells with the same affinity as the native ones, their ability to activate the hormone-responsive adenylate cyclase is drastically decreased (Sairam, 1989). The role of carbohydrates in the activity of erythropoietin has been the subject of intense study (Wasley *et al.*, 1991; Takeuchi and Kobata, 1991). Desialylation of erythropoietin enhanced its *in vitro* activity by increasing its affinity for the receptor, but decreased its activity *in vivo*, presumably by decreasing its life-time in circulation. Examination of several preparations of recombinant erythropoietin that differ in the degree of branching of their N-glycans revealed that the *in vivo* activity of the hormone increased with the ratio of tetraantennary to biantennary saccharides (Takeuchi *et al.* 1989). The non-glycosylated hormone has several fold higher specific activity than the native one (Higuchi *et al.*, 1992).

1.9.3.3 Clearance Markers: Carbohydrate serves as an important recognition marker on glycoproteins in the circulation, which controls the half-life of serum glycoprotein in the circulatory system as well as their uptake into liver cells (Pricer and Ashwell, 1971). The classic work of Gilbert Ashwell *et al.* has demonstrated that removal of sialic acid from circulating glycoproteins by sialidase leads to a dramatic enhancement in the rate of glycoprotein clearance from the circulatory system of rabbits, rats, and mice (Ashwell and Harford, 1982). Detailed investigations of this phenomenon have revealed that the asialoglycoproteins are rapidly taken up and catabolized by the liver (Schengrund *et al.*, 1972). This uptake depended on recognition by the liver cells of galactose residues on the glycoprotein which were exposed by the removal of sialic acid. Indeed, a receptor that specifically binds asialoglycoproteins has been isolated from rabbit liver membranes and has been designated as the hepatic (carbohydrate) binding protein (hepatic asialoglycoprotein receptor). This receptor is responsible for removal of asialoglycoproteins from the circulation (Pricer *et al.*, 1974, Stockert, 1992).

1.10 Rationale and Objectives

AT is the principal anticoagulant protein that inhibits thrombin and factor Xa in plasma through the formation of AT-proteinase complexes. This anticoagulant protein is synthesized in hepatocytes and secreted into the circulation. As is the case for many plasma proteins, AT is glycosylated during the course of its synthesis.

Protein and cDNA sequence of AT from both the human and rabbit have shown the presence of four consensus sequences for N-linked glycosylation. In the human molecule, these potential glycosylation sites are located at amino acid positions Asn 96,

135, 155, and 192, by comparison, they are at Asn 97, 136, 156, 193 in rabbit molecule, due to the presence of a single additional amino acid residue, Glu 7, in the rabbit. Interestingly, two isoforms of AT have been isolated from human and rabbit plasmas. While the major α-form of AT is glycosylated at all four sites, the β-isoform is not glycosylated at Asn 135 in the human or Asn136 in the rabbit molecule. Compared with the α-AT isoform, the partially deglycosylated β-AT isoform binds to immobilized heparin with greater affinity and inactivates thrombin faster in the presence of either heparin or heparan sulphate (Turk *et al.*, 1997; Witmer and Hatton, 1991). In addition, the β-AT isoform has been shown to associate more readily than the α-AT isoform with both uninjured and de-endothelialized rabbit aortic vessel walls. Moreover, the β-AT isoform has been demonstrated to have a shorter *in vivo* half-life than the α isoform (Witmer *et al.*, 1992). A recent *in vitro* experiment demonstrated that the carbohydrate side chain at Asn-135 of human AT reduces the heparin affinity of α-AT primarily by interfering with heparin-induced conformational change (Turk *et al.*, 1997). These observations have demonstrated that the degree of AT glycosylation affects its biological function as well as its *in vivo* catabolism and distribution. However, it is not clear whether or not this effect is entirely due to the removal of the charged sialic acid residues upon removal of the entire glycosidic side chain, or it is simply due to removing steric interference around asparagine-135 as seen in the β-isoform. In addition, the role of the glycans on positions 96, 155, and 192 in the biological function of AT is not known. Previous investigations suggested that the Asn-135 oligosaccharide of α-AT is oriented away from the heparin binding site and does not interfere with the first step of heparin

binding. It has been hypothesized that the initial binding of heparin to AT induces conformational changes involving extension of helix D into the adjacent region containing Asn-135, which are transmitted to the reactive center loop (Belzar *et al.*, 2002; Turk *et al.*, 1997). The resulting decreased conformational flexibility of the Asn-135 oligosaccharide may be responsible for a decreased heparin binding affinity (Turk, 1997). This model suggests that the decreased heparin affinity seen in the α-AT is due to the close vicinity of the oligsaccharide at Asn 135 to the heparin binding site. Therefore, we felt that it would be of great interest to evaluate the role of other individual glycans, at position 97, 156, and 193, in the biological function of rabbit AT.

To address these issues, and to investigate possible contributions of the each individual glycan chain to the *in vitro* and *in vivo* biological functions of AT, we systematically and individually eliminated each of the four potential glycosylation sites of rabbit AT by substituting an Asn residue to a Gln residue. Using this approach, we created four underglycosylated forms of rabbit AT. Each molecule only possesses three of four glycosylation consensus sites. Two specific objectives were proposed for this study: (1). To investigate the effect of each glycan chain on the *in vivo* half-life of rabbit AT; (2). To investigate the effect of each glycan chain on the *in vitro* biological function of AT including heparin binding affinity and thrombin inhibitory activity.

The availability of the rabbit AT cDNA enabled us to express this protein in a mammalian system. By introducing recombinant rabbit AT molecules into the rabbit circulation system provided us with a unique opportunity to study the *in vivo* behavior of underglycosylated AT in a partially homologous system in that studies of the

recombinant ATs *in vivo* were performed in the same species as that from which the cDNA that we used was derived. Although the potential glycosylation sites in rabbit AT are located at Asn97, 136, 156, and 192, the glycosylation site numbering corresponding to human AT (Asn 96, 135, 155, and 192) will be used in the discussion. This is mainly for the purpose of comparison with previous studies in which human AT was used.

2. MATERIALS AND METHODS

2.1 Materials

2.1.1 Source of Chemicals and Reagents

Electrophoresis grade agarose was purchased from Bethesda Research Laboratories (BRL) (Burlington, ON). Ethidium bromide (EtBr), 5-bromo-4-chloro-3-indolyl phosphate (BCIP), nitro blue tetrazolium (NBT), and phosphatase substrate, p-nitrophenyl phosphate (PNPP) disodium hexahydrate, iodoacetamide, 3-(N-morpholino) propanesulfonic acid (MOPS), Nonidet P-40 (NP-40), ampicillin, chloramphenicol, and kanamycin were purchased from Sigma Chemical Company (St. Louis, MO). Ammonium acetate (NH_4OAc), boric acid, ethylene-diamine-tetraacetic acid (EDTA), glycerol, polyethylene glycol (PEG), dimethyl sulphoxide (DMSO), potassium acetate (KOAc) and sodium acetate (NaOAc) were purchased from BDH Chemicals (Toronto, ON). Acrylamide, ammonium persulfate (APS), N, N'-methylene-bis-acrylamide (BIS), bromophenol blue, Coomassie Brilliant Blue R-250, glycine, sodium dodecyl sulfate (SDS), N,N,N',N'-tetramethylethylenediamine hydrochloride (TEMED), Tris(hydroxymethyl) aminomethane (TRIS) and urea were purchased from Bio-Rad Laboratories (Mississauga, ON). Dithiothreitol (DTT), 5-bromo-4-chloro-3-indolyl-β-D-galactoside (X-gal) and β-D-isopropyl-thiogalactopyranoside (IPTG) were purchased from Bethesda Research Laboratories (Gibco BRL) products from Life Technologies (Burlington, ON). All other chemicals and reagents were of the highest quality available.

2.1.2 Radiochemicals

For metabolic radiolabeling of cultured mammalian cells, the radioactive products [^{35}S]-methionine and [^{35}S] cysteine (Tran^{35}Slabel) were obtained from ICN (Mississauga, ON). [^{35}S]-dATP and Na^{125}I and Na^{131}I were from Mandel (Toronto, ON). α-[^{32}P]dATP (3000 Ci/mmol, 10 μCi/μl) was purchased from Amersham (Oakville, ON).

2.1.3 Enzymes

Restriction endonucleases were purchased either from Pharmacia LKB Biotechnology (Baie d'Urfe, QC) or Gibco BRL. T4 DNA ligase, T4 DNA polymerase were purchased from either Pharmacia (Baie d'Urfe, QC) or Promega-Biotec (Toronto, ON). The enzymes were used according to the manufacturer's product data sheet.

2.1.4 Bacterial Cell Lines and Helper Phages

Routine transformations were carried out in either competent *E.coli* DH5α cells or DH10B cells purchased from Canadian Life Technologies (Burlington, ON). Transformed *E.coli* cells were routinely grown at 37°C with shaking in Lauria-Broth (LB) medium [1% bacto-tryptone, 0.5% (w/v) bacto-yeast extract, 1% (w/v) NaCl, pH 7.5] supplemented with 100 μg/ml ampicillin. Since both pGEM3Zf(+) and pCMV5 carry the ampicillin resistance gene, 100 μg/ml ampicillin was supplemented in the LB-agar plates for selection of transformed resistance bacteria. Transformed *E.coli* cells were initially selected on LB plates containing 1.5% (w/v) bacto-agar. The generation of single-stranded DNA from phagemid vectors for site directed mutagenesis was carried out in

competent *E.coli* DH5αF' cells purchased from BRL. M13K07 helper phage (1-5X 10^{11} pfu/ml) was purchased from Bio-Rad Laboratories (Richmond, CA).

2.1.5 Mammalian Cell Expression Vector

The pCMV5 mammalian expression vector was constructed in Dr. David W. Russell's laboratory and was kindly provided by him (University of Pennsylvania, Philadelphia, PA) (shown in Figure. 2.1). This vector contains the promoter-enhancer region of the major immediate early gene of the human cytomegalovirus, a synthetic polylinker sequence containing unique cleavage sites for restriction enzymes, the transcription termination and polyadenylation region of the human growth hormone gene, and the SV_{40} virus DNA replication origin and early region enhancer. After introduction into mammalian cells, the vector is designed such that transcription originating from the strong cytomegalovirus promoter will traverse the polylinker sequences including the inserted cDNA, and terminate in the human growth hormone gene region. The presence of the SV_{40} origin of replication in pCMV5 results in the amplification of plasmid sequences, when the vector is transfected into mammalian cells previously transformed with the large T antigen of SV_{40}, such as simian COS cells. Thus, this vector can be used to express a protein in both transient as well as stable cell line expression systems. The pCMV5 vector also carries the ampicillin resistance gene (Anderson et al., 1989).

Plasmid pSV2Neo contains a dominant neomycin (geneticin) resistance gene which can be expressed in eukaryotic cells. Introduction of this gene into cells confers resistance to geneticin, enabling the cells to grow in media containing geneticin (Kaufman, 1990).

Figure 2.1 Structure of plasmid pCMV5 expression vector. (Modified from Anderson et al., 1989; copyright permission obtained.).

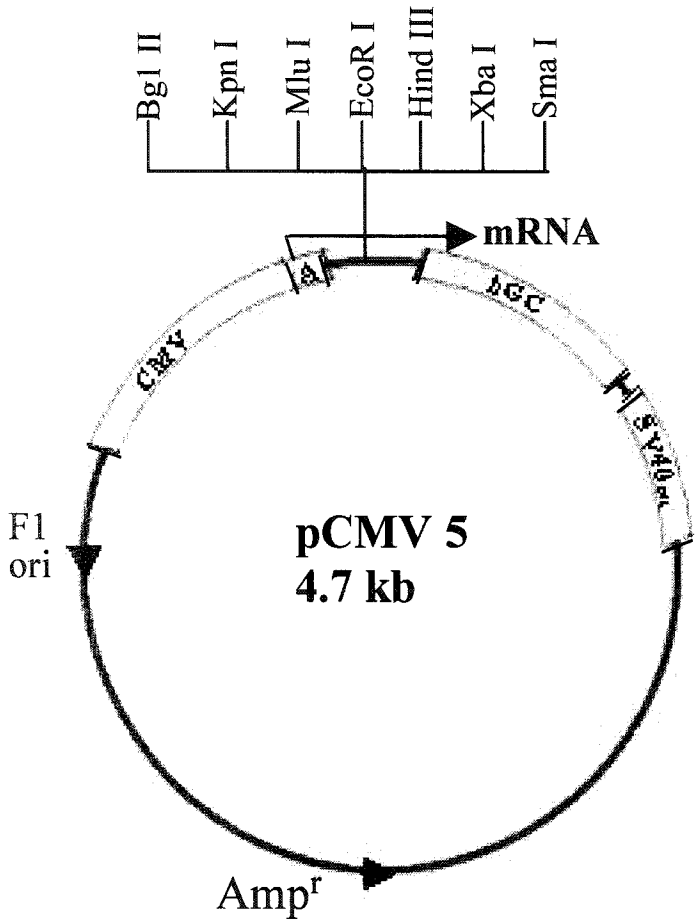
Bg1 II
Kpn I
Mlu I
EcoR I
Hind III
Xba I
Sma I
mRNA
CMV
SV40 pA
F1
ori
pCMV 5
4.7 kb
Amp^r

2.1.6 Mammalian Expression Cell Lines

COS-1 and CHO cells (pro5-CHO) were purchased from the American Type Culture Collection (ATCC) (Rockville, MD). The pro-5 CHO cell line (ovary, proline auxotrophy, Chinese hamster) was a clonal derivative of the original Chinese hamster ovary cell line (CHO). One of the advantages of this cell line is that it can be maintained in either a suspension or a monolayer system. This feature facilitated the expansion of the culture to a large scale to produce large quantities of AT sufficient for its purification and further extensive characterization.

COS-1 was a fibroblast-like cell line established from CV-1 simian cells which were transformed by an origin-defective mutant of simian virus 40 (SV_{40}) which codes for wild-type T antigen. These COS cells express high level of the SV_{40} large tumor (T) antigen which supports the replication of viral DNA. The T antigen-mediated replication can amplify the plasmid copy number to a great extent, allowing high expression of the transfected DNA.

2.1.7 Media and Regents for Cell Cultures

Dulbeco's modified eagle medium without L-Gln, L-Met, and L-Cys (D-MEM-Gln-Met-Cys-) were bought from ICN (Mississauga, ON). Geneticin^R reagent (G-418 Sulfate), heat-inactivated fetal bovine serum (FBS), penicillin-streptomycin, and trypsin-EDTA (1X) (0.05% trypsin, 0.53 mM EDTA) were Gibco BRL products. Minimum essential α-medium (α-MEM), and sterile phosphate-buffered saline (PBS) were supplied from McMaster University (Hamilton, ON).

2.1.8 Source of Rabbit AT cDNA

The rabbit cDNA encoding AT, including its secretory signal sequence, was isolated and subcloned into the phagemid pGEM3zf(+) in Dr. Blajchman's laboratory. This cDNA was used in this study. It contained 96 nucleotides encoding the 32 amino-acid signal peptide, and 1299 nucleotides encoding the 433 amino acids of the mature rabbit AT-III protein (Sheffield et al. 1992).

2.1.9 Oligodeoxyribonucleotides

The following oligodeoxyribonucleotides designed as primers for site-directed mutagenesis were synthesized at the Institute for Molecular Biology and Biotechnology, McMaster University.

N96Q (5'-GGTGCCTGT**CAA**GATACCCTC-3')

N135Q (5'-CGAAAAGCC**CAG**AAATCCTCC-3')

N155Q (5'-CTTAACTTC**CAA**GAGACCTAT-3')

N192Q (5'-TGGATCTCC**CAG**AAGACGGAG-3')

2.1.10 Protein Standards

The low range prestained protein molecular weight standards (KDa) used for molecular mass determination on SDS-PAGE were purchased from BioRad Labs (Oakville, ON). They included: 112 KDa, rabbit muscle phosphorylase b; 84 KDa, bovine serum albumin; 53.2 KDa, ovalbumin; 34.9 KDa, carbonic anhydrase; 28.7 KDa, soybean trypsin inhibitor; and 20.5 KDa, lysozyme.

2.1.11 Antibodies

Sheep anti-rabbit AT antibody, polyclonal (IgG) was prepared by Mr. M. Kulczyky in Dr. Blajchman's laboratory. This antibody was used as the primary antibody in Western blotting and in immunoprecipitation. This IgG was biotinylated in accordance with the manufacturer's instruction. The biotinylated IgG was used in the ELISA.

The affinity-purified rabbit anti-sheep IgG (H+L)-alkaline phosphatase (AP) conjugate served as the secondary antibody in Western blotting was from Zymed Laboratories (Burlington, CA). S&S NC^{TM} nitrocellulose was purchased from Schleicher & Schuell (Keene, NH).

2.1.12 Other Biological Materials

Human α-thrombin (>3300 NIH units/mg; >93% active as determined by active-site titration) was provided by Dr. J. Fenton (New York State Division of Biologicals, Albany, NY). DNA sequencing (^{T7}Sequencing^{TM}) kit, adenosine 5'-triphosphate (ATP), CNBr-activated Sepharose 4B, Hitrap^{R} heparin affinity columns, Heparin-Sepharose^{R} CL-6B, Q-Sepharose^{R} fast flow, and Sephaglas^{TM} BandPrep kit were purchased from Pharmacia Biotech (Baie d'Urfe, QC). QIAGEN^{R} plasmid DNA isolation kits were purchased from Qiagen (Chatsworth, CA). The thrombin inhibitor D-phenylalanyl-L-propyl-arginine chloromethyl ketone (PPACK), and Ominisorb^{TM} cells were purchased from Calbiochem (La Jolla, CA). Lipofectin^{R} reagent was purchased from Canadian Life Technologies, Inc. (Burlington, ON). The DIG Glycan Differentiation Kit was from Boehringer Mannheim Canada (Mississauga, ON). Alkaline phosphatase conjugated rabbit anti-sheep IgG was from Jackson Labs (Bar Harbour, ME). Recombinant

endoglycosidase F (PNGase F) was from New England Biolabs (Beverly, MA). The oligonucleotide-directed *in vitro* mutagenesis system was purchased from Amersham (Oakville, ON). The 1 Kb DNA ladder suitable for sizing linear ds DNA fragments from 500 bp to 12 Kb was a Gibco BRL product. The chromogenic substrate S-2238 was purchased from Chromogenix (Molndal, Sweden). IODO-GEN™ Iodination Reagent was purchased from Pierce (Rockford, IL, USA). Rabbit plasma AT was purified from rabbit plasma as described by Miller-Anderson *et al.* (Miller-Anderson et al, 1974).

2.1.13 Animals

Healthy male New Zealand White rabbits whose weight ranged from 2.5 to 3.3 Kg were used. The rabbits were supplied by Maple Lane Rabbits (Clifford, ON).

2.1.14 Apparatus

Precision pipettes (Pipetman P20, P200, P1000) were purchased from Gilson through Mandel Scientific. Accumet™ pH meter model 620 was from Fisher Scientific (Pittsburgh, PA). Sorvall™ RC-5 superspeed refrigerated centrifuge and Sorvall™ RT6000B refrigerated centrifuge were from DuPont Canada. Eppendorf® micro centrifuge model 5415C was from Brinkmann (Mississauga, ON). Hoefer HE 33 mini and Hoefer HE 99X max submarine electrophoresis units were from Pharmacia. Fotodyne™ transilluminator Foto/prep I and Fotodyne™ Polaroid camera were purchased through Bio/Can Scientific. Model S2 sequencing gel electrophoresis apparatus was a Gibco BRL product. Electrophoresis constant power supply ECPS 3000/150 was from Pharmacia. Model 583 gel dryer was from Bio-Rad. A Mini-Protein II electrophoresis cell suitable for SDS-polyacrylamide gel electrophoresis (SDS-PAGE)

with discontinuous buffer system and mini trans-blot electrophoretic transfer cell for transfer of proteins from SDS-polyacrylamide gel to solid support were from Bio-Rad. Electrophoresis power supply EC-105, used for agarose and SDS-polyacrylamide gel electrophoresis as well as protein transfer, was purchased through Mandel Scientific. Prep/Scale^{TM}-TFF 1 ft^2 cartridges (PLTK 30K ultrafiltration membrane) and MasterFlex^R industrial/process Easy-Load^R pump were from Millipore (Mississauga, ON). Peristaltic pump P-1, fraction collector, and Gradient mixer GM-1 were from Pharmacia. Fluorescence measurements were made on a luminescence spectrometer LS 50 from Perkin Elmer (Mississauga, ON) and was made available for use by Dr. V.S. Ananthanarayanan (McMaster University). Radioactivity measurements were performed on a Beckman Model 5500 gamma count (Beckman Instruments, Palo Alto, California).

2.2 Site-Directed Mutagenesis and DNA Sequencing

2.2.1 Preparation of Single-Stranded Phagemid DNA

A fresh culture of *E.coli* DH5α cells harbouring the phagemid pGEM3zf(+)-AT was grown in 4 ml of LB medium containing 100 μg/ml ampicillin at 37°C with vigorous shaking (220 rpm). The cells were then diluted 100-fold in 50 ml of TYP medium [1.6% (w/v) bacto-tryptone, 1.6% (w/v) bacto-yeast extract, 0.5% (w/v) NaCl, 0.25% K_2HPO4, pH 7.5] containing 20 mM glucose and 100 μg/ml ampicillin. The cells were grown at 37°C with vigorous agitation to an OD_{550} of 0.05. At this time, M13K07 helper phage was added to the cell cultures at a ratio of phagemid to phage particles of 20:1. After incubation at 37°C with shaking for 1 hour, kanamycin was then added at a

final concentration of 75 μg/ml. The addition of kanamycin inhibits the growth of the *E.coli* DH5α cells but allows growth of the cells infected with M13K07 helper phage. The cell culture was then grown overnight at 37°C with vigorous shaking.

The overnight culture were transferred to a sterile 50 ml centrifuge tube (Nalgene) and centrifuged at 4°C in an SS34 rotor at 12,000 X g for 10 minutes. The supernatant containing the phagemid particles was transferred to another 50 ml centrifuge tube and centrifuged at 4°C at 15,000 X g for an additional 15 minutes to pellet remaining cells and cellular debris. The supernatant was then transferred to a 50 ml capped conical tube (Falcon) and incubated at room temperature for 30 minutes in the presence of RNase at a final concentration of 10 μg/ml. After the RNase treatment, 0.25 vol of a 20% (w/v) PEG/2.5 M NaCl solution was added to the supernatant and the tube was placed at 4°C overnight with rocking. The supernatant was transferred to a 50 ml centrifuge tube and centrifuged at 15,000 X g for 20 minutes at 4°C to pellet the phagemid particles. The supernatant was carefully drained off and the phagemid pellet was allowed to air dry. The phagemid pellet was then resuspended in 0.5 ml of 10 mM Tris-HCl (pH 8.0), 1 mM EDTA (pH 8.0) and transferred to a 1.5 ml microcentrifuge tube.

The resuspended phagemid particles were subsequently extracted with 1 volume of phenol once, with 1 volume of phenol:chloroform:isoamyl alcohol (25:24:1) twice, and 1 vol of chloroform:isoamyl alcohol (24:1) for five times. The phagemid DNA was then precipitated in 0.1 volume of 7.8 M NH_4OAc solution and 2.5 volumes of ice-cold absolute ethanol. The reaction mixture was incubated at -70°C for 1-2 hours and

centrifuged at 14,000 rpm for 15 minutes at 4°C. The phagemid pellet was washed once with ice-cold 70% ethanol, dried in a SpeedVac concentrator, resuspended in 50 µl of 10 mM Tris-HCl (pH 8.0), 1 mM EDTA (pH 8.0) and stored at -20°C. The single-stranded phagemid DNA was then routinely used for site-directed mutagenesis.

2.2.2 Site-Directed Mutagenesis of Rabbit AT cDNA

In vitro site-directed mutagenesis was adapted from the method of Taylor et al. (1985) using the reagents and protocol as outlined in the Amersham mutagenesis kit and shown in Figure 2.2. Greater than 60% success rate was achieved using this method.

Approximately 5µg of single-stranded DNA template [derived from the pGEM-3Zf(+)-AT constructs] was annealed to 10-20 pmol of phosphorylated mutant deoxyoligonucleotide in 17 µl annealing buffer [20 mM Tris-HCl (pH 7.4), 2 mM $MgCl_2$, 50 mM NaCl, 1mM DTT]. The reaction mixture was heated to 70°C for 3 minutes and allowed to cool down to 37°C in the water bath. The synthesis and ligation of the mutagenic DNA strand was accomplished by adding $MgCl_2$ to a final concentration of 12 mM, 6 U of Klenow fragment, 6 U of T4 DNA ligase and a dNTP mix containing dCTPαS instead of dCTP. After overnight incubation at 14°C, the remaining unconverted single-stranded DNA was removed by centrifugation of the reaction mixture through a nitrocellulose filter unit which binds to the unwanted single-stranded DNA. The double-stranded DNA mixture was then precipitated in 0.1 vol 3 M sodium acetate (pH 5.2), 2.5 vol of ice-cold absolute ethanol and pelleted by centrifugation. After washing with ice-cold 70% ethanol, the double-stranded DNA solution was nicked with 5 U of Nci I and

Figure 2.2 Oligonucleotide-directed *in vitro* mutagenesis system.

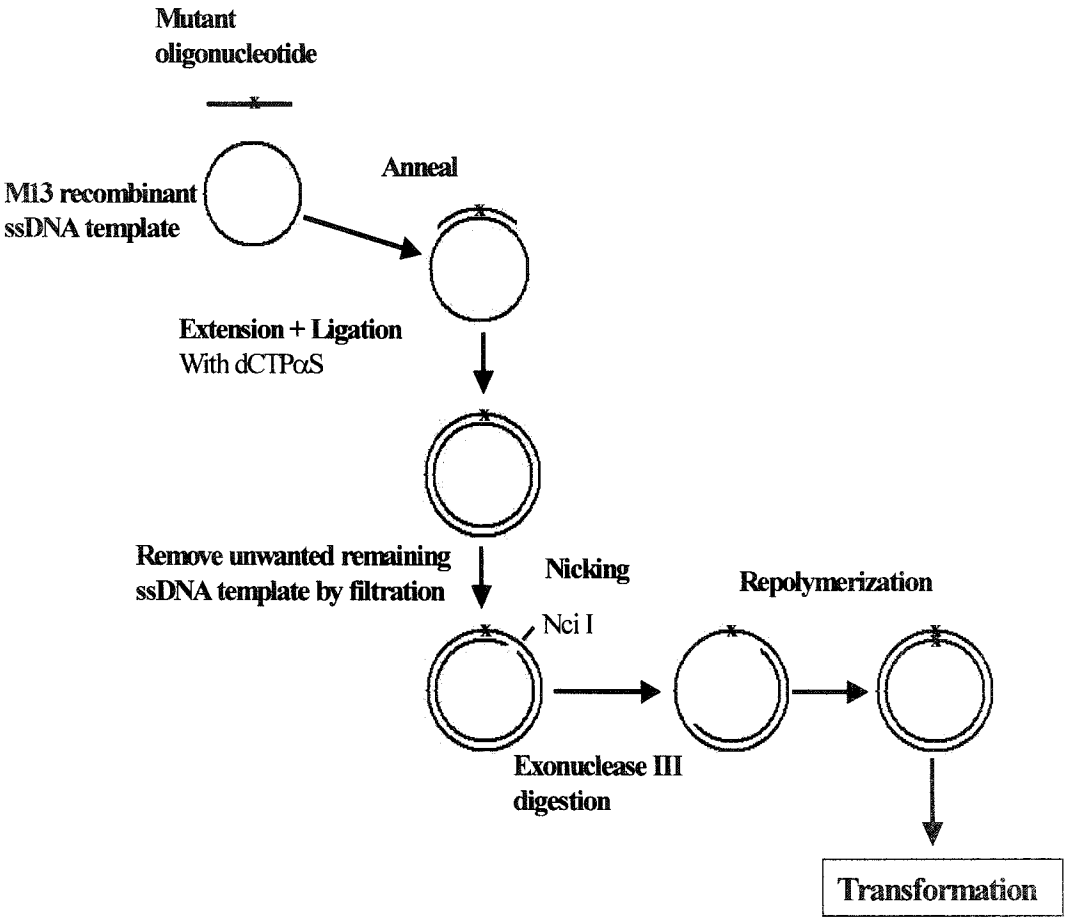
Mutant
oligonucleotide
M13 recombinant
ssDNA template
Anneal
Extension + Ligation
With dCTPαS
Remove unwanted remaining
ssDNA template by filtration
Nicking
Nci I
Repolymerization
Exonuclease III
digestion
Transformation

the non-mutant strand was digested with 50 U of Exo III for 15 minutes at 37°C. Repolymerization and ligation of the gapped DNA heteroduplex was accomplished by adding $MgCl_2$ to a final concentration of 5 mM, 3U T4 DNA polymerase I, 2U T4 DNA ligase and a dNTP mix with dCTP instead of dCTPαS. The reaction mixture was allowed to incubate at 14°C for 4 hours. Finally, 3 μl of the reaction mix was used to transform *E.coli* DH5α cells.

2.2.3 DNA Sequencing

To confirm the introduction of the desired mutations in rabbit AT cDNA, regions of interest were sequenced using the ^{T7}Sequencing^{TM} kit, based on the dideoxy sequencing method of Sanger *et al.*(1977). Double-stranded plasmid DNA templates were obtained as described below. Prior to sequencing, 3 to 5 μg of the double-stranded plasmid DNA was denatured by adding denaturing buffer [0.2 M NaOH, 0.2 mM EDTA (pH 8.0)]. The mixture was then incubated at 37°C for 15 minutes. The denatured DNA was precipitated by the addition of 0.1 vol of 3 M NaOAc (pH 5.2) and 2.5 vol of ice-cold absolute ethanol, followed by incubation at -70°C for 1-2 hours. The denatured DNA was recovered by centrifugation at 14,000 rpm for 15 minutes at 4°C. After the supernatant was carefully drained off, the DNA pellet was washed once with 70% ethanol, dried in a SpeedVac and resuspended in 7 μl of sterile distilled water. DNA sequencing was then carried out by the modified T7 DNA polymerase method using the ^{T7}Sequenase^{TM} kit with specific internal AT primers based on previous sequencing information. The sequencing reactions were then boiled for 2 minutes, quick cooled on

ice and loaded onto a pre-run sequencing gel which was prepared by mixing the following reagents to obtain a final concentration of 8% (w/v) acrylamide [acrylamide stock solution containing 38% (w/v) acrylamide and 2% (w/v) BIS, 1X TBE (0.089 M Tris-HCl, 0.089 M boric acid, 0.002 M EDTA (pH 8.0) and 8 M urea]. The sequencing gel was overlaid with 1X TBS and run using a BRL sequencing gel electrophoresis system (model 50) at a constant power of 50 W for approximately 4 h. After electrophoresis, the sequencing gel was transferred to Whatman 3 mm chromatography paper and dried under vacuum at 80°C for 2 hours on a Bio-Rad slab gel dryer. The dried gel was then exposed to Kodak X-Omat XK-1 film at room temperature overnight.

2.3 Construction of Mammalian Expression Plasmids

This section describes the experimental procedures used to synthesize the mammalian expression vectors. Authenticity of each mutation was confirmed by double-stranded DNA sequencing using the modified T7 polymerase method.

2.3.1 Transformation of *E.coli* Cells with Plasmids

E.coli DH10B^{TM} and DH5α competent cells were transformed with plasmid DNA or ligation mixture according to the manufacture's protocol. An aliquot containing 50 µl of competent *E.coli* cells was removed from a -70°C freezer and thawed on ice for 30 minutes. Approximately 1 to 10 ng of plasmid DNA or 20 ng of ligation reaction were added to the cells and incubated on ice for 30 minutes. The cells were then heat shocked by incubation at 37°C for 20 seconds and placed on ice. After 5 minutes, 0.95 ml of room temperature LB medium was gently added and the cell suspension was incubated for 1 h

at 37°C with shaking (225 rpm). The cells were then pelleted by centrifugation for 5 seconds and the supernatant was carefully drained off. The cells were resuspended in 100 µl of LB medium. The cell suspension was spreaded onto two LB plates containing 100 µg/ml ampicillin with 10 µl and 90 µl of solution respectively. The plates were incubated overnight at 37°C. Following characterization, the desired individual transformants were cultured in LB broth and stored at -70°C in the presence of 20% glycerol.

2.3.2 Extraction and Purification of Plasmid DNA

Plasmid DNA used for sequencing, restriction enzyme digestion analysis, transformation and subcloning was prepared using a modified alkaline lysis miniprep method (Zhou *et al.* 1990). Bacterial cells harbouring the plasmid of interest were grown overnight in 3 ml of LB medium containing 100 µg/ml ampicillin in 37°C with vigorous shaking. The bacterial cells were then transferred to 1.5 ml sterile microcentrifuge tubes and harvested by centrifugation at 12,000 rpm for 1 minute in an Eppendorf microcentrifuge. The supernatant was removed by aspiration and the bacterial pellet was resuspended in 100 µl of LB medium. 300 µl of a freshly prepared alkali solution TENS [10 mM Tris-HCl, 1mM EDTA, 0.1N NaOH, and 0.5% (w/v) SDS] was added to the resuspended cells, followed by the addition of 150 µl 3.0 M NaOAc (pH 5.2). Cell debris and chromosomal DNA were removed by centrifugation, and the supernatant was transferred to a fresh tube, and mixed with 0.9 ml of 100% ethanol which had been precooled to -20°C. Plasmid DNA and RNA were then pelleted by centrifugation. The pellet was washed twice with 1 ml of 70% ethanol, dried under vacuum, and resuspended

in 20 μl of TE buffer [10 mM Tris-Cl, 1 mM EDTA, pH 8.0] containing 25 μg/ml of RNase.

Plasmid DNA used for transfecting mammalian cells was prepared using the QIAGEN^{R} plasmid kit. *E coli* DH10B^{TM} competent cells transformed by wild-type and mutant recombinant pCMV5 plasmids, were cultured overnight in 125 ml of LB medium containing 100 μg/ml of ampicillin. After harvesting and resuspension, the cells were lysed in NaOH/SDS, in the presence of RNase A. The lysate was neutralized by the addition of acidic potassium acetate and precipitated debris was removed by high speed centrifugation. The supernatant was then applied to a pre-equilibrated QIAGEN-tip by gravity flow. Plasmid DNA bound to QIAGEN anion-exchange resin under appropriate low salt and pH conditions, while degraded RNA and cellular proteins were not retained on the resin. The QIAGEN-tip was then washed with 1M NaCl and the bound DNA was eluted from the QIAGEN-tip with elution buffer. Finally, the eluted plasmid DNA is desalted and concentrated by isopropanol precipitation, and resuspended in 100 μl of TE buffer.

2.3.3 Analysis of Nucleic Acids

Techniques and protocols used for analysis of nucleic acids were carried out according to either the product data sheets, the methods of Maniatis *et al.* (1982), or Current Protocols in Molecular Biology (Ausubel *et al.*, 1992). All standard buffers and reagents are also described from these sources. The information presented in this section

represents an overview of experimental procedures combined with additional modifications.

2.3.3.1 Gel Preparation and Electrophoresis of DNA

Gel preparation and electrophoresis of DNA was performed essentially as described by Maniatis et al. (1982). Agarose gels were prepared by heating a 1 % electrophoresis grade agarose in 1X TAE (40 mM Tris-acetate, 1mM EDTA, pH 8.0). Once all the agarose had dissolved, the solution was cooled to 50°C and the fluorescent dye EtBr was added to a final concentration of 0.5 μg/ml. The melted agarose mixture was cast in gel trays (containing sample well combs). DNA samples were prepared in gel loading dye [0.25 % (w/v) bromophenol blue, 0.25% (w/v) xylene cyanol, 40% (w/v) sucrose] and loaded into the pre-formed wells. The gel was electrophoresed in 1X TAE at 60 V for 1-2 h. The separated DNA bands were visualized and photographed.

2.3.3.2 Recovery of DNA Fragments From Polyacrylamide

Extraction of individual DNA bands from agarose gels following electrophoresis was carried out using Sephaglas^{TM} BandPrep kit (Pharmacia) as instructed by the manufacturer (Baie d'Urfe, QC). After electrophoresis, the agarose slices containing the DNA fragments were excised and chopped into small pieces using a sterile razor blade. The agarose pieces were placed in a 1.5 ml microcentrifuge tube and was solubilized in sodium iodide. Sephaglas^{TM} BandPrep was added to allow the binding of the DNA fragment. The matrix-bound DNA was then washed with an ethanol based buffer and allowed to air-dry. Finally, the DNA was recovered from the dry matrix in an elution buffer of low ionic strength. The resulting DNA was ready for further manipulation.

2.3.3.3 Quantitation of Nucleic Acids

The concentration of nucleic acid was determined by spectrophotometric measurement of the amount of ultraviolet (UV) irradiation absorbed by the base. A 1 to 10 μl of the DNA sample was diluted to 1 ml in dd H_2O, and the optical density (OD) reading were taken at 260 nm and 280 nm. The nucleic acid concentration was then determined based on the assumption that an OD_{260} of 1 corresponded to approximately 50 μg/ml double-stranded DNA and 40 μg/ml for single-stranded DNA and RNA (Sambrook et al., 1989a). Ratios between the reading at 260 nm and 280 nm (OD 260/OD280) provided an estimate of sample purity.

2.3.4 Construction of AT Expression Plasmid in pCMV5

To create AT mammalian expression constructs, the wild type and four mutant variants of rabbit AT cDNA were liberated from their plasmid backbone pGEM3Zf(+) by using EcoRI, and introduced into the EcoRI site of pCMV5. To generate these constructs, pGEM3Zf(+)-AT and pCMV5 plasmids were initially digested with EcoRI. Such restriction enzyme digestions linearized pCMV5 and released the AT cDNA insert from its plasmid backbone pGEM3Zf(+). The excised AT cDNA and pCMV5 were purified using SephaglasTM BandPrep Kit as described above, and joined together by T4 DNA ligase to assemble the pCMV5-AT constructs. Ligation was carried out at 16°C overnight in One Phor All^R buffer supplemented with 1 mM ATP. An aliquot of the ligation reaction mixture was then used to transform *E.coli* DH10B cells. The desired insert with the correct orientation was first selected by restriction enzyme mapping and

then confirmed by DNA sequencing analysis. The resulting expression plasmid were designated pCMV5-AT-WT and pCMV5-AT-N, where N represents the location of the mutagenic oligonucleotide. Four mutant variants were obtained which included AT-N96Q, AT-N135Q, AT-N155Q, and AT-N192Q.

2.4 Expression of AT in Mammalian Cells

2.4.1 Expression of AT in COS Cells

Wild-type (AT-WT) and the mutant variants of rabbit AT moieties were transiently expressed in COS-1 cells. To express the AT-WT and mutant variants of AT, COS-1 cells were transfected with various pCMV5 mammalian expression constructs, respectively. Transfection was carried out by employing a liposome mediated technique using lipofectin^R reagent. COS-1 cells were maintained in DUL media (Dulbeco's minimal essential medium) containing 10% fetal bovine serum, 100U/ml of penicillin and 100μg/ml streptomycin. Transfection was initiated when the cells reached 80 to 90% confluence. The cells were washed twice with sterile PBS. For a 100 mm tissue culture plate, transfection was conducted in 4 ml of serum-free DUL media containing 20μg of DNA and 100 μg of lipofectin^R reagent. The cells were incubated at 37°C for 18 hours when the DNA-containing medium was replaced by 10 ml of DUL medium containing 10% fetal bovine serum. Forty-eight hours after the transfection, the cells were metabolically radiolabeled with [^{35}S]-methionine in methionine-deficient Eagle's modified minimum essential medium. To increase the efficiency of incorporation of the radiolabeled methionine, the intracellular pools of these amino acids were depleted by

maintaining cells in Met and Cys deficient D-MEM media for 30 minutes. The starved cells were then washed with PBS and incubated with 5 ml of Met and Cys deficient medium supplemented with 200 μCi of ^{35}S-labeled Met and Cys for 3 hours. The conditioned media of the radiolabeled cells was then harvested and clarified by centrifugation, aliquoted, and frozen at -70°C for further analysis.

2.4.2 Establishment of Permanent AT Producing CHO Cell Lines

2.4.2.1 Transfection of CHO Cells: To establish permanent cell lines that could produce AT, AT-WT and mutant forms of pCMV5-AT expression plasmids were cotransfected with a neomycin resistant plasmid (pSV2Neo) into the CHO cells using the lipofectin^{R} reagent. CHO cells were maintained in α-MEM media containing 10% fetal bovine serum, 100 U/ml of penicillin, and 100 μg/ml of streptomycin. Transfection was performed when cells were 30% to 50% confluent. For each 100 mm tissue culture plate, co-transfection was conducted in 4 ml of serum-free α-MEM media containing 100 μg of lipofectin^{R} reagent, 25 μg of pCMV5-AT expression plasmids and 2 μg of the neomycin resistant plasmid (pSV2Neo). The cells were then incubated at 37°C for 18 hours when the DNA containing medium was replaced by 10 ml of α-MEM medium containing 10% fetal bovine serum (Kaufman, 1990).

2.4.2.2 Selection of AT Producing CHO Cells: Twenty-four hours after the transfection, the cells were subcultured 1:10 into α-MEM media containing 1mg/ml of geneticin (G418), 10% fetal bovine serum, 100 U/ml of penicillin and 100 μg/ml of streptomycin. After 10 days, viable colonies resistant to G418 were isolated using a glass

cylinder. Briefly, the sterilized cylinder was glued to the plate around the colony to be picked up. The cells within the cylinder were detached by incubated with trypsin for 2 minutes and then transferred to a well in a 24-well tissue plate. Cells from each well were transferred to a 60-mm plate. These transfected cells were then cultured using the selection concentration of geneticin at 250 μg/ml. To screen for their AT production levels, the cells were incubated in serum free medium for 24 hours and the conditioned medium was assayed for AT by an enzyme-linked immunosorbent assay (ELISA) using sheep anti-rabbit AT antibody (IgG). Of the G418 resistant clones tested, 65% of them secreted AT into the culture medium. The expression rates of these clones ranged from 0.02 μg to 15 μg of AT/10^6 cells/24 hours. The clones secreting from 1 μg to 15 μg of AT/10^6/24 hours were chosen and stored in liquid nitrogen in α-MEM medium in the presence of 20% FBS and 10% DMSO.

2.4.2.3 Propagation of AT Producing CHO Cells: AT producing CHO cell lines were grown in α-MEM media containing 250 μg/ml of G418, 10% fetal bovine serum, 100 U/ml of penicillin and 100 μg/ml of streptomycin in 100 mm plates. Cells from two such plates were transferred into five 150-mm plates. When cells reached 90-95% confluent, they were washed with PBS, detached by trypsinization, and collected by centrifugation. Approximately 5X10^8 cells were rinsed with PBS and then transferred to 500 ml suspension tissue culture bottle (Cytostir). The cells were fed with 400 ml of serum-free α-MEM media supplemented with 100 U/ml of penicillin and 100 μg/ml of streptomycin, and stirred at 30 rpm in suspension. Forty-eight hours later, the conditioned

media were harvested by centrifugation to pellet the cells. The supernatants were stored at -20°C for further purification.

2.4.2.4 Pulse-Chase Studies in AT Producing CHO Cell Lines: To evaluate the secretion and intracellular transportation of newly synthesized AT, the clones producing wild-type and mutant variants of AT were used for pulse-chase experiments. 4 X 10^5 AT producing CHO cells were transferred to a 60 mm tissue culture plate and allowed to grow overnight in α-MEM media containing 10% fetal bovine serum, 250 μg/ml of G418, 100 U/ml of penicillin and 100 μg/ml of streptomycin. The cells were washed with PBS twice and once with α-MEM media lacking methionine and cysteine. The cells were then starved for methionine and cysteine for 30 minutes by maintaining in methionine- and cysteine- deficient α-MEM media. At this point, the starved cells were washed once with methionine and cysteine deficient α-MEM media and fed with 200 μCi/ml of ^{35}S-methionine and ^{35}S-cysteine. The cells were pulse labeled for 30 minutes. The medium was then removed and replaced with complete α-MEM media. At 15 min, 30 min, 60min, 2h, 4h, 6h, 8h, 10h, and 12h after pulse labeling, conditioned media were harvested from individual plates and clarified by centrifugation and the cells were rinsed once with PBS and lysed in situ with radioimmune precipitation (RIPA) buffer supplemented with Triton X-100 to a final concentration of 2% (v/v). Cell debris was pelleted by centrifugation and the cleared cell extracts were transferred to a fresh tube and stored at -20°C for further analysis. Conditioned media and cell extracts were

immunoprecipitated using a sheep anti-rabbit AT antibody, and a commercially available preparation of heated-inactivated protein A-bearing *Streptococcus* cells.

2.4.2.5 Analysis of Radiolabeled AT by Immunoprecipitation: Immuno-precipitation coupled with SDS-PAGE was used to detect and analyze radioactive AT produced from both COS-1 and CHO cells. Immunoprecipitation was performed by using the method of Dorner (Dorner and Kaufman, 1990), and employed a sheep anti-rabbit AT IgG. 300µl of conditioned medium or 100µl of cell extract was incubated with 3µg of the antibody (IgG) in 1ml of 1X radioimmune precipitation (RIPA) buffer consisting of 150 mM NaCl, 20 mM Tris (pH 7.5), 0.5 mM EDTA, 0.1% (w/v) sodium deoxycholate, 1% (v/v) Triton X-100, 1 mM phenylmethanesulphonyl fluoride (PMSF), and 1 mg/ml soybean trypsin inhibitor at 4°C for overnight (Norner and Kaufman, 1990). The antigen-antibody complex was precipitated by incubation with 100µl of the 10% Omnisorb^{TM} cell suspension pre-equilibrated with Tris-buffered saline (TBS) [20 mM Tris-CL, 150 mM NaCl, (pH 7.4)] for 2 hours at 4°C. Cell-bound immune complexes were pelleted by centrifugation and the cells were washed sequentially with 1 ml of 1X RIPA buffer three times, TBS twice, and dd H_2O once. The cells were then suspended in 50 µl of 4X SDS-PAGE sample buffer containing DTT [10 mM Tris-Cl (pH 6.8), 1 mM EDTA, 5% (w/v) SDS, 10% glycerol, 0.025% (w/v) bromophenol blue, 200 mM DTT]. The protein associated with cells were denatured by heating to 100°C for 3 minutes. Subsequently, the cells, which had served as the immunoabsorbent, were removed by centrifugation. The samples were analyzed by SDS-PAGE under reducing conditions followed by

autoradiography. Phospho-imager analysis was used to quantitate the autoradiographic images.

2.4.2.6 Sodium Dodecyl Sulphate-Polyacrylamide Gel Electrophoresis: One dimensional sodium dodecyl sulphate-polyacrylamide gel electrophoresis (SDS-PAGE) was performed using the Bio-Rad Mini-PROTEIN II dual slab cell system. All electrophoretic runs were done using the discontinuous buffer system in vertical gels that were composed of an upper stacking gel and a lower resolving gel. Resolving gels were prepared by combining the following reagents to obtain a final concentration of 10% (w/v) acrylamide [acrylamide stock solution (29.2% (w/v) acrylamide and 0.8% (w/v) BIS), 0.375 M Tris-HCl (pH 8.8), 0.1% (w/v) SDS, 0.05% (w/v) APS, 0.05% (w/v) APS and 0.05% (v/v) TEMED]. To ensure an even surface, the resolving gel was overlaid with isopropyl alcohol until polymerization was completed. The stacking gel was prepared by mixing the following components to obtain a final concentration of 3% (w/v) acrylamide [acrylamide stock solution same as resolving gel, 0.125 M Tris-HCl (pH 6.8), 0.1% (w/v) SDS, 0.5% (w/v) APS and 0.1% (v/v) TEMED].

Samples subjected to electrophoretic analysis were prepared under reducing conditions essentially as described by Bulleid and Freedman (1988). Samples were mixed with 3 volumes of 4 x SDS-PAGE sample buffer containing DTT [20 mM Tris-Cl, (pH 6.8), 2 mM EDTA, 10% (w/v) SDS, 20% (w/v) glycerol, 0.05%(w/v) bromophenol blue, 400 mM DTT], and heated at 100°C for 5 minutes. The samples were then added to their respective wells, overlaid with 1X electrophoresis gel running buffer [0.30% (w/v) Tris-

base, 1.44% (w/v) glycine, 0.1% (w/v) SDS, pH 8.3)] and electrophoresed at 200V until the tracking dye migrated to the bottom of the gel which took approximately 45 minutes.

After electrophoresis, gels were fixed and stained by soaking in staining solution [35% (v/v) methanol, 10% (v/v) glacial acetic acid, 0.05%(w/v) Coomassie brilliant blue R-250] for 1-2 hour at room temperature with shaking. Gels were then destained in destaining solution [35% (v/v) methanol, 10% (v/v) glacial acid] and then dried on Whatman #3 chromatography paper using a Bio-Rad slab gel dryer at 80°C for 1 h.

When fluorographic treatment was indicated for ^{35}S- radiolabeled samples, following electrophoresis the gel was soaked in destaining solution for 30 minutes to fix the protein. The gels were washed with distilled water once and then transferred into Amplify™ for 15 minutes. The gel was then dried on the gel dryer with the temperature reduced to 70°C so as not to destroy the fluor. The gel was then exposed to X-ray film (Kodak Z-Omast XAR-1 or XK-1) at -70°C for an appropriate length of time for autoradiography.

2.4.2.7 Western Immunoblot Analysis: Following SDS-PAGE, the gel was equilibrated in 500 ml of transfer buffer (25 mM Tris, 192 mM glycine, pH 8.3) for 30 min at room temperature, and the transfer apparatus was assembled according to the method described by Sambrook et al (1989b). Electrotransfer was accomplished using an LKB transfer chamber at 400 milliamps for 3 hours at 4°C. Immediately following transfer, the nitrocellulose membranes to be probed with the sheep anti-rabbit AT antibody were incubated in Blotto (5% dry skim milk powder in TBS) for 1 h at room

temperature to saturate nonspecific binding sites on the membrane followed by three washes with TBS-T. The membrane was then incubated with primary antibody, the sheep anti-rabbit AT IgG, at the final concentration of 10μg/ml in 15 ml of Blotto, at room temperature for 1 h. Following the incubation and three washes for 15 minutes each in TBS-T, the membrane was then incubated with the second antibody, AP-rabbit anti-sheep IgG. After three washes with TBS, the AT proteins which were immobilized on the nitrocellulose and probed by the antibodies were then visualized by incubating the blot with chromogenic substrate mixture [33 μg/ml BCIP and 60 μg/ml NBT] in 10 ml of AP buffer [100 mM Tris-Cl (pH 9.5), 100 mM NaCl, 5 mM $MgCl_2$] for 5-15 min at room temperature in dark (Sambrook et al., 1989b).

2.4.2.8 Quantitation of AT by an ELISA: An ELISA was performed to quantitate rabbit AT. For each experiment, each polystyrene microtiter plate well was coated with the sheep anti-rabbit AT IgG by incubating 1μg of this IgG in coating buffer [100 mM Na_2CO_3, pH 9.6] at 4°C for overnight. The unbound IgG was removed by washing plates with TBS-T [10 mM Tris-Cl, 0.526 mM NaCl, 0.05% Tween-20, pH 7.4] three times. Each well was then incubated with 200 μl of Blotto [1% skim milk powder in TBS-T] for 1 h at room temperature to block nonspecific binding sites. The coated wells were then incubated either with samples to be tested or with standard rabbit plasma AT in triplicate. The concentration of the AT standard ranged from 5 ng/ml to 250 ng/ml. After three washes with TBS-T, each well was incubated with 100 ng of the biotinylated sheep anti-rabbit AT IgG in TBS-T+BSA [1% BSA in TBS-T] at 37°C for 1 h. Each well was

then washed three times with TBS-T and incubated with streptavidin-AP (diluted 1/5000 in TBS-T+BSA) for 1 h at 37°C. Following three subsequent washes, 100 μg PNPP in DEA substrate buffer [1 M DEA, 0.5 mM $MgCl_2$, pH 9.8] was added. After an one hour incubation in the dark at room temperature, the colour reaction was stopped by adding 30 μl of 100 mM NaOH to each well. Finally, the OD reading of each well was taken at 405 nm by an ELISA plate reader. The data obtained were analyzed by Minitab™ (version 8.0), and the standard curve was generated. The AT concentration of the sample tested was calculated based on a standard curve obtained from AT standards which was run on each plate.

2.5 Purification of Recombinant AT From CHO Cell-Derived Media

2.5.1 Affinity Chromatography of Recombinant AT on Heparin-Sepharose

Recombinant AT proteins produced by CHO cell lines were purified from the conditioned media by affinity chromatography using a heparin-Sepharose column, Hitrap®. Three liters of conditioned media were concentrated to 100 ml using a Prep/Scale-TFF Cartridge with PLTK ultrafiltration membrane with a molecular weight cut-off of 30 KDa (Millipore). The concentrated media was clarified by centrifugation and applied to a heparin-Sepharose column (1X3 cm, HitrapR) equilibrated with 0.02 M Tris-Cl buffer (pH 7.4) containing 0.15 M NaCl at a flow rate of 0.5ml/min. The column was then washed thoroughly with TBS buffer until the OD_{280} reading reached 0 (usually approximately 50 ml of TBS buffer). The bound proteins were then eluted with a linear gradient from 0.15 M NaCl to 3 M NaCl in TBS buffer in a gradient mixer. The AT recovery rate was initially determined spectrophotometrically by absorption

measurements at $OD_{280\,nm}$ with the use of specific absorption coefficient of 0.65 $\cdot g^{-1} \cdot cm^{-1}$ and a molecular weight of 58,000 Dalton (Nordenman *et al.*, 1977). Two major peaks were observed based on the OD_{280} reading. Fractions from peak 1 and 2 were pooled separately and each dialyzed against TBS buffer. The samples from each peak were analyzed on SDS-PAGE followed by Coomassie Blue staining, Western immunoblot and ELISA, which showed that the second peak containing purified recombinant rabbit AT.

2.5.2 Ion-Exchange Chromatography Using Q-Sepharose

In order to further purify recombinant AT from the conditioned media and to remove any possible contaminating free heparin in the preparation, the fractions from the second peak were pooled and dialyzed against TBS buffer (0.02M Tris-Cl, 0.15 M NaCl) overnight at 4°C. The pooled fraction was then loaded to a Q-Sepharose column (1X3 cm) previously equilibrated with TBS buffer (pH 7.4). The flow-through fraction was collected and the column was washed with 3 volumes of the equilibrating buffer. The column was then eluted stepwise with 0.02 M Tris-Cl containing NaCl in concentrations of 0.3M, 0.5M, 1M, and 2M. The flow-through and the wash fractions were collected and pooled. The resultant fractions were dialyzed against TBS buffer and subjected to electrophoresis on SDS-PAGE gel under reducing conditions followed by Coomassie Blue staining and Western immunoblot analysis. The result showed that the AT was in the flow-through fraction and washing fractions. The final reparation of purified AT was concentrated and stored at -20°C for further characterization.

2.6 *In vitro* Functional Characterization of Recombinant AT

2.6.1 Preparation of High Affinity Heparin

High affinity heparin was isolated through affinity chromatography on an AT-Sepharose column. The AT column was prepared by coupling 140 mg of AT to 4 g CNBr-activated Sepharose 4B in 14 ml of TBS for 2 hours at room temperature. The Sepharose was then packed to a column at 4°C for overnight. The column was equilibrated with TBS buffer. 150 mg of standard heparin sodium salt was dissolved in 1 ml of TBS buffer and applied onto the pre-equilibrated AT-Sepharose column (2x5 cm). The column was washed thoroughly with 200 ml of TBS buffer, and the bound heparin was eluted with TBS containing 2.0 M NaCl. The heparin concentration in each fraction was determined by a protamine sulphate assay. The heparin-containing fractions were pooled and dialyzed against 4 L of TBS overnight at 4°C. After dialysis, the heparin concentration was determined again by the protamine sulphate assay and the final preparation was kept at 4°C.

2.6.2 Thrombin-AT Complex Formation

To evaluate the thrombin inhibitory activity of the recombinant wt and singly deglycosylated mutant variants, AT was assayed for its ability to form covalent complexes with thrombin in the presence of heparin. In each experiment, 10 μg of AT-WT or mutant forms of AT were incubated with 12 μg of human α-thrombin in the presence of heparin at a final concentration of 0.5 μmole at 37°C in a total volume of 400 μl. At 0, 10, 30, 60, 120, 300, 600, 1200, and 1800 seconds after incubation, a 40 μl

aliquot of reaction mixture was taken to a fresh tube containing 10 µl of 50 µmole PPACK, which stopped the reaction. The reaction mixture was then electrophoresed on 10% SDS-PAGE gels under reducing conditions. Finally, each gel was stained with Coomassie Blue.

2.6.3 Second Order Rate Constant K_2 (Pseudo-First-Order Rate Constant)

A discontinuous kinetic assay was used to determine the rate of inhibition of thrombin by wild-type and the singly underglycosylated mutant variants of recombinant AT under pseudo-first order conditions, in the presence or absence of heparin. The analysis was conducted in a two-stage assay using the chromogenic thrombin substrate S-2238. For each experiment, 400 nmole of AT was incubated with 60 nmole of thrombin in a total volume of a 20 µL in TSP buffer. When heparin was included in the reaction, heparin was pre-incubated with AT at final concentration of 40 nmole before the incubation with thrombin. At different times, the reaction was quenched by diluting the reaction mixture with 200 µL of solution of 200 µmole of S-2238 (with a final concentration at 2 µmole). The residual thrombin activity was determined by monitoring the initial rate of substrate hydrolysis spectroscopically at 405 nM for several minutes, using a plate reader set to kinetic mode. A graph was plotted using time vs the logarithm of the change in optical density at 405 nm [ln(O.D)]. The slope of the line on this graph, which gives the observed rate constant (K_1 or K_{obs}) was determined. The second order rate constant (K_2) was then calculated by dividing K_1 with the concentration of AT used (Olson et al., 1993b).

2.6.4 Heparin Affinity of COS-Derived AT

Heparin-Sepharose chromatography was performed to measure heparin binding affinity of COS cell-derived wild-type AT. Heparin-Sepharose previously equilibrated with PBS (pH 7.5) was incubated with five volumes of COS-derived conditioned medium. The slurry was rotated at room temperature for one hour, then transferred to a mini-column. After washing with 10 volumes of PBS, proteins were eluted stepwise with two column volumes of TBS containing NaCl in concentrations of 0.2, 0.4, 0.6, 0.8, 1, 1.2, 1.4, 1.6, 1.8 and 2.0 mol/L. The resultant fractions were subjected to immunoprecipitation and electrophoresis on SDS-PAGE gel under reducing conditions, followed by autoradiography.

2.6.5 Thrombin-AT Complex Formation of COS-Derived AT

The COS cell-derived wild type recombinant AT was assayed for its ability to form a covalent complex with thrombin in the absence of heparin. One ml of the conditioned culture medium containing [^{35}S]-Met labeled AT at the concentration of 5μg/ml (86 nM) was incubated with human α-thrombin at the final concentration of 25 μg/ml (684 nM) at 37°C. At 0, 30, 60, 120, 300, 600, 1200, and 1800 seconds after incubation, a 100 μl aliquot of reaction mixture was taken to a fresh tube containing 10 μl of PPACK (50 μmole), which stopped the reaction. The reaction mixtures were then immunoprecipitated with sheep anti-rabbit AT antibody (IgG), electrophoresed on 8% SDS-PAGE gels under reducing condition, and visualized by autoradiography as described above.

2.6.6 Determination of Heparin-AT Dissociation Constants

Dissociation constants (K_d) of heparin-AT complex were determined spectrofluorometrically by monitoring changes in endogenous tryptophan fluorescence of AT that accompanies the binding. Fluorescence measurements were made on a LS-50 Luminescence Spectrometer. The analyses were carried out at 25°C. A cuvette containing AT (100 nmole) in 600 µl of TBS [0.02 M Tris-Cl/0.15 M NaCl, pH 7.4] was titrated by successive additions of 1µl aliquots of a concentrated high affinity heparin solution (with a stock concentration of 73 µmole). Heparin stock solutions were of concentration such that no more than 5% volume change occurred during the titration. The excitation and emission wavelengths were 280 and 340 nm respectively, and the bandwidths were 5 nm for both excitation and emission. Protein fluorescence was measured before titration and after each addition of the heparin. Three readings were taken and averaged for each titration point. Fluorescence data, corrected for dilution and assuming a 1:1 stoichiometry for complex formation, were fitted by nonlinear least-squares analysis using the following equation (Olson et al., 1993b):

$$\frac{\Delta F}{F_0} = \frac{\Delta F_{max}}{F_0} \times \frac{[AT]_0 + n[H]_0 + K_d - \{([AT]_0 + n[H]_0 + K_d)^2 - 4[AT]_0 n[H]_0\}^{1/2}}{2[AT]_0}$$

K_d was determined by nonlinear least-squares analysis using the SigmaPlot^R program. $[AT]_0$ represents total AT concentration; $[H]_0$ represents total heparin concentration; F_0 represents AT fluorescence before the titration; F represents observed fluorescence after each addition of the heparin; F_{max} represents the maximal fluorescence

change; and n represents the apparent stoichiometry for the interaction, which was assumed to be 1.

2.7 *In vivo* Behavior of Recombinant AT

2.7.1 Preparation of Radioiodinated AT

The purified recombinant rabbit wild-type and singly deglycosylated mutant variants of AT, as well as purified plasma-derived AT were labeled by IODO-GEN^{TM} using the procedure described by the manufacturer. For each labeling, 100 μg of AT was added to a reaction vessel that had been coated with 5 μg of IODOGEN. In a total reaction volume of 300 μl, 1 mCi of $Na^{125}I$ (3 μl of $Na^{125}I$ at a stock concentration of 369.51 mCi/ml) was added to the reaction mixture. One preparation of plasma derived AT was radiolabeled with 1mCi of $Na^{131}I$ using the same method. The reaction was allowed to proceed with gentle agitation for 5 minutes, at that time, the reaction mixture was then transferred to a dialysis tubing (molecular weight cut-off at 14,000 Daltons) and dialyzed against TBS buffer overnight, with three changes of buffer with 3 liters for each change. Radioactivity was measured with a Beckman Model 5500 gamma counter. Approximately $1X10^7$cpm/μg protein was obtained for each labeling. Each preparation of the radiolabeled AT was subjected to SDS-PAGE analysis. The gels were dried and exposed to Kodak X-AR5 film.

2.7.2 Animal Experiments

Healthy male New Zealand White rabbits (2.5-3.3 kg) were used and six rabbits were assigned for each experiment. Each rabbit was injected with approximately 150 μCi

of ^{125}I-labeled recombinant AT (approximately 1x 10^8 cpm) through left lateral ear vein. Blood samples (1.5 ml) were taken at 5, 30, 60, 120, 240, 360, and 480 min after injection, and then daily thereafter for up to 7 days. Blood samples were mixed with one-tenth volume of 0.13 mol/L sodium citrate. After centrifugation of the blood samples for 5 minutes at 14,000 rpm, 0.5 ml of plasma was collected to polystyrene tubes (75X12 mm) containing 0.5 ml of normal saline. Radioactivity was measured by a Beckman Model 5500 gamma counter. To compare the *in vivo* behavior of plasma-derived AT and recombinant wild-type AT, each of six rabbits was injected with both ^{125}I labeled recombinant wt AT and ^{131}I labeled plasma-derived AT contemporaneously with a similar dose. Radioactivities of ^{125}I and ^{131}I of plasma samples were measured.

Plasma non-protein-bound radioactivity was determined by trichloroacetic acid (TCA) precipitation. TCA treatment consisted of a mixture of 200 ml of plasma, 600 ml of normal saline, and 200 ml of 50% TCA. Precipitation was performed at room temperature for 10 minutes. The samples were then centrifuged at 14,000 rpm for 10 minutes and the radioactivity of supernatant was counted. Protein-bound radioactivity was determined using the following formula (Witmer and Hatton,1991):
plasma protein-bound radioactivity = (total plasma counts)-(plasma non-protein-bound counts).

2.7.3 Radioactivity Data Analysis

A plasma clearance curve was constructed for each radiolabeled AT. The corrected radioactivity data was fitted to a three-compartment model which includes intravascular space (plasma compartment), noncirculating vascular wall associated

compartment, and extravascular space (Carlson et al., 1985). This three compartment model is described by the following equation (Carlson et al. 1985):

$$A_p = C_1 e^{-a1t} + C_2 e^{-a2t} C_3 e^{-a3t}$$

where A_p is the fraction of radiolabeled protein remaining in the circulation at time t; the terms C_1, C_2, and C_3 are the fractional constants for compartments 1, 2 and 3; and the terms a_1, a_2, and a_3 are the respective rate constants of exchange between those compartments. The catabolic rates of each AT were calculated using a Lotus-based computer program. Briefly, the protein-bound radioactivity content of the first plasma sample, obtained 5-6 min after injection, was taken as 100% dose, and each subsequent measurement was expressed as a percentage of this value. The logarithm of the residual radioactivity was plotted against the time after injection in decimal days. The terminal exponential phase of the clearance was curve-fit using linear regression. Subtraction of the equation describing this line from the remaining data yielded a residual curve, which was also curve-fit using linear regression to complete the analysis second exponential phase. In turn, subtraction of the equation describe the second exponential phase from the remaining data yielded a residual curve which was curve-fit using linear regression to complete the analysis in a three-compartment model.

2.8 Analysis of the Carbohydrate Composition of AT

2.8.1 Glycosidase Treatment of AT

10μg of purified recombinant AT or plasma derived AT were reacted with N-glycosidase F under denaturing conditions. The reaction mixture was heated to 100°C for 10 minutes in the denaturing buffer [0.5% SDS and 1%–mercaptoethanol], and then

cooled to 37°C. The samples were reacted with 5,000 unit of N-glycosidase F in the reaction buffer [0.05 M Na phosphate (pH 7.5), containing 1% NP-40] at 37°C for 18 hours. The samples were then subjected to electrophoresis on SDS-PAGE gel under reducing conditions followed by Coomassie Blue staining or Western immunoblot with a sheep anti-rabbit AT IgG as described in section 2.4.2.7.

2.8.2 Analysis of Terminal Sialic Acid Structure on AT

A glycan differentiation kit was used to identify the type of carbohydrate chains present on recombinant AT. Recombinant AT and rabbit plasma-derived AT were electrophoresed on SDS-PAGE gels and transferred to nitrocellulose membranes for binding of glycan-specific lectins. Different carbohydrate structures were then identified by binding to specific lectins. Each lectin was digoxigenin-labeled and was exposed to anti-digoxigenin antibody coupled to alkaline phosphatase. The presence of bound lectin, and thus of a given carbohydrate structure, was demonstrated by the development of colour, through the alkaline phosphatase-catalyzed hydrolysis of 5-bromo-4-choloro-3-indolyl-phosphate (BCIP) in the presence of 4-nitro blue tetrazolium chloride (NBT). Briefly, for each lectin binding experiment, approximately 2 μg of AT was electrophoresed on SDS-PAGE gel under reduced conditions, and then transferred onto a nitrocellulose membrane. The membranes were incubated with 20 ml of blocking solution (provided by Boehringer Mannheim Biochemica) for 1 h. The membranes were then washed twice with TBS and once with binding buffer [0.05 mol Tris-HCl, 0.15 mol NaCl, 1 mmol $MgCl_2$, 1 mmol $MnCl_2$, and 1 mmol $CaCl_2$, (pH 7.5). Each membrane was

incubated with individual lectin in 10 ml of binding buffer for 1 h. After washing with TBS for 3 times, the membranes were incubated with anti-digoxigenin-AP in TBS for 1 h. Following 3 washes with TBS, the membranes were then stained with 50 μl of NBT and 37.5 μl x-phosphate in the buffer containing 0.1 mol Tris-HCl, 0.05 mol $MgCl_2$, and 0.1mol NaCl (pH 9.5).

Five different lectins were used in this experiment which include: 1) *Galanthus nivalis* agglutinin (GNA) with the specificity for terminal mannose; 2) *Sambucus nigra* agglutinin (SNA) with the specificity for terminal α(2-6)-linked sialic acid; 3) *Maackia amurensis* agglutinin (MAA) with the specificity for terminal α(2-3)-linked sialic acid; 4) Peanut agglutinin (PNA) with the specificity for terminal galactose-β(1-3)-N-acetylgalactosamine (present in O-linked glycans); and 5) *Datura stramonium* agglutinin (DSA) with the specificity for terminal galactose-β-(1-4)-acetylglucosamine (present in N-linked complex and hybrid glycans).

2.9 Statistical Analysis

Statistical analyses were performed using a two-way analysis of variance (ANOVA). When variance was found, further analysis was performed using a Neuman-Keuls multiple Student's t test to detect which specific pairs of data were statistically different at P values of <0.05. When the experiment was designed to compare results of the wild-type recombinant AT with that of plasma derived AT, the Student t test was performed.

3. RESULTS

3.1 Generation of Mutant Variants of AT cDNA By Site Directed Mutagenesis

The rabbit cDNA encoding AT, including its secretory signal sequence, was isolated and subcloned into the phagemid pGEM3zf(+). When superinfected with M13K07 helper bacteriophage, this vector produces single-stranded DNA which can be used for mutagenesis. Four mutant variants of rabbit AT cDNA were created by site-directed mutagenesis that was carried out as described in section 2.2.2. In each mutant AT cDNA, one of the four potential glycosylation Asn sites was substituted to a Gln residue which is incapable of N-linked glycosylation. These mutant AT cDNA constructs were verified by double-stranded DNA sequencing as described in section 2.2.3 (Shown in Fig. 3.1).

3.2 Construction of the Rabbit AT Mammalian Cell Expression Vectors

The pCMV5 mammalian expression plasmid constructs that allow expression of wild type and mutant forms of rabbit AT were assembled as described in section 2.3.7. To eliminate the possibility of errors introduced during the steps of excision of the AT cDNA and ligation into the pCMV5 plasmid, DNA sequencing analysis was carried out prior to transfection of mammalian cells. The resulting expression plasmid constructs were designated pCMV5-AT-WT, and pCMV5-AT-N where WT presents wild type and N represents the position of the mutagenic oligonucleotide. Five expression plasmid constructs were obtained which are shown schematically in Fig. 3.2 and Fig.3.3.

Figure 3.1 Sequence analysis shows that the codon for Asn (AAC) at amino acid position 155 in the wild type AT was substituted to Gln (CAA) in the mutant variant.

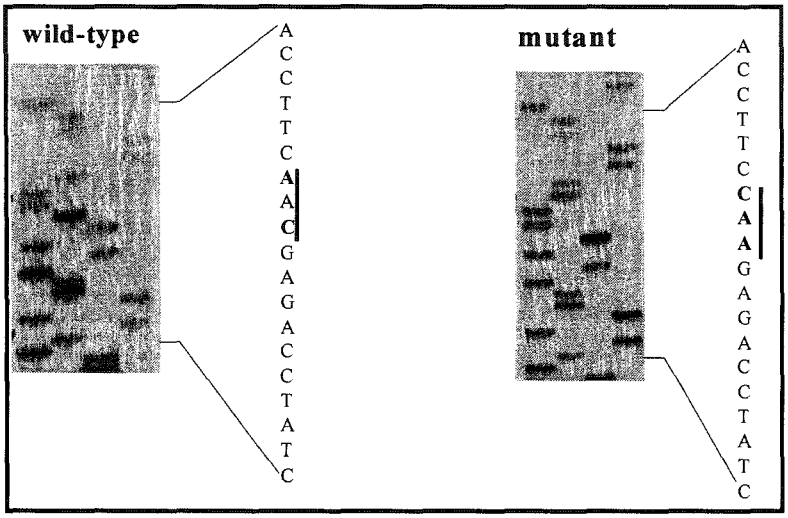
wild-type
ACCTTTCAACGAGACCTATC
mutant
ACCTTTCCAAGAGACCTATC

Figure 3.2 Panel A, The plasmid vector used for mammalian cell expression of wild type AT. Panel B schematically illustrates the glycosylated form of wild type α-AT that contains four N-linked glycans as illustrated by tailed diamond at positions 96, 135, 155, and 192. N indicates amino terminus while C indicates carboxyl terminus.

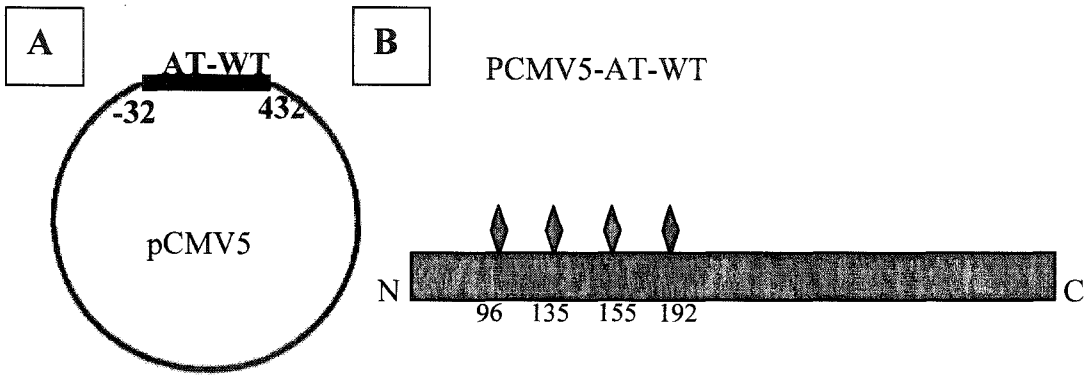
A
AT-WT
-32
432
pCMV5
B
PCMV5-AT-WT
N
C
96
135
155
192

Figure 3.3 Panel A. The plasmid vector used for mammalian cell expression of mutant forms of AT. Panel B schematically illustrates each mutant variant of AT containing only three of the four glycosylation sites; Tailed diamonds represent each N-linked glycan, whether at 96, 135, 155,or 192. N indicates amino terminus while C indicates carboxyl terminus.

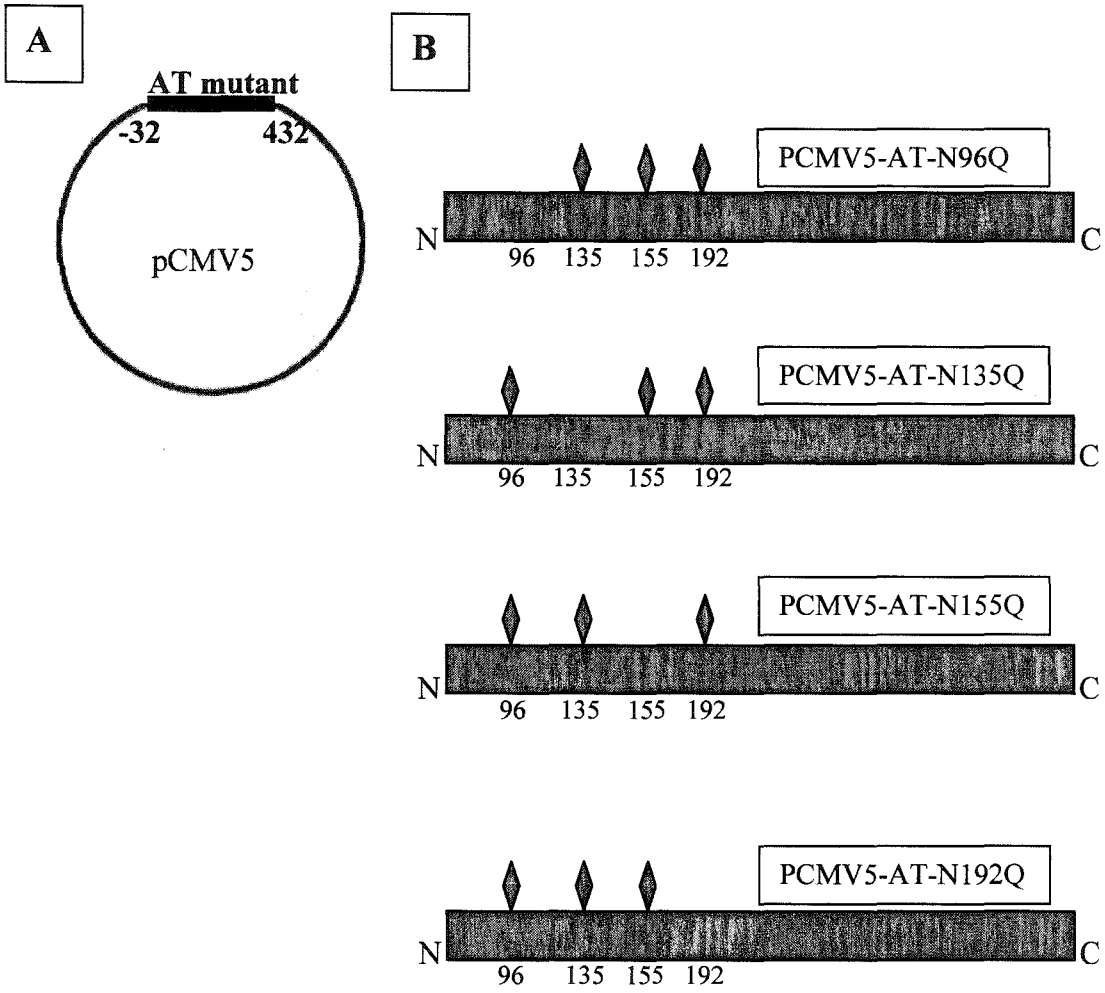
A
AT mutant
-32
432
pCMV5
B
PCMV5-AT-N96Q
N
C
96 135 155 192
PCMV5-AT-N135Q
N
C
96 135 155 192
PCMV5-AT-N155Q
N
C
96 135 155 192
PCMV5-AT-N192Q
N
C
96 135 155 192

3.3 Expression of Wild-Type and Mutant Variants of AT in COS-1 Cells

Wild-type and mutant variants of rabbit AT were transiently expressed in COS-1 cells as outlined in section 2.4.1. In order to detect the recombinant AT proteins, the transfected COS-1 cells were metabolically radiolabeled with L-[^{35}S]-Met and L-[^{35}S] Cys as detailed in section 2.4.1. The conditioned media were immuno-precipitated and electrophoresed on SDS-PAGE gel followed by autoradiography as described in section 2.4.2.5. The results demonstrated a band with an apparent molecular weight of 65 KDa that was recognized and precipitated by the sheep-anti-rabbit AT IgG. This band was not observed in media from non-transfected COS-1 cells and cells transfected with the pCMV5 plasmid alone (Shown in Fig. 3.4). The molecular size of this band is very similar to the previously described molecular weight of rabbit plasma-derived AT. This recombinant protein, therefore, was the COS-expressed AT-WT. Novel synthesis of protein that could be immunoprecipitated by sheep-anti-rabbit AT IgG was also observed in COS-1 cells transfected with the expression constructs containing mutant variants of cDNA. The mutant variants of AT migrated slightly faster than wild-type AT (shown in Fig. 3.5). The increased mobility of the mutant variants suggested that they had a decreased apparent molecular weight due to the lack of one of the four glycans, which is consistent with the underglycosylated form of AT protein.

A band with an apparent molecular weight of 49 KDa is also co-precipitated with AT. However, this band is present in the medium from non-transfected COS-1 cells and cells transfected with the pCMV5 plasmid alone (Shown in Fig. 3.4). Therefore, it is

Figure 3.4 SDS-PAGE analysis of rabbit AT secreted by COS cells. Lane 1 represents conditioned medium from COS cells without transfection; Lane 2 represents COS cells transfected with pCMV5 plasmid without AT cDNA insert; Lane 3, and 4 represent conditioned media from COS cells transfected with pCMV5-AT-WT expression plasmid construct.

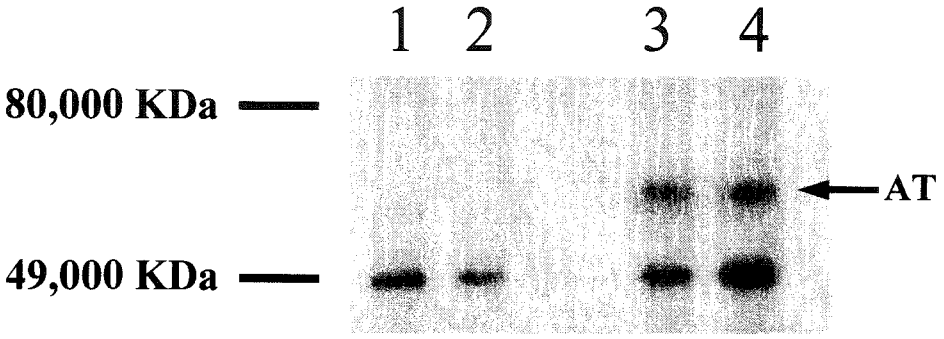
1 2 3 4
80,000 KDa
49,000 KDa
AT

Figure 3.5 Electrophoresis of conditioned media from COS cells expressing either AT-WT or mutant variants. Lane 1 represents pCMV5-AT-WT; lane 2 represents pCMV5-AT-N96Q; Lane 3 represents pCMV5-AT-N135Q; Lane 4 represents pCMV5-AT-N155Q; Lane 5 represents pCMV5-AT-N192Q; and lane 6 represents media collected from the COS cells transfected with pCMV5 plasmid without AT cDNA insert.

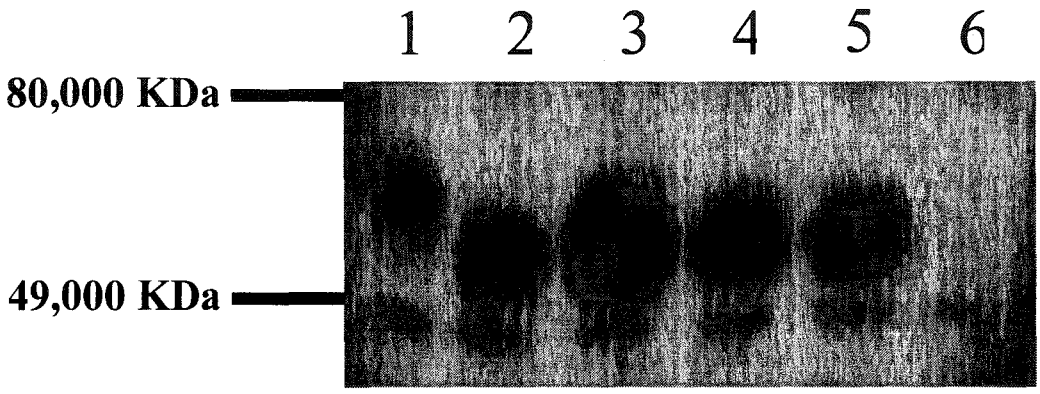
1 2 3 4 5 6
80,000 KDa
49,000 KDa

considered that this band is not related to AT, although the nature of this band is not known.

3.4 Functional Characterization of COS-1 Cell Expressed AT-WT

3.4.1 Thrombin-AT Complex Formation

The thrombin inhibitory activity of COS-1 cell derived AT-WT was determined by thrombin-AT complex formation assay as described in 2.6.5. The results demonstrated that COS-1 cell-derived AT and human α-thrombin formed a complex of molecular size of approximately 96 KDa (Figure 3.6). This 96 KDa complex is clearly visible after 30 seconds of incubation and reached a maximum after 5 minutes. Beyond 10 minutes of incubation, the amount of complex declined, either through degradation or dissociation.

3.4.2 Heparin-Binding Affinity of COS-1 Cell Derived AT-WT

Heparin-Sepharose chromatography was performed to measure the heparin affinity of COS-1 cell-derived AT-WT as described in section 2.6.4. The results showed that the majority of COS-1 cell-derived AT-WT could be eluted with TBS buffers containing 1 to 1.2 M NaCl. This heparin-binding profile was similar to that of plasma-derived rabbit AT.

3.5 Establishment of Rabbit AT Producing Cell Lines

Expression of foreign DNA sequence in transfected COS-1 cells only lasted for a short period of time after transfection (usually three to four days). Eventually the transfected cells died, presumably because they could not tolerate the high levels of DNA. Therefore, it was difficult to produce sufficient AT for purification and further characterization by using this system. As a result, AT producing permanent cell lines

Figure 3.6 Time-dependent reaction between human α-thrombin and COS-1- cell-derived rabbit AT to produce complexes of thrombin-AT (TAT). Panel (A) represents AT-WT; Panel (B) represents a mutant variant of AT (AT-N155Q).

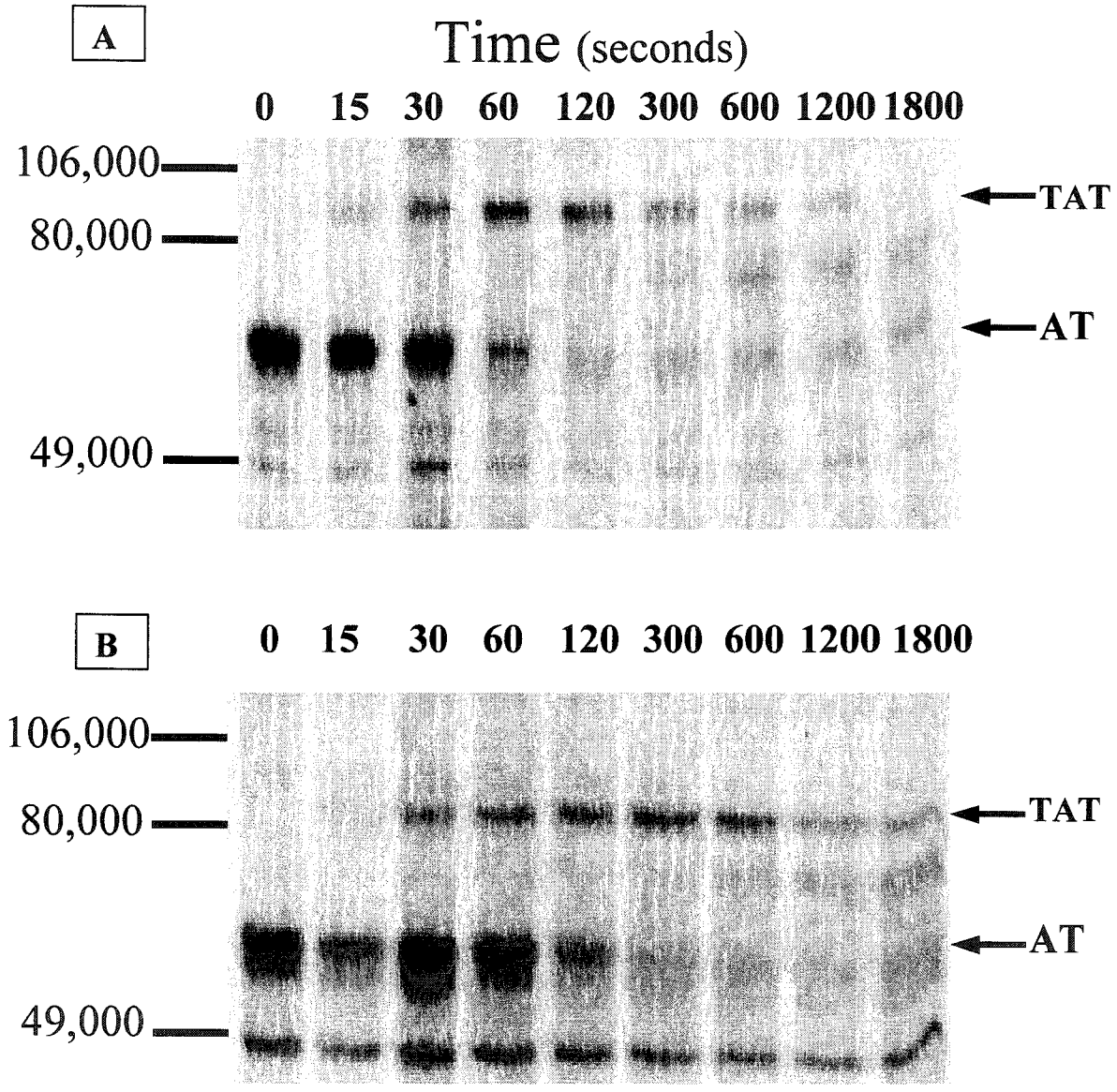
A
Time (seconds)
0 15 30 60 120 300 600 1200 1800
106,000
80,000
49,000
TAT
AT
B
0 15 30 60 120 300 600 1200 1800
106,000
80,000
49,000
TAT
AT

were established. These cell lines produced sufficient amount of AT for the purification and further characterization. To establish permanent AT-producing CHO cell lines, a neomycin-resistant plasmid pSV2Neo and mammalian expression plasmid constructs pCMV5 containing either wild type or mutant variants of AT cDNA were co-transfected into CHO cells as described in section 2.4.2.1. Transfection with the plasmid pSV2Neo would confer geneticin resistance to the cells, thus allowing the selection of the cells. Since the two plasmids were employed in a molar ratio of pCMV5-AT:pSV2Neo of 10:1, most of the cells which were transfected with pSV2Neo should theoretically have been transfected with pCMV5-AT. Thus, the transfected cells were first selected by resistance to geneticin and subsequently screened for AT production. Based on ELISA-based quantification, among the 50 geneticin resistant colonies that were exposed to the AT-WT expression constructs, 65% were positive for AT expression. For the constructs expressing mutant variants of AT, 64 to 67% of colonies were producing AT. The expression rates of these clones ranged from 0.02 μg to 15 μg of AT/10^6 cells /24 h. The clones secreting from 1 μg to 15 μg of AT/10^6 cells/24 h were chosen for further study and stored in liquid nitrogen. Ten clones were randomly selected from cell lines producing either AT-WT or each mutant variant of AT. Their AT producing levels were compared based on the ELISA quantitation measurements. No statistically significant difference was observed in comparing the AT secretion of the wild type and each mutant variant (Table 3.1).

Table 3.1 PRODUCTION BY CHO CELLS OF WT AND MUTANT AT VARIANTS

AT	Sample Size (n)	rAT production ($\mu g/10^6$ cells/24 hours)	P value
AT	10	2.32 ± 1.13	
AT-N96-Q	10	2.31 ± 1.89	0.99
AT-N135Q	10	2.33 ± 1.50	0.99
AT-N155Q	10	2.25 ± 1.50	0.91
AT-N192Q	10	2.25 ± 1.13	0.89

3.6 Pulse-Chase Studies in AT Producing CHO Cell Lines

To evaluate the secretion and intracellular transportation of newly synthesized AT, clones producing wild type and each mutant variant of AT were used for pulse-chase experiments as described in section 2.4.2.4.

Intracellular nascent wild-type AT seen at 0 and 1 hour gradually decreased in the cells and radiolabeled AT appeared in the extracellular medium at 2 hours after pulse labeling. At 6 hours after pulse labeling, most of the AT was found in the culture medium (Fig. 3.7, and 3.8). Similar patterns of AT secretion were observed in AT-N96Q, AT-N135Q, AT-N155Q, and AT-N192Q mutant variants. This similarity was quantified by determining the time required for 50% of the initially labeled intracellular AT to disappear from the cell (Figure 3.9). The half-life was shown in table 3.2. No statistically significant difference in AT production between cell lines expressing wild type and mutant variants was found.

3.7 Purification of Recombinant AT From CHO Cell-Derived Media

To produce wild-type and singly underglycosylated mutant variants of AT in quantities sufficient for their purification and characterization, AT producing CHO cell lines were grown and scaled up in suspension culture. Cells were allowed to express and secrete AT into serum-free medium. The expression levels were checked by an ELISA. The viability of cells was monitored by Trypan Blue staining.

The conditioned media were concentrated 20 times using a Prep/Scale-TFF cartridges and affinity purified with a heparin-Sepharose column as described in section 2.5.1. The AT was eluted with a gradient from 0.15 M NaCl to 3 M NaCl. A typical

Figure 3.7 Synthesis and secretion of rabbit AT-WT . A pulse-chase study in which duplicate plates of permanently transfected CHO cells producing AT-WT were pulse labeled with (^{35}S)-methionine and (^{35}S)-cysteine for 30 minutes, then chased in the absence of radioactivity. At the times (in hours) indicated below the panels, equivalent aliquots of cell lysates [upper (A): intracellular] or conditioned cell media [lower (B): extracellular] from parallel plates were immunoprecipitated with affinity-purified sheep anti-rabbit AT IgG and analyzed by SDS-PAGE and fluorography.

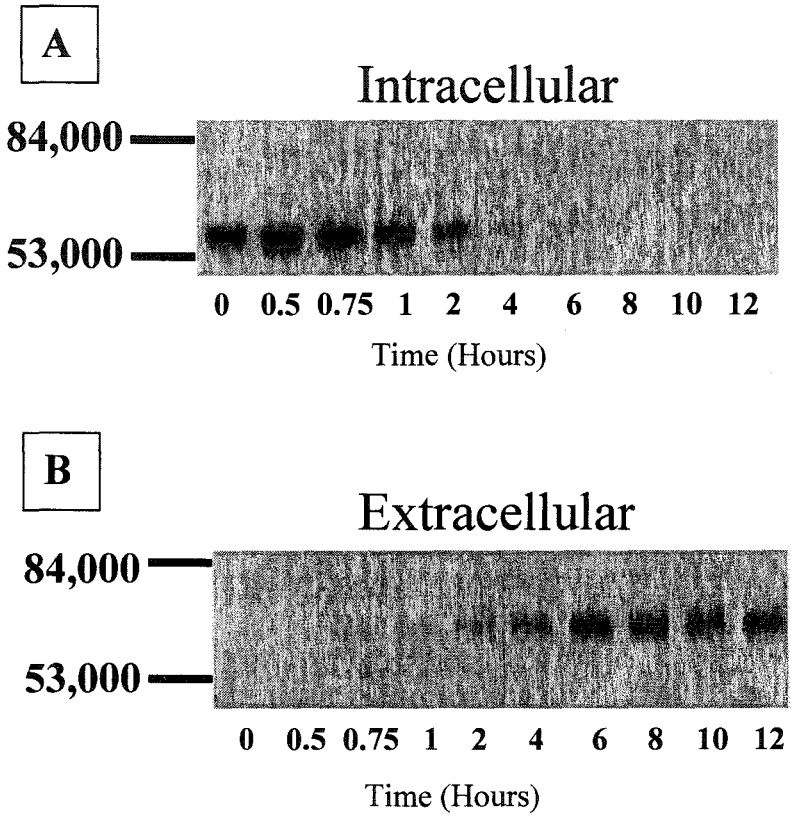
A
Intracellular
84,000
53,000
0 0.5 0.75 1 2 4 6 8 10 12
Time (Hours)
B
Extracellular
84,000
53,000
0 0.5 0.75 1 2 4 6 8 10 12
Time (Hours)

Figure 3.8 Synthesis and secretion of rabbit mutant variants of AT. Panel A represents AT-N96Q and panel B represents AT-N155Q

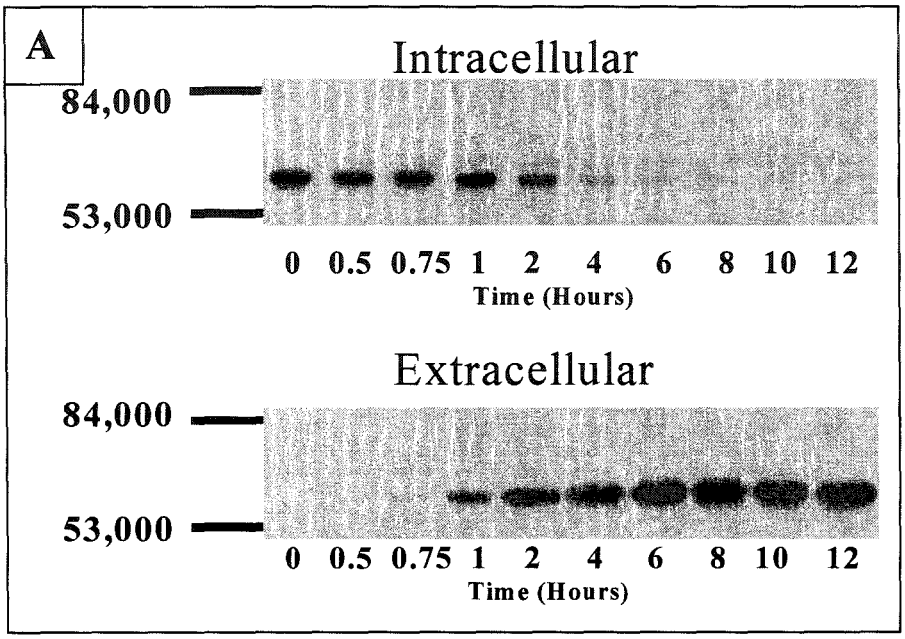
A
Intracellular
84,000
53,000
0 0.5 0.75 1 2 4 6 8 10 12
Time (Hours)
Extracellular
84,000
53,000
0 0.5 0.75 1 2 4 6 8 10 12
Time (Hours)

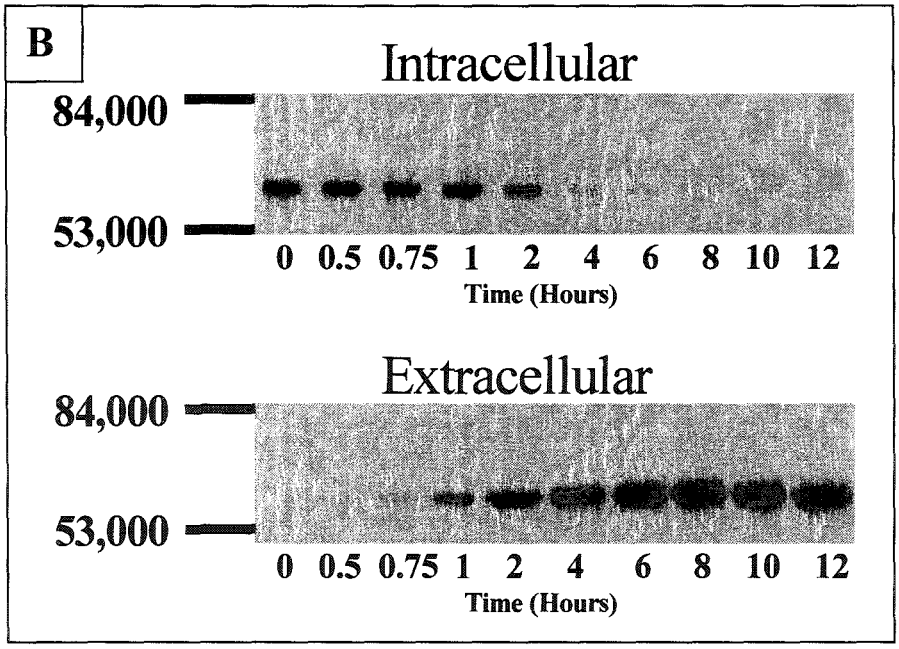
B
Intracellular
84,000
53,000
0 0.5 0.75 1 2 4 6 8 10 12
Time (Hours)
Extracellular
84,000
53,000
0 0.5 0.75 1 2 4 6 8 10 12
Time (Hours)

Figure 3.9 Quantitative analysis of pulse-chase study of AT-WT production and secretion in CHO cell line. AT-WT means radiolabeled wild type AT; ▲ represents intracellular AT; ● represents AT in the conditioned medium.

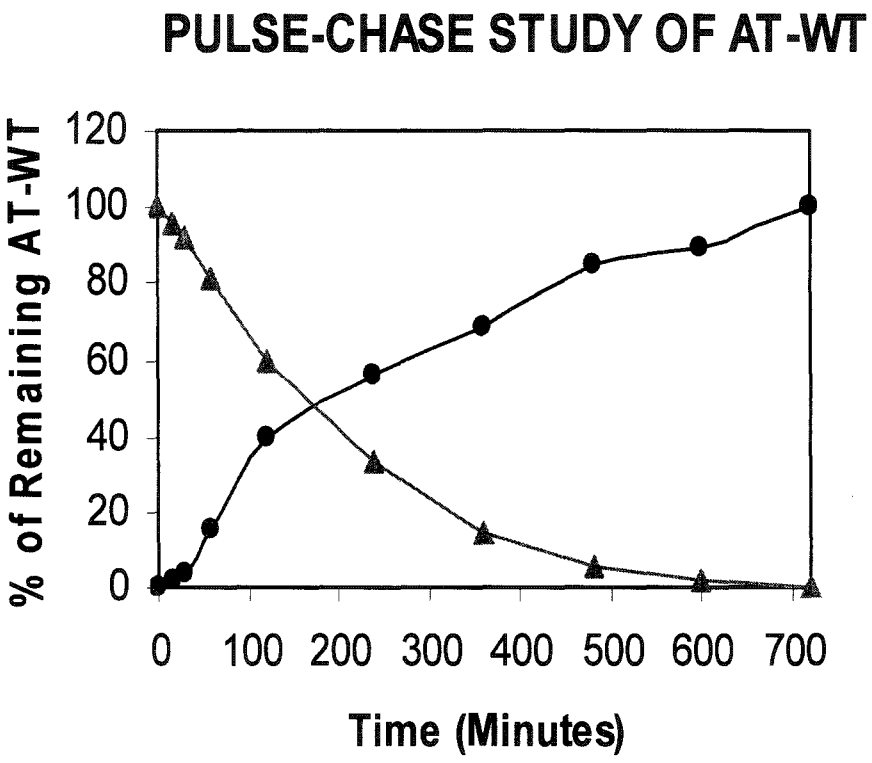
PULSE-CHASE STUDY OF AT-WT
% of Remaining AT-WT
120
100
80
60
40
20
0
0
100
200
300
400
500
600
700
Time (Minutes)

Table 3.2 $T_{1/2}$ OF INTRACELLULAR RADIOLABELED AT SYNTHESIZED IN CHO CELLS

AT	Sample Size	$T_{1/2}$ (Hours)	P value
Wild-type	4	2.63 ± 0.20	
AT-N96-Q	3	2.55 ± 0.07	P>0.05
AT-N135Q	3	2.43 ± 0.08	P>0.05
AT-N155Q	3	2.66 ± 0.15	P>0.05
AT-N192Q	3	2.46 ± 0.17	P>0.05

No statistically significant difference was identified in comparison of AT-WT with mutant AT variants (P>0.05).

elution profile for wild-type AT is shown in Fig. 3.10. Two major peaks were observed. While peak 1 eluted off the heparin-Sepharose at less than 0.5 M NaCl, peak 2 eluted off at approximately 1.2 M NaCl. Fractions from peak 1 and peak 2 were pooled separately and analyzed on SDS-PAGE gel. Whereas many proteins with different molecular weights constituted the fraction of peak 1, the sample from the second peak contains a major protein band with a molecular weight of approximately 65 KDa as shown in figure 3.11. The sample from the second peak was further subjected to Western blotting analysis with a sheep anti-rabbit AT antibody (IgG). The results demonstrated that the 65 KDa band was recognized by this antibody. Heparin affinity chromatography elution profiles of mutant forms of AT are shown in Figure 3.12. The AT-WT, AT-N96Q, AT-N135Q and AT-N192Q have a similar elution profiles. It appears that the affinity of AT-N155Q for heparin was decreased as manifested by the fact that this variant was eluted with TBS containing 0.8 M of NaCl.

In order to further purify recombinant AT from the conditioned media and to remove any possible contaminating free heparin in the preparation, the fractions from the second peak which was eluted off the heparin –Sepharose at 0.8 to 1.5 M NaCl were pooled and dialyzed against TBS buffer. The preparation was then applied to an anion exchange Q-Sepharose. The AT was present in the flow through and the low salt wash up to 0.3 NaCl. These fractions were pooled, concentrated and dialyzed against TBS. The resultant preparation was subjected to electrophoresis on SDS-PAGE gel under reducing conditions followed by Coomassie blue staining or Western blot analysis with a sheep anti-rabbit AT antibody (IgG). The purified recombinant AT protein migrated with an

Figure 3.10 Heparin-Sepharose chromatography of CHO cell derived conditioned media containing AT-WT. Linear gradient elution was from 0.15M NaCl to 3 M.

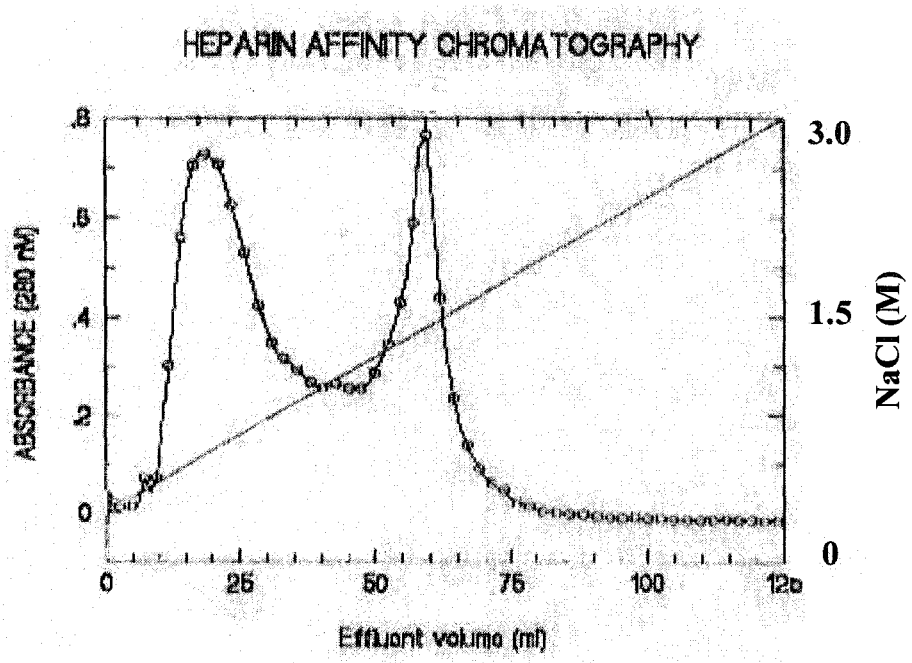
HEPARIN AFFINITY CHROMATOGRAPHY
ABSORBANCE (280 nM)
.8
.6
.4
.2
0
0
25
50
75
100
125
Effluent volume (ml)
3.0
1.5
0
NaCl (M)

Figure 3.11 SDS-polyacrylamide gel of pooled fractions from heparin-Sepharose chromatography. The gel was run under reducing conditions followed by Coomassie blue staining. Lane 1. pooled fraction from the first peak; lane 2. pooled fraction from the second peak; lane 3. low range molecular mass standards.

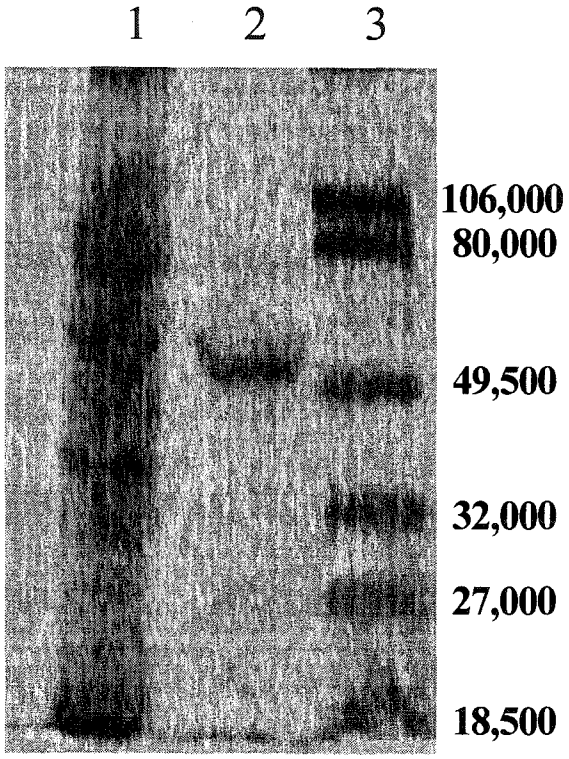
1
2
3
106,000
80,000
49,500
32,000
27,000
18,500

Figure 3.12. Heparin affinity chromatography elution profiles of the underglycosylated mutant variants of AT. Linear gradient elution was from 0.15 M NaCl to 3 M NaCl. Panel A represents AT-N96Q; panel B represents AT-N135Q; panel C represents AT-N155Q; and panel D represents AT-N192Q.

A

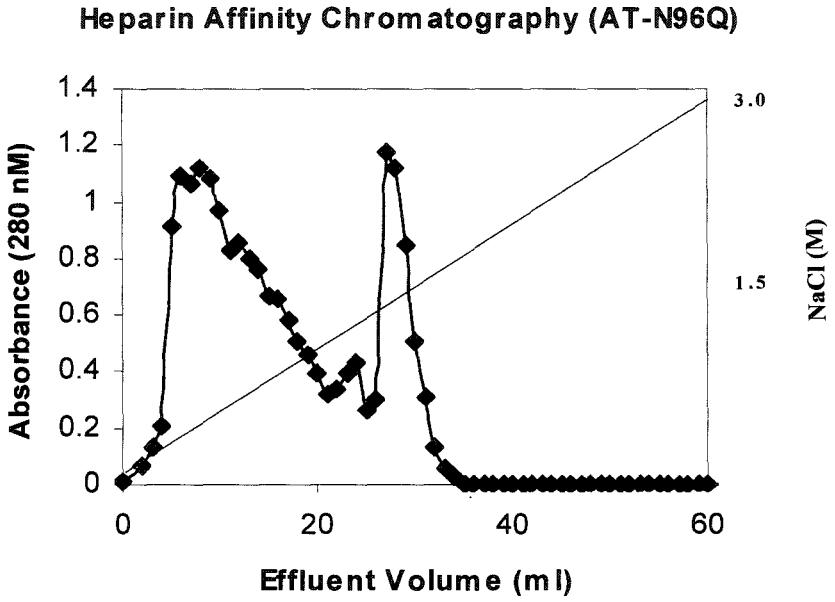
Heparin Affinity Chromatography (AT-N96Q)
Absorbance (280 nM)
1.4
1.2
1
0.8
0.6
0.4
0.2
0
0
20
40
60
Effluent Volume (ml)
3.0
1.5
NaCl (M)

B

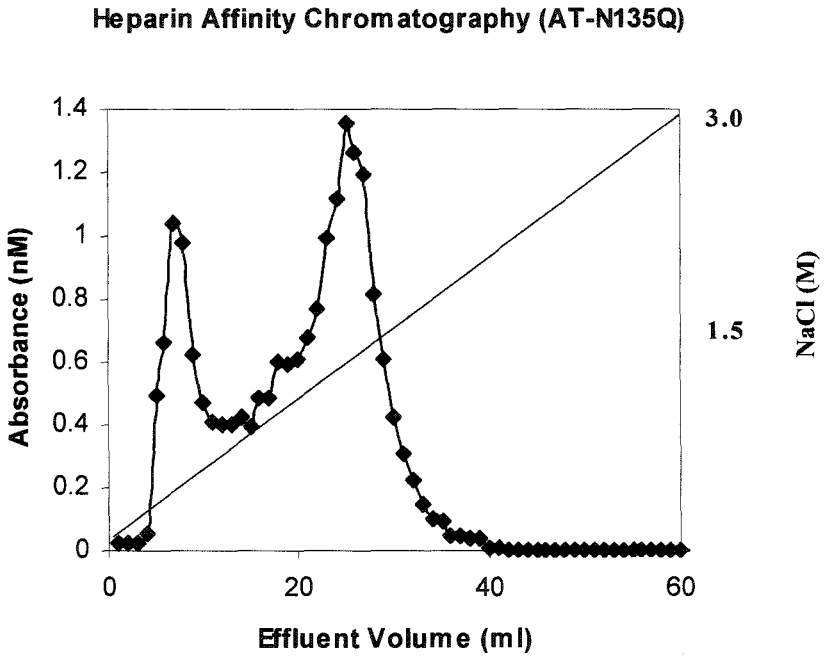
Heparin Affinity Chromatography (AT-N135Q)
Absorbance (nM)
1.4
1.2
1
0.8
0.6
0.4
0.2
0
0
20
40
60
Effluent Volume (ml)
3.0
1.5
NaCl (M)

C

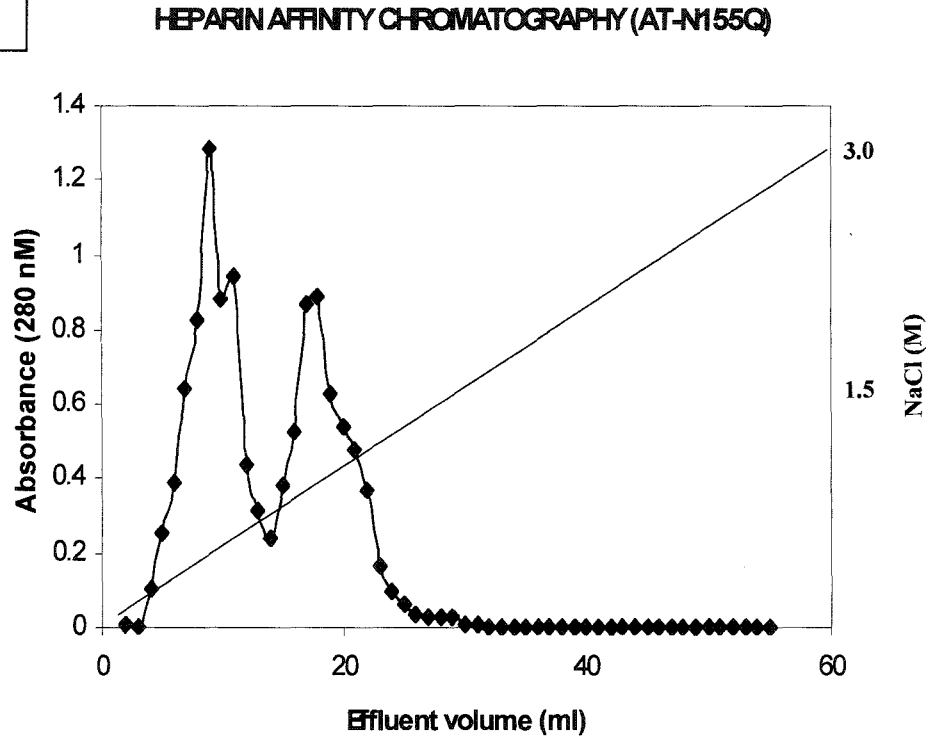
HEPARIN AFFINITY CHROMATOGRAPHY (AT-N155Q)
Absorbance (280 nM)
1.4
1.2
1
0.8
0.6
0.4
0.2
0
0
20
40
60
Effluent volume (ml)
3.0
1.5
NaCl (M)

D

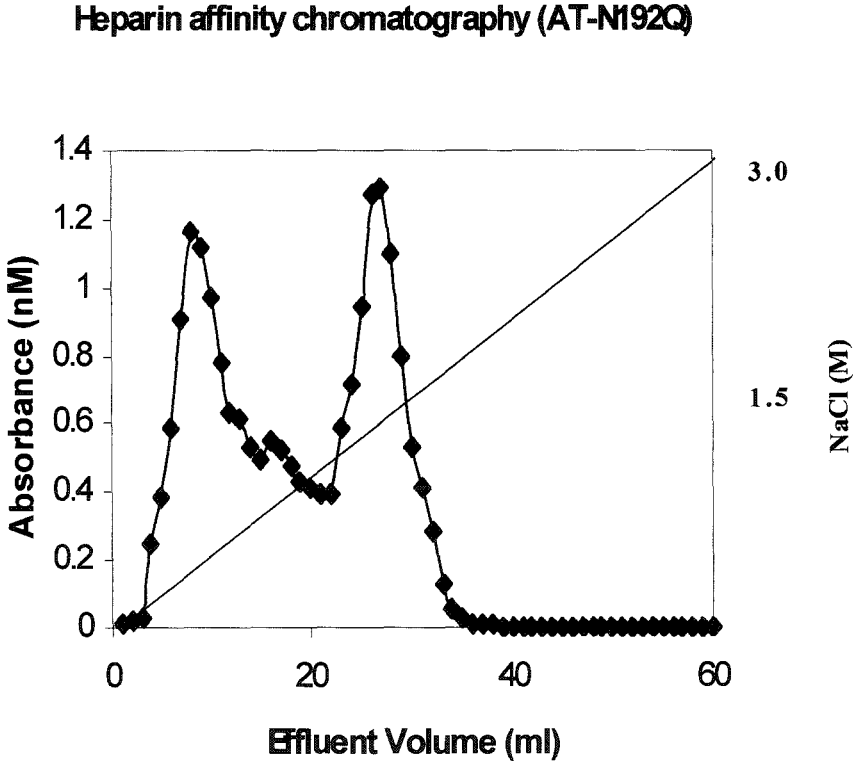
Heparin affinity chromatography (AT-N192Q)
Absorbance (nM)
1.4
1.2
1
0.8
0.6
0.4
0.2
0
0
20
40
60
Effluent Volume (ml)
3.0
1.5
NaCl (M)

apparent molecular weight similar to that of plasma-derived AT and could be recognized by the sheep anti-rabbit AT IgG (Fig. 3.13). The recombinant AT was, therefore, purified with heparin Sepharose followed by Q-Sepharose chromatography.

The underglycosylated mutant variants of AT migrated slightly faster than wild-type AT as shown in Figure 3.14. The increased mobility of the mutant variants suggests that they have a decreased apparent molecular weight due to the lack of one of the four glycans.

3.8 Functional Characterization of Recombinant AT

3.8.1 Thrombin-AT Complex Formation

The thrombin inhibitory activity of wild-type and underglycosylated mutant variants of AT were investigated by testing their ability to form SDS-stable complexes with human α-thrombin in the presence of heparin as described in section 2.6.2. The wild-type and all four underglycosylated variants of AT were capable of forming complexes with thrombin (Fig. 3.15). The complexes, with molecular weight of approximately 96 KDa, were clearly visible at 10 seconds after incubation. Beyond 1 minute of incubation, the degradation products started to appear with apparent molecular weights ranging from 70 KDa to 90 KDa. Concurrently, the amount of complex seen was declining. The results demonstrated that the recombinant ATs, both wild-type and underglycosylated variants, were biologically active. No difference was seen qualitatively between wild-type and all four underglycosylated variants as judged by their ability to form a complex with human α-thrombin.

Figure 3.13 Comparison of recombinant wild-type (AT-WT) and plasma-derived (pd-AT) rabbit AT preparation. Electrophoresis of 400 ng per lane of purified AT-WT and purified pd-AT. Lane M shows molecular weight markers corresponding to 94, 67, 43, and 30 kDa.

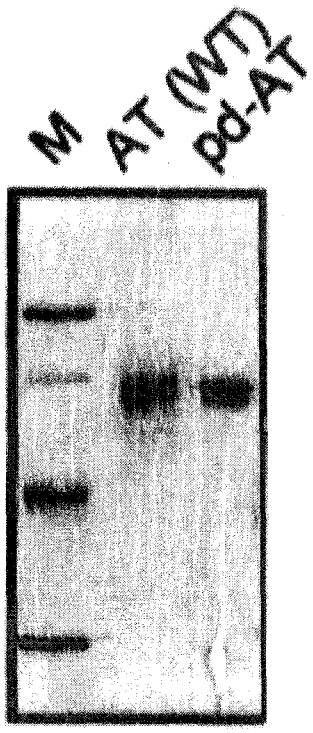
M
AT (WT)
pd-AT

Figure 3.14 SDS-PAGE co-electrophoresis of AT produced from CHO cells expressing either AT-WT or underglycosylated mutant variants. Lane 1 represents AT-WT; lane 2 represents AT-N96Q; Lane 3 represents AT-N135Q; Lane 4 represents AT-N155Q; and Lane 5 represents AT-N192Q.

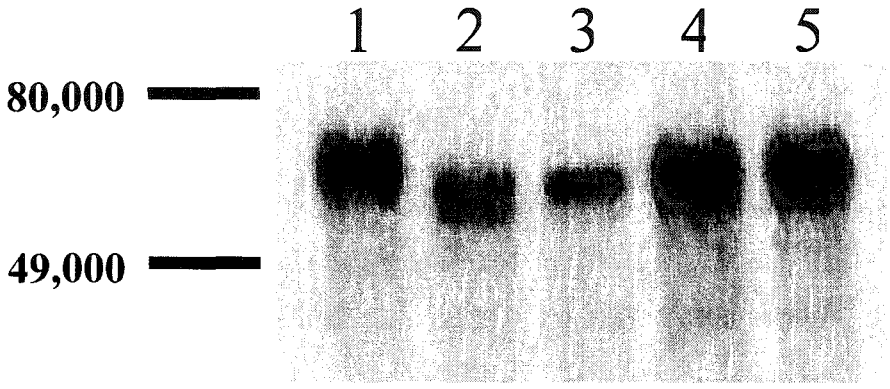
1
2
3
4
5
80,000
49,000

Figure 3.15 Biological activity of wild-type AT and underglycosylated mutant variants of AT. SDS-polyacrylamide gel under reducing conditions showing thrombin-AT complexes (TAT) formation. Panel A represents AT-WT; Panel B represents AT-N96Q; Panel C represents AT-N135Q; Panel D represents AT-N155Q; and Panel E represents AT-N192Q. TAT indicates thrombin-AT complexes.

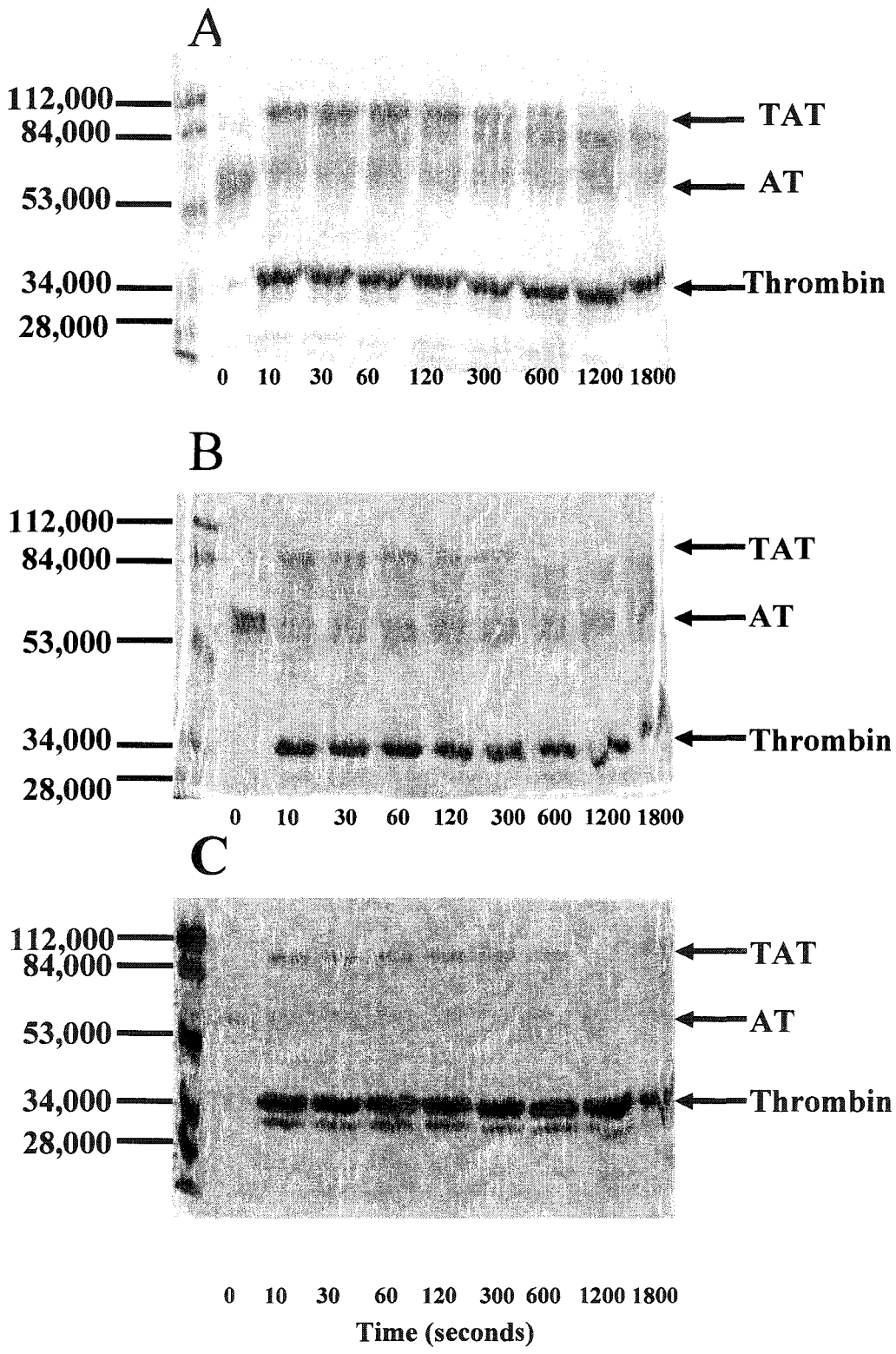
A
112,000
84,000
53,000
34,000
28,000
TAT
AT
Thrombin
0 10 30 60 120 300 600 1200 1800
B
112,000
84,000
53,000
34,000
28,000
TAT
AT
Thrombin
0 10 30 60 120 300 600 1200 1800
C
112,000
84,000
53,000
34,000
28,000
TAT
AT
Thrombin
0 10 30 60 120 300 600 1200 1800
Time (seconds)

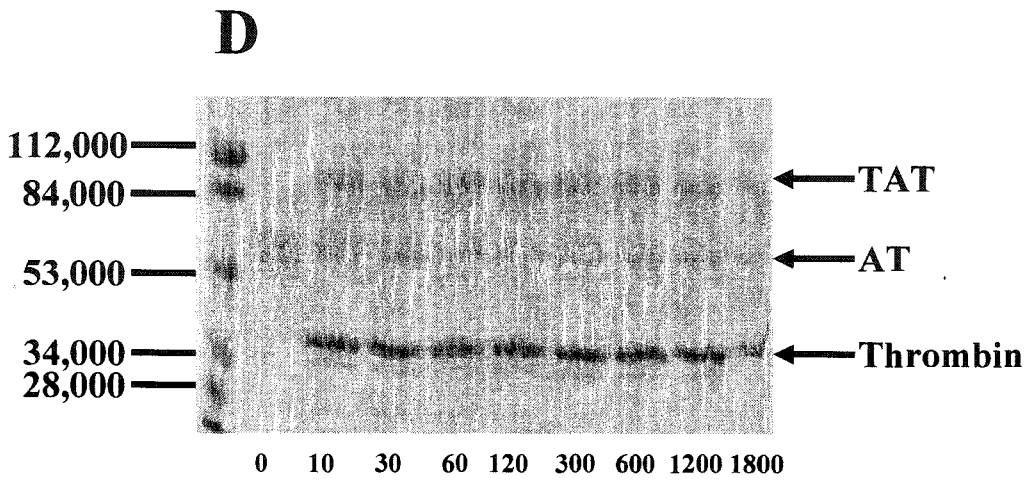
D
112,000
84,000
53,000
34,000
28,000
TAT
AT
Thrombin
0 10 30 60 120 300 600 1200 1800

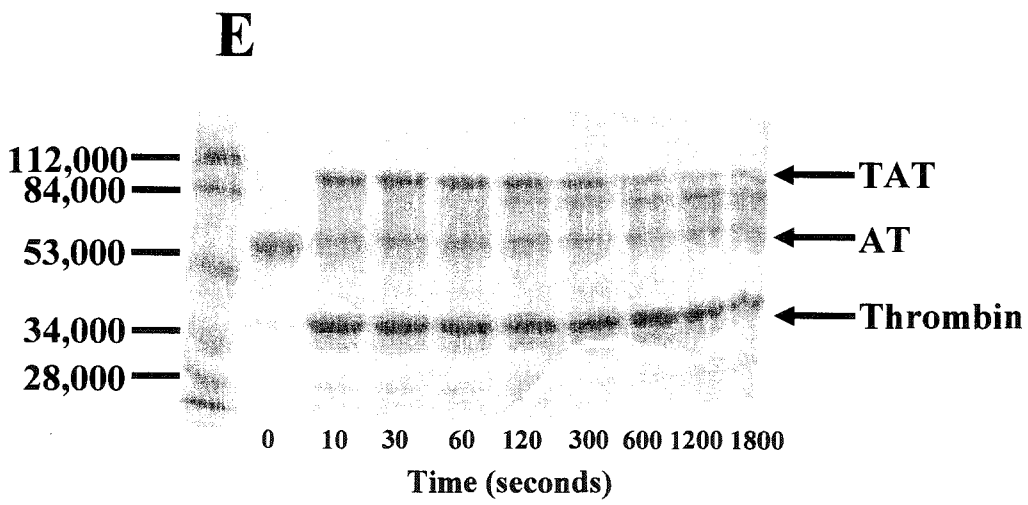
E
112,000
84,000
53,000
34,000
28,000
TAT
AT
Thrombin
0 10 30 60 120 300 600 1200 1800
Time (seconds)

3.8.2 Second Order Rate Constant K_2 (Pseudo-First-Order Rate Constant)

To further characterize the thrombin inhibitory activity of the wild-type and the underglycosylated variants, kinetic analysis of the inactivation of thrombin was conducted in a two-stage assay using the chromogenic thrombin substrate S-2238. Under pseudo-first order conditions, second order rate constants (k_2) were calculated for the inhibitory effect of each variant of AT. In initial experiments, the k_2 for the inhibition of human α-thrombin by rabbit plasma-derived AT was found to be 9.32 ± 0.72 X10^3 M^{-1} sec^{-1}. Use of high-affinity heparin increased this rate constant to 1.63 ± 0.13 X10^6 M^{-1} sec^{-1}, a 175 times enhancement (Table 3.3).

As shown in Table 3.3, the recombinant CHO-derived wild-type AT was less active than the human plasma-derived AT by a factor of 6. No statistically significant differences were observed between the recombinant wild-type and three underglycosylated variants, AT-N96Q, AT-N135Q and AT-N192Q ($P>0.05$). However, the AT-N155Q mutant showed 2.2 and 21-fold less active than the wild-type AT in the absence and presence of heparin, respectively ($P<0.007$).

3.8.3 Determination of Heparin-AT Dissociation Constants

The interaction of heparin with AT results in an enhancement of endogenous tryptophan fluorescence. This fluorescence change arises from buried tryptophan residues, and thus reflects the heparin-induced conformational change in AT. Therefore, the increase in intrinsic fluorescence of AT can be used to monitor the binding of heparin and evaluate the heparin binding affinity of AT.

Table 3.3 SECOND ORDER RATE CONSTANTS (k_2) OF AT VARIANTS

		k_2 ($M^{-1}sec^{-1}$)	
AT	Sample Size (n)	- Heparin ($X10^3$)	+Heparin ($X10^6$)
Plasma-derived	4	9.32 ± 0.72*	1.63 ± 0.132*
Wild-type	4	1.15 ± 0.23	0.11 ±0.032
AT-N96-Q	4	1.16 ± 0.04	0.10 ± 0.031
AT-N135Q	4	1.22 ± 0.20	0.13 ± 0.019
AT-N155Q	4	0.52 ± 0.14*	0.0053 ± 0.0001*
AT-N192Q	4	1.17 ± 0.11	0.14 ± 0.029

* Indicates statistically significant difference ($P<0.05$) in comparison with recombinant wild-type AT.

Interaction of high affinity heparin with wild-type AT and mutant forms of AT were studied as described in section 2.6.6. When excited at 280 nm, the fluorescence emission spectrum of both recombinant and rabbit plasma derived ATs exhibited a maximum at 340 nm with a range of 290-400 nm. The characteristic fluorescence emission maximum at 340-nm indicates that the fluorescence is primarily due to four Trp residues of the AT. No peak or shoulder was observed in the 280-nm excited spectrum at 300-310 nm, suggesting that Tyr emission was minor. The fluorescence emission spectrum of AT in comparison with rabbit plasma derived AT is shown in Fig. 3.16. Upon binding, heparin induced a 40% increase in Trp fluorescence in the plasma derived AT, consistent with what has been reported in the literature (Nordenman and Bjork, 1978a; Nordenman *et al.*, 1978b). The fluorescence spectrum of recombinant AT-WT was very similar to that of rabbit plasma derived AT, in terms of the shape of the curve, relative intensity and the fluorescence emission maximum at 340 nm. The same held true for three underglycosylated mutant variants, AT-N96Q, AT-N135Q, and AT-N192Q, when compared with both plasma-derived and recombinant AT-WT (Figure 3.17). The effect of mass ratios of heparin to wild-type and these three mutant variants on the relative fluorescence enhancement of AT were similar (Fig. 3.17). However, the mass ratio of heparin to the AT-N155Q variant was decreased (Figure 3.17). The binding of heparin to this mutant variant resulted in an increase in fluorescence intensity of only 16%, demonstrating a two-fold reduction in maximal fluorescence change in AT-N155Q.

In order to determine the K_d values of these complexes, the emission spectrum at 340 nM of each AT moiety after excitation at 280 nM was measured on a luminescence

Figure 3.16 Effect of mass ratio of heparin to AT on the relative fluorescence enhancement of plasma-derived antithrombin (panel A) and recombinant wt AT (AT-WT) (panel B).

A

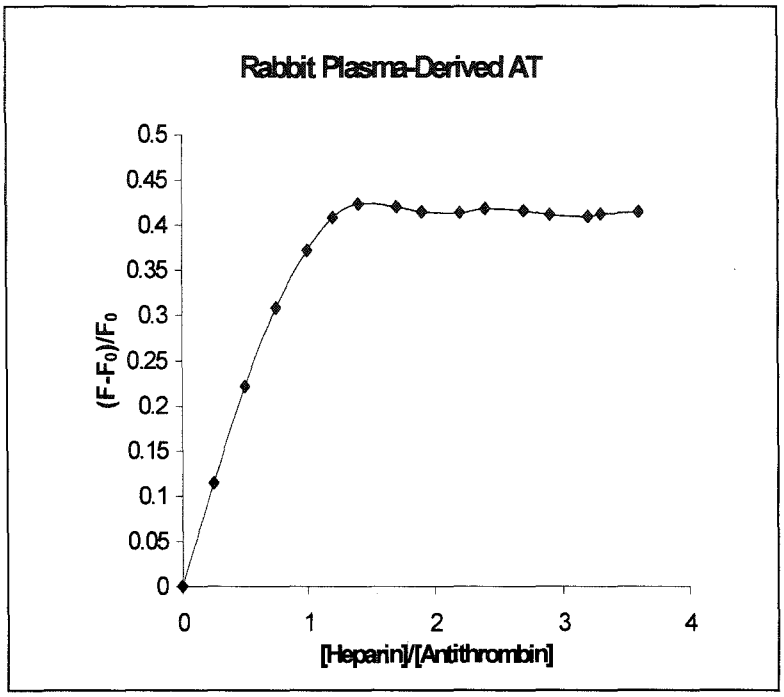
Rabbit Plasma-Derived AT
(F-F0)/F0
0.5
0.45
0.4
0.35
0.3
0.25
0.2
0.15
0.1
0.05
0
0
1
2
3
4
[Heparin]/[Antithrombin]

B

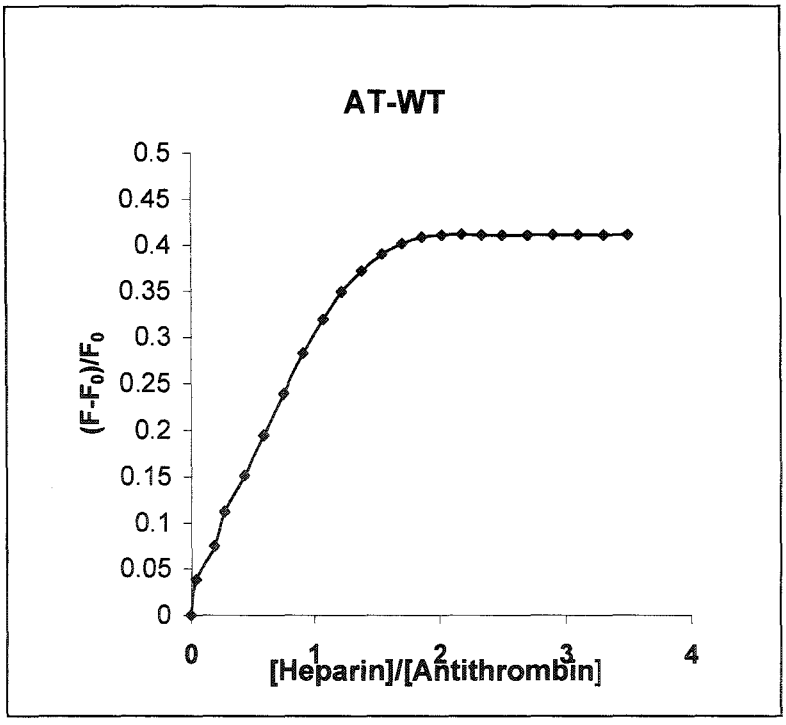
AT-WT
(F-F0)/F0
0.5
0.45
0.4
0.35
0.3
0.25
0.2
0.15
0.1
0.05
0
0
1
2
3
4
[Heparin]/[Antithrombin]

Figure 3.17 Effect of mass ratio of heparin to AT on the relative fluorescence enhancement of the underglycosylated mutant variants of AT. Panel (A). represents AT-N96Q; panel (B). represents AT-N135Q; panel (C). represents AT-N155Q; and panel (D). represents AT-N192Q.

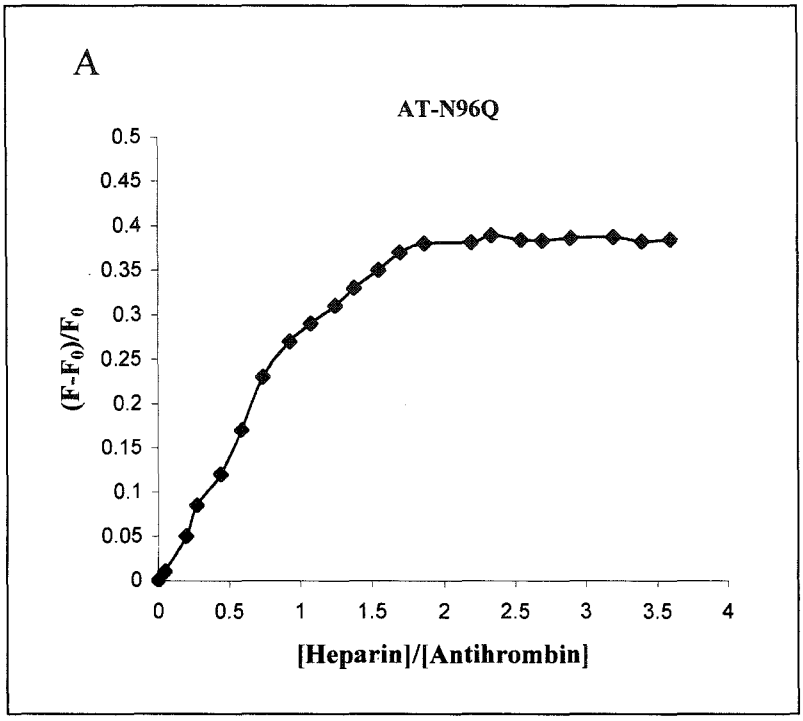
A
AT-N96Q
(F-F0)/F0
0.5
0.45
0.4
0.35
0.3
0.25
0.2
0.15
0.1
0.05
0
0 0.5 1 1.5 2 2.5 3 3.5 4
[Heparin]/[Antihrombin]

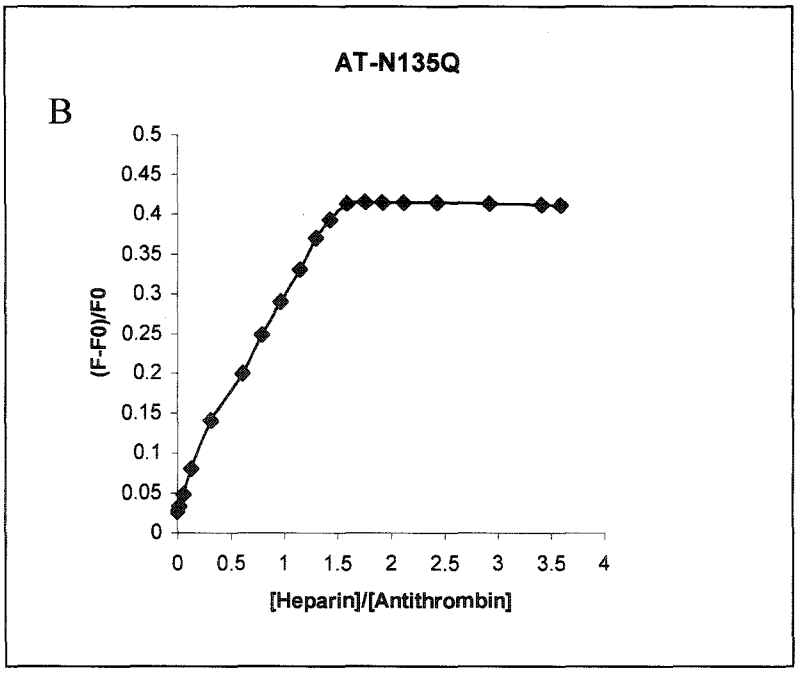
B
AT-N135Q
(F-F0)/F0
0.5
0.45
0.4
0.35
0.3
0.25
0.2
0.15
0.1
0.05
0
0 0.5 1 1.5 2 2.5 3 3.5 4
[Heparin]/[Antithrombin]

C

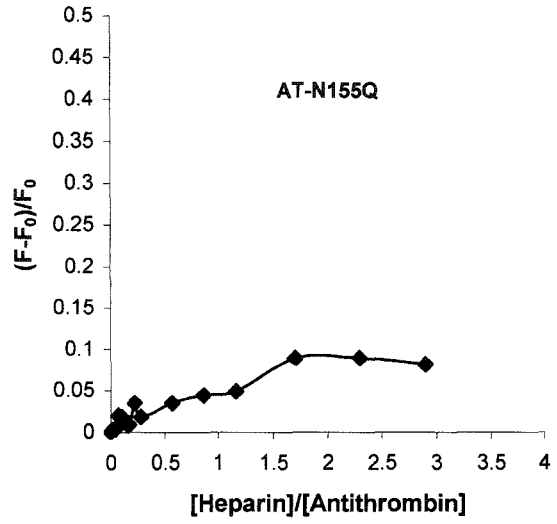
AT-N155Q
(F-F0)/F0
0.5
0.45
0.4
0.35
0.3
0.25
0.2
0.15
0.1
0.05
0
0 0.5 1 1.5 2 2.5 3 3.5 4
[Heparin]/[Antithrombin]

D

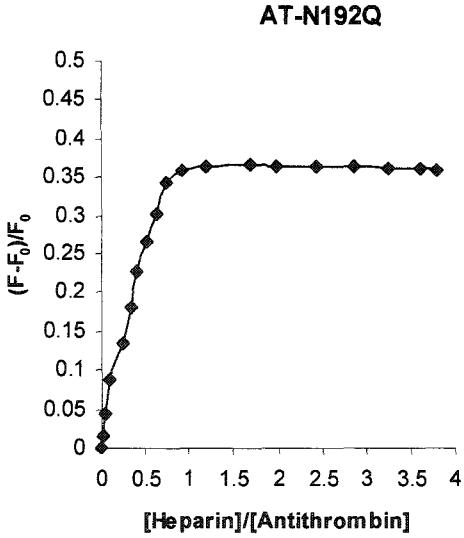
AT-N192Q
(F-F0)/F0
0.5
0.45
0.4
0.35
0.3
0.25
0.2
0.15
0.1
0.05
0
0 0.5 1 1.5 2 2.5 3 3.5 4
[Heparin]/[Antithrombin]

spectrophotometer before titration and after the each addition of heparin. K_d values for each AT moieties were determined by nonlinear least-square fitting of the observed endogenous Trp fluorescence enhancement upon titration with heparin. Table 3.4. summaries the K_d values for the complex formed with each of these AT moieties. The K_d values for heparin and rabbit plasma-derived AT were estimated in this experimental system, to be 3.47±1.70 nM at physiological pH and ionic strength (0.15M). The observed K_d of 6.3 ±1.97 nM for heparin and recombinant AT-WT suggested a 2 fold reduction in the heparin affinity of recombinant AT. Compared with AT-WT, there is a 6-fold decrease in the affinity of AT-N155Q variant for heparin. AT-N96Q showed a small (2-fold) increase in K_d. No difference of K_d was observed between AT-WT and AT-N135Q and AT-N192Q mutant variants.

3.9 *In Vivo* Behavior of Recombinant AT

3.9.1 Purity and Function of Radiolabeled Recombinant AT

Radiolabeling of AT with $Na^{125}I$ or $Na^{131}I$ was undertaken using the IODO-GEN reagent as described in section 2.7.1. Approximately $1X10^7$cpm/μg protein was obtained for each labeling. Each radiolabeled AT moiety was analyzed by SDS-PAGE followed by autoradiography. The result showed that the radiolabeled AT ran as a single band and coincidentally with its unlabeled counterpart. The radiolabeled AT was also capable of forming SDS-stable complexes with human α-thrombin (Fig. 3.18).

Table 3.4 DISSOCIATION CONSTANT (Kd) OF AT

AT	Sample Size (n)	K_d (nM)	Δ Fmax
Plasma-derived	4	3.47 ± 1.70	0.39 ± 0.04
Wild-type	4	6.30 ±1.97	0.37 ± 0.03
AT-N96-Q	4	8.52 ± 3.09	0.36 ± 0.05
AT-N135Q	4	4.88 ±1.56	0.36 ± 0.03
AT-N155Q	6	36.15 ± 4.33*	0.21 ± 0.05*
AT-N192Q	4	4.32 ±2.26	0.38 ± 0.06

* Indicates statistically significant difference in comparison with recombinant wild-type AT ($P<0.05$).

Figure 3.18 Autoradiogram of radioiodinated AT-WT (lane 1). Lane 2 represents radioiodinated AT-WT forming a thrombin-AT complex [^{125}I-AT-WT and unlabeled AT-WT (total 43 pmole) were incubated with human α-thrombin (82 pmole) for 15 minutes].

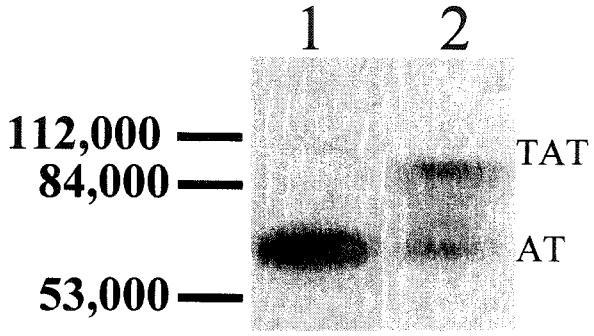
1
2
112,000
84,000
53,000
TAT
AT

3.9.2 Behavior of Radiolabeled Recombinant Rabbit AT and Rabbit Plasma-Derived AT

To compare the terminal plasma clearance of recombinant rabbit AT-WT with that of plasma-derived AT (pAT), ^{125}I-labeled AT-WT and ^{131}I-labeled pAT were injected into six rabbits. Each rabbit was injected with approximately 150 μCi of ^{125}I-labeled AT-WT and ^{131}I-labeled pAT. Plasma samples were collected at designated time points and plasma ^{125}I and ^{131}I radioactivities were counted as described in section 2.7.2. Plasma clearance curves were constructed as shown in figure 3.19. A three-compartment model proposed previously for AT catabolism in the rabbit was used (Carlson et al. 1984). Following curve peeling of each clearance curve from each experiment, it was possible to calculate the rate constants and fractional constants using the equation as described in section 2.7.3. As shown in Table 3.5, no statistically significant difference was observed in a_1 between pAT (0.25 ± 0.03) and recombinant AT-WT (0.24 ± 0.01). The a_1 is a metabolic rate constant that corresponds to the terminal slope of the clearance curve, and pertains to the total body catabolic rate of a protein (Carlson et al., 1985). The extravascular compartment half-lives which represent the terminal clearance of protein from the circulation showed no statistically significant difference between pAT (67.52 ± 7.83 hours) and recombinant AT-WT (70.15 ± 3.12 hours) (Shown in Table 3.6). The rate constant of exchange for the plasma compartment is significant higher in recombinant AT-WT (43.77 ± 10.43) than pAT (14.49 ± 11.90) as shown in Table 3.5.

Figure 3.19 Mean plasma clearance of radiolabeled rabbit ATs in rabbits over 7 days. Each value represents a mean of six determinations. Error bars represent the standard error of the means (n=6), and where not shown are less than the size of the symbol.

(▲) represents pAT

(■) represents AT-WT

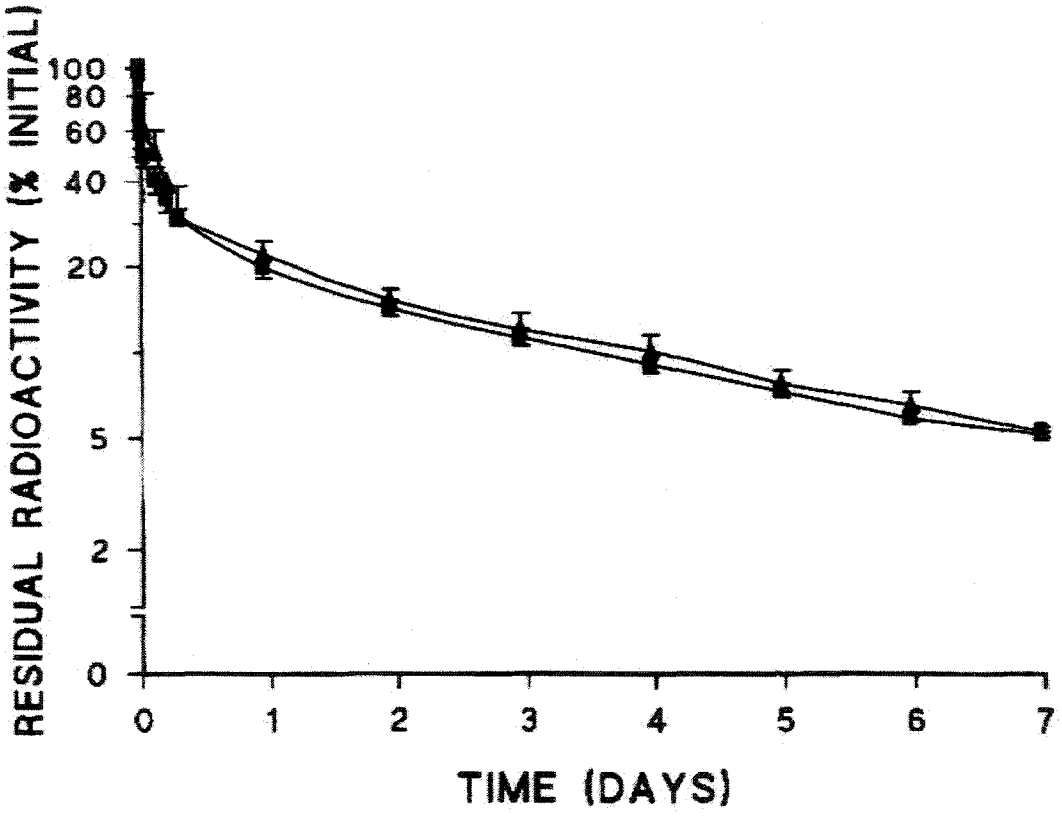
RESIDUAL RADIOACTIVITY (% INITIAL)
100
80
60
40
20
5
2
0
0
1
2
3
4
5
6
7
TIME (DAYS)

3.9.3 Behavior of Radiolabeled Recombinant Singly Underglycosylated AT Variants

The plasma survival of underglycosylated mutant variants of AT was compared with that of recombinant AT-WT. Following iodination with ^{125}I and confirmation of radiochemical purity by autoradiography of dried SDS-PAGE gels, each of the AT-WT and underglycosylated AT variants was injected into rabbits (six rabbit for each group). Plasma ^{125}I radioactivities were counted and a plasma clearance curve was constructed for each rabbit (Fig. 3.20, and Fig. 3.21). The rate constants and fractional constants for each curve in each individual rabbit were then obtained by curve-peeling using a clearance equation in a three-compartment model. The terminal catabolic rate (a_1) is significantly higher in all underglycosylated variants than AT-WT (Shown in Table 3.5). As shown in Table 3.6, in comparison with AT-WT (70.16± 3.12 h), all underglycosylated variants of AT demonstrated an increased rate of terminal clearance, as indicated by their significantly reduced half-lives, with a value of 58.86± 3.70 h, 52.43 ±2.54 h, 55.84±5.87 h and 57.80±2.98 h for AT-N96Q, AT-N-135Q, and AT-N155Q , and AT-N192Q, respectively ($P \leq 0.015$). With regard to the rate constant of exchange for the plasma compartment (a_2 and a_3), no statistically significant difference was observed between recombinant AT-WT and underglycosylated mutant variant (Table 3.5).

The fractional constants for compartment 1 (C1) are lower in mutant variants than that of AT-WT. The fractional constants for compartment 3 (C3) are higher in underglycosylated mutant variants in comparison with AT-WT (Shown in Table 3.7).

Table 3.5 RATE CONSTANTS FOR COMPARTMENT CHANGES OF RABBIT AT

AT	Sample Size (n)	a_1	a_2	a_3
pAT	6	0.25 ± 0.03	3.97 ± 2.22	14.49 ± 11.90*
AT-WT	6	0.24 ± 0.01	3.68 ± 1.79	43.77 ± 10.43
AT-N96Q	6	0.28 ± 0.02*	4.29 ± 1.73	43.29 ± 13.41
AT-N135Q	6	0.31 ± 0.02*	5.36 ± 2.31	43.79 ± 14.29
AT-N155Q	6	0.30 ± 0.03*	5.86 ± 2.00	43.34 ± 14.64
AT-N192Q	6	0.29 ± 0.01*	4.13 ± 1.56	33.49 ± 11.22

* Indicates statistically significant difference ($P<0.05$) in comparison with recombinant AT-WT.

pAT indicates rabbit plasma derived AT.

Table 3.6 SURVIVAL ($t_{1/2}$)OF RABBIT ANTITHROMBIN IN THE CIRCULATION

AT	Sample Size (n)	R^2	$t_{1/2}$ (Hours)	P
pAT	6	0.98	67.52 ± 7.83	0.20
AT-WT	6	0.95	70.16 ± 3.12	
AT-N96-Q	6	0.91	58.86 ± 3.70	0.0001*
AT-N135Q	6	0.99	52.43 ± 2.54	0.00001*
AT-N155Q	6	0.94	55.84 ± 5.87	0.004*
AT-N192Q	6	0.93	57.80 ± 2.98	0.0003*

* indicates statistically significant difference compared with WT

Table 3.7 FRACTIONAL CONSTANTS OF RABBIT AT

AT	Sample Size (n)	C1	C2	C3	Σ C
pAT	6	0.25 ± 0.04	0.35 ± 0.09	0.41 ± 0.11	1.01
AT-WT	6	0.22 ± 0.02	0.45 ± 0.07	0.30 ± 0.10	0.97
AT-N96Q	6	0.13 ± 0.02*	0.46 ± 0.11	0.36 ± 0.15	0.95
AT-N135Q	6	0.12 ± 0.02*	0.41 ± 0.13	0.48 ± 0.10*	1.01
AT-N155Q	6	0.17 ± 0.03*	0.34 ± 0.15	0.44 ± 0.13*	0.95
AT-N192Q	6	0.11 ± 0.02*	0.50 ± 0.12	0.35 ± 0.17	0.96

* Indicates statistically significant difference ($P<0.05$) in comparison with recombinant AT-WT.

Figure 3.20 Mean plasma clearance of radiolabeled rabbit AT over 7 days. Each value represents a mean of six determinations.

(■) represents AT-WT.

(●) represents AT-N96Q

(*) represents AT-N135Q

(▲) represents AT-N155Q

(□) represents AT-N192Q

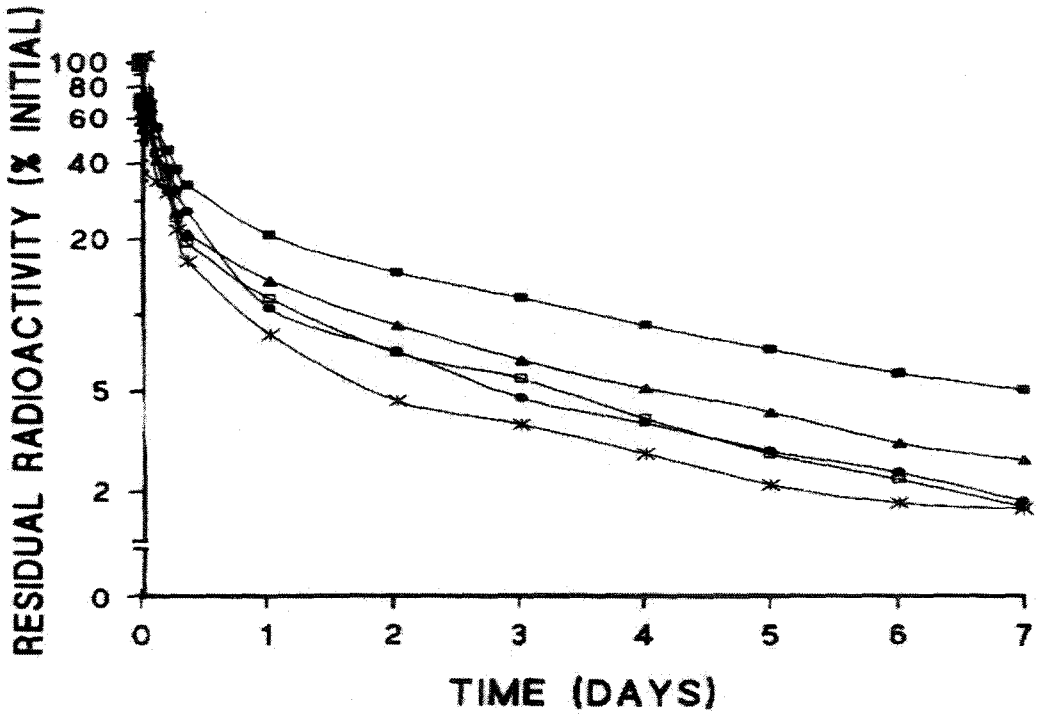
RESIDUAL RADIOACTIVITY (% INITIAL)
100
80
60
40
20
5
2
0
0
1
2
3
4
5
6
7
TIME (DAYS)

Figure 3.21 Clearance of recombinant AT-WT and the AT-N155Q variant from rabbit plasma *in vivo*. Squares correspond to the AT-WT curves, while triangles correspond to AT-N155Q. Error bars represent the standard error of the means (n=6), and where not shown are less than the size of the symbol.

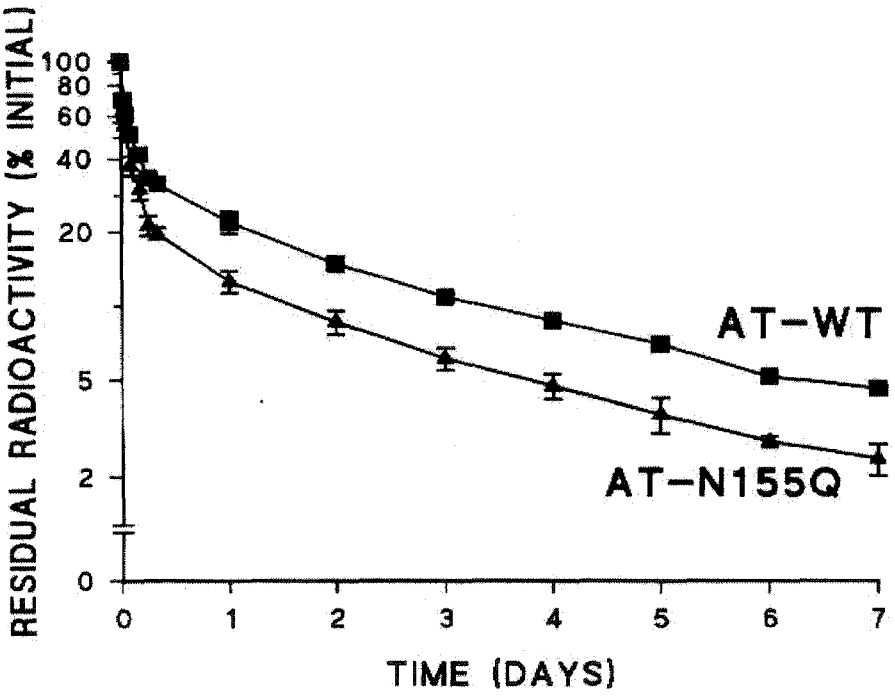
RESIDUAL RADIOACTIVITY (% INITIAL)
100
80
60
40
20
5
2
0
0
1
2
3
4
5
6
7
TIME (DAYS)
AT-WT
AT-N155Q

Although a statistically significant difference was only obtained for AT-N135Q, and AT-N155Q, the values of C3 are higher for AT-N96Q (0.36 ± 0.15) and AT-N192Q (0.35 ± 0.17) compared to that of AT-WT (0.30 ± 0.10). The failure to obtain a statistically significant difference for AT-N96Q and AT-N192Q is probably due to the small sample size used in this study that included 6 rabbits in each experiment. The lower fractional constants for compartment one with higher fractional constants for compartment three are most likely due to the comparatively high catabolic rate of underglycosylated mutant variants.

3.9.4 Radiolabeled Recombinant AT in The Plasma

To exclude the possibility that recombinant AT was breaking down after injection into rabbit circulation, plasma samples containing radiolabeled AT were obtained from a rabbit injected with ^{125}I-labeled AT and subjected for electrophoresis on 8% SDS-PAGE gels under reducing condition, followed by autoradiography. The result demonstrated that radiolabeled AT was intact up to 2 days in circulation as indicated by a single band with a molecular weight of approximately 65 KDa (shown in Fig 3.22). After 2 days, the radioactive band became very faint.

3.10 Analysis of Carbohydrate Composition of AT

3.10.1 Glycosidase F (PNGase F) Treatment of AT

Glycosidase F (PNGase F) cleaves the bond linking the innermost GlcNAc of oligosaccharides and the asparagine residue of N-linked glycoprotein. CHO cell derived AT-WT and underglycosylated

Figure 3.22 Autoradiogram of plasma samples containing radiolabeled AT obtained from a rabbit injected with ^{125}I-labeled AT-WT.

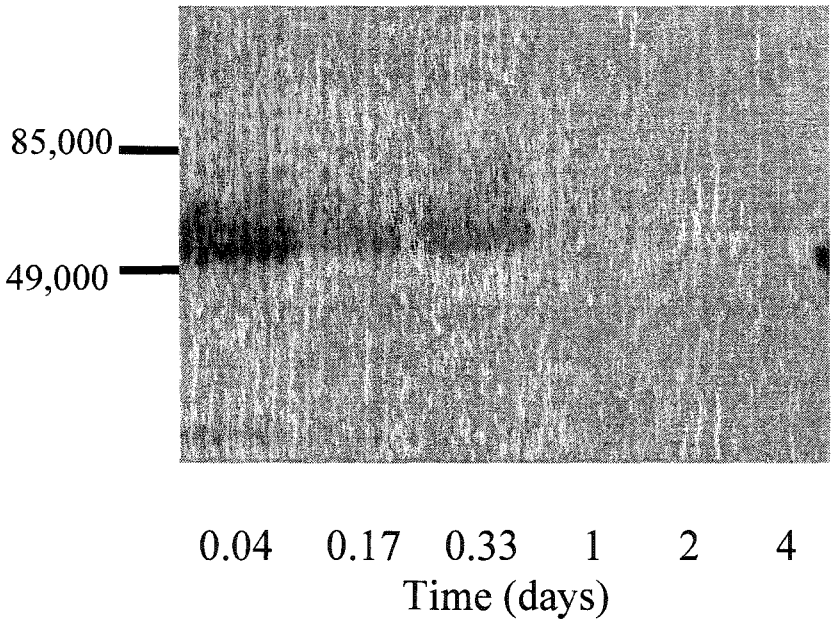
85,000
49,000
0.04 0.17 0.33 1 2 4
Time (days)

mutant variants were reacted with N-glycosidase F under denaturing conditions as described in section 2.8.1. Following reaction with PNGase F, both AT-WT and underglycosylated AT variants migrated faster with a similar molecular weight of approximately 45 KDa, which is expected for the deglycosylated AT. In addition, enzymatic removal of the N-linked glycans eliminated the bulk of the heterogeneity of recombinant AT (Fig. 3.23).

3.10.2 Determination of Terminal Sialic Acid Structure of Recombinant AT

To identify the type of carbohydrate chains present on AT, CHO cell-derived recombinant AT-WT and rabbit plasma-derived AT were electrophoresed on SDS-PAGE gel and transferred to nitrocellulose for binding of glycan-specific lectins as described in section 2.8.2.

The results (table 3.8) demonstrate that CHO cell-derived recombinant AT bound to the lectin MAA, suggesting the presence of terminal α2-3 linked sialic acid. In contrast, the rabbit plasma-derived AT bound to SNA, indicating the presence of terminal α2-6 linked sialic acid. Neither plasma-derived AT nor recombinant AT-WT reacted with GNA, PNA or DSA, which suggested that terminal mannose, O-linked glycans, or terminal galactose-β-(1-4)-N-acetylglucosamine were not present on these ATs.

Figure 3.23 An immunoblot probed with anti-rabbit AT IgG of AT-WT or rabbit plasma derived AT (pd-AT) treated in the presence (+) or absence (-) of PNGase F.

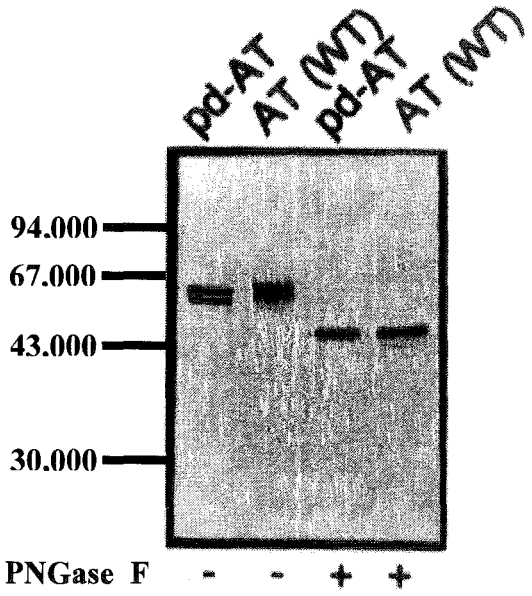
pd-AT
AT (WT)
pd-AT
AT (WT)
94.000
67.000
43.000
30.000
PNGase F - - + +

Table 3.8 SUMMARY OF LECTIN AFFINITY

	GNA	SNA	MAA	PNA	DSA
pAT	-	+	-	-	-
AT-WT	-	-	+	-	-

GNA: *Galanthus nivalis* agglutinin
SNA: *Sambucus nigra* agglutinin
MAA: *Maackia amurensis* agglutinin
PNA: Peanut agglutinin
DSA: *Datura stramonium* agglutinin

4. DISCUSSION

Antithrombin (AT) is the principal anticoagulant protein that inhibits thrombin and factor Xa in plasma (Bauer and Rosenberg, 1991). This 58-KDa anticoagulant protein is synthesized in hepatocytes and secreted into the circulation. During the course of its synthesis, AT is modified at four locations of Asn-X-Ser/Thr N-glycosylation consensus sequences with N-glycosidically linked complex oligosaccharides (Peterson *et al.*, 1979). In the human molecule, the four glycosylation sites correspond to Asn 96, 135, 155, and 192 (Chandra *et al.*, 1983). Because of the presence of a single additional amino acid, Glu7, in the rabbit AT, the N-linked glycosylation Asn residues are located at position 97, 136, 156, and 193 (Sheffield *et al.*, 1992). For the purpose of easy comparison with previous studies using human AT molecule, glycosylation site numbering corresponding to human AT is used throughout the thesis.

Previous studies have demonstrated that different glycoforms of AT have different heparin affinity and proteinase inhibitory activity (Turk, *et al.*, 1997). This is best demonstrated by comparison of the biological function of α-AT and β-AT. While α-AT is fully glycosylated, the β-AT is not glycosylated at Asn 135 position (Brennan *et al.*, 1987). Compared with α-AT, the underglycosylated β-AT isoform binds to immobilized heparin with greater affinity and inactivates thrombin faster in the presence of either heparin or heparan sulfate (Turk *et al.*, 1997; Witmer and Hatton, 1991). In addition, variation of glycosylation affecting biological function of AT has also been shown in a family with mutation in which 7 Ile of AT is substituted to Asn (Brennan *et al.*, 1988). This mutation introduced a new glycosylation site that was partially utilized

for glycosylation. The overglycosylated AT isolated from a patient with this mutation suffering from pulmonary embolism showed a reduced heparin affinity (Brennan *et al.*, 1988). These observations prompted us to examine the effect of individual carbohydrate chains on the biological function of AT. To investigate possible contributions of each glycan chain to the *in vitro* and *in vivo* biological functions of AT, we have systemically and individually mutated each potential N-linked glycosylation site of rabbit AT by substituting the Asn residue to a Gln residue. By using this approach, we have created four underglycosylated forms of AT. Thus, each molecule only possesses three of four glycosylation consensus sites. Two specific objectives were set up for this study: (1). To investigate the effect of each glycan chain on the *in vivo* clearance of rabbit AT; (2). To investigate the effect of each glycan chain on the *in vitro* biological function of AT including heparin binding ability and thrombin inhibitory activity.

4.1 Expression of the AT-WT and Mutant Variants of AT in COS cells

Four underglycosylated mutant AT variants were created by site-directed mutagenesis. The wild-type and mutant variants of rabbit cDNA were inserted into the mammalian expression vector, pCMV5. This vector contains the promoter-enhancer region of the major immediate early gene of the human cytomegalovirus, a synthetic polylinker sequence containing unique cleavage sites, the transcription termination and polyadenylation region of the human growth hormone gene, and the SV40 virus DNA replication origin and early region enhancer (Anderson *et al.*, 1989). The presence of the SV40 origin of replication in pCMV5 results in the amplification of plasmid sequences, when the vector is transfected into mammalian cells previously transformed with the

large T antigen of SV40, such as simian COS cells. Thus, this vector can be used to express a protein in both transient as well as stable cell line expression systems.

To determine if the alteration in glycosylation pattern affected the secretion of AT, wild-type and mutant AT variants were initially transiently expressed in COS-1 cells. Although the COS cell transient expression system only produces limited amounts of protein, it can generate recombinant protein in a relatively rapid and convenient fashion (Kaufman, 1990). This property of the COS cell expression system makes it an ideal means to test the expressibility of pCMV5-AT expression constructs. In the event that the introduced mutations or altered glycosylation pattern affect the folding of the protein and therefore the passage of the protein through the secretion pathway, the transient expression system would allow the detection of this defect and would save the time required to establish permanent cell lines. Therefore, the COS cell system was chosen as an initial step to express AT-WT as well as underglycosylated mutant AT variants.

Transfected COS-1 cells expressed and secreted AT-WT as well as the four mutant AT variants. These recombinant AT molecules were biologically functional as demonstrated by their capability to form thrombin-AT complexes and to bind to heparin. The results demonstrated that all of the AT expression constructs could be expressed in mammalian cells.

4.2 Expression of AT-WT and Mutant Variants of AT in CHO cells

Cell lines that can produce AT-WT as well as underglycosylated variants of AT were established using CHO cells. CHO cells have been used as a predominant system

to produce many therapeutic proteins, including many biologically functional proteins involved in blood coagulation, such as AT, tissue plasminogen activator, factor VIII, and factor IX (Wasley *et al.*, 1991; Zettlmeissl *et al.*, 1994; Spellman *et al.*,1989; Pittman *et al.* 1992; Adamson *et al.*, 1998).

Glycosylation is the most common form of post-translational processing associated with protein synthesis (Sharon and Lis, 1982). The general function of N-glycosylation is to aid in folding of the nascent polypeptide chain and in stabilization of the conformation of the mature glycoprotein (Lis and Sharon, 1993). When this is prevented, some proteins have been shown to undergo degradation, and therefore not be secreted from the cells in which they are synthesized (Dube *et al.*, 1988). Such effects have been demonstrated in human protein C, a serine protease that acts as a natural anticoagulant by inactivating factor Va and factor VIIIa. Single elimination of the carbohydrate side chain at Asn-97 of protein C decreased the efficiency of its production, with a 70-75% reduction in secretion (Grinnell *et al.*, 1991). On the other hand, addition of an extra carbohydrate side chain may also affect protein secretion. This is best illustrated by recently characterized antithrombin deficient family in which the creation of an additional glycosylation site in AT molecule blocks AT secretion, resulting in type I antithrombin deficiency (Fitches *et al.*, 2001).

To determine if the alteration in glycosylation pattern affected the secretion of AT in our study, we compared the AT secretion levels of AT-WT with each underglycosylated AT variant. The wild-type and mutant AT variants were expressed by CHO cells. No differences in the production levels were found between AT-WT and the

four underglycosylated AT variants. To exclude the possibility that some variants were being synthesized at higher rates, but only being secreted at wild-type levels due to intracellular sequestration, pulse chase studies were carried out. Inspection of immunoprecipitated intracellular and extracellular samples showed no differences between the wild-type and four underglycosylated AT cell lines. This similarity was quantified by determining the time required for 50% of the initially labeled intracellular AT to disappear from the cells. The values of the intracellular half-life did not differ significantly between the AT-WT and underglycosylated AT producing cell lines. Therefore, we conclude that the elimination of any single glycan from AT did not affect its intracellular transportation and secretion. Although the pulse chase studies did not include AT producing clones that secreted AT level lower than 0.02 $\mu g/10^6$ cells/24 hours and that a more definite conclusion could not be made before we analyze these clones with lower AT production, our current results are consistent with the yields of human AT obtained by others (Zettlmeissl *et al.*, 1989; Olson *et al.* 1997). Recently, a family with antithrombin deficiency caused by Asn135Thr mutation was reported (Bayston *et al.*, 1999). This mutation results in overexpression of β-AT. Expression of this mutant form of antithrombin in COS cells indicated that the absence of glycosylation at Asn 135 did not affect the secretion of antithrombin from hepatocytes (Bayston *et al.*, 1999). These findings further support our conclusion that the elimination of a single glycan from AT does not affect its secretion.

4.3 Purification of Recombinant AT-WT and Mutant Variants of AT

Purification of AT-WT and mutant variants of AT was achieved by affinity chromatography on heparin-Sepharose followed by Q-Sepharose chromatography. The use of Q-Sepharose chromatography following heparin-Sepharose chromatography also permitted the removal of any possible contaminating free heparin in the preparation, which could have interfered with further characterization of AT molecules.

The purified recombinant wild-type AT preparation showed heterogeneity in that it contained two isoforms, a slow migrating major form and a more rapidly migrating minor form. This electrophoretic mobility pattern is similar to that observed in plasma derived AT preparation that contains α and β isoforms. The difference between α and β isoforms from plasma derived AT is due to incomplete glycosylation of Asn 135. While the majority of AT found in plasma is fully glycosylated (α isoform), approximately 10% of the AT is not glycosylated at Asn 135 (β isoform) (Peterson and Blackburn, 1985; Brennan *et al.*, 1987; Carlson and Atencio, 1982; Turk *et al.*, 1997). The presence of fast moving minor forms in AT-N96Q, AT-N155Q, and AT-N192Q preparations, but the lack of such forms in the AT-N135Q preparation strongly suggested that the minor form in the recombinant AT preparation is derived from incomplete glycosylation of Asn 135, like the plasma-derived β–AT isoform. This conclusion is further supported by the fact that the digestion with N-glycosidase F eliminated this apparent molecular weight difference. Therefore, each preparation of AT-N96Q, AT-N155Q, and AT-N192Q contains two forms of AT in which the major form contains three glycans while the minor form contains two glycans. However, in each case of these three mutant

variants, following purification, this two-glycan isoform was present in lesser quantities than the three-glycan major form. This distribution likely arose due to differences in heparin affinity, and allowed us to make meaningful conclusions about the three-glycan forms, because of their predominance.

It has been shown in both rabbit and human AT that the consensus sequence for N-linked glycosylation at positions 96, 135, 155 is Asn-X-Thr, while the 135 consensus sequence is Asn-X-Ser. Previous studies have demonstrated that Asn-X-Ser consensus sequences are used less efficiently than Asn-X-Thr consensus sequences during N-glycosylation (Bause and Legler, 1981). Recently, Picard *et al.* have substituted Asn-135 consensus sequence in AT cDNA from a code for Asn-X-Ser to a code for Asn-X-Thr using a site-directed mutagenesis technique (Picard *et al.*, 1995). AT with Asn-X-Ser and Asn-X-Thr consensus sequences were expressed in baculovirus-infected insect cells. In contrast to the Asn-X-Ser sequence, which expressed a mixture of α-AT and β-AT molecules, the Asn-X-Thr variant produced the α-AT form exclusively. These results suggested that the preference of the oligosaccharyl transferase for Thr, rather than Ser, at the third position of the Asn-135 consensus sequence was responsible for the production of partially glycosylated β-isoform of AT (Picard *et al.*, 1995). Although baculovirus system was used in this study, it is likely that this explanation could be applied to mammalian cells.

4.4 Carbohydrate Composition of CHO-Derived AT

The glycosylation potential in CHO cells has been well characterized. CHO cells allow processing to multi-antennary and poly-N-acetyllactosamine oligosaccharides. It

has been demonstrated that CHO cells do not transfer sialic acid in an α2-6 linkage; instead an α2-3 linkage was identified on the CHO-derived protein. Fucosylation of recombinant proteins also occurred in CHO-derived recombinant glycoproteins (Spellman *et al.*, 1989).

The SDS-PAGE analysis showed that the bands exhibited by AT produced by CHO cells were more diffuse than those obtained with plasma-derived AT. The digestion with N-glycosidase F markedly decreased the apparent size heterogeneity. Each N-glycosidase F-treated deglycosylated recombinant AT thus migrated in SDS/PAGE under reducing conditions essentially as a single sharp band with no discernible difference in mobility from the band given by deglycosylated plasma AT. These results suggested that the diffuse bands were caused by relative size heterogeneity possibly due to the heterogeneous glycosylation of recombinant AT. Considerable heterogeneity of CHO-derived recombinant AT was also noted in previous reports (Zettlmeissl *et al.*, 1989; Bjork *et al.*, 1992). Bjork *et al.*, performed an analysis of the carbohydrate structures of CHO-derived AT and demonstrated the heterogeneity could be attributed to the presence of different types of carbohydrate chains, including bi, tri, and tetra-antennary complex chains (Bjork *et al.*, 1992). This observation is in agreement with the report from Zettlmeissl *et al.* who found that the recombinant human AT from CHO cells contains a considerable proportion of tri- and tetra-antennary chains in addition to bi-antennary chains (Zettlmeissl *et al.*, 1989).

Similar heterogeneity of recombinant AT was also reported in human AT expressed in BHK cells (Fan *et al.*, 1993). Fan *et al.* reported three different forms of

AT derived from BHK cells, which differ in their carbohydrate composition and affinity for heparin. The form I had the lowest affinity and contained a high proportion of highly branched complex carbohydrate. The form II had higher affinity and contained both complex and high mannose-type chains. The form III had the highest affinity and was similar to form II in the type of carbohydrate present, but had a lower level of glycosylation, consistent with the absence of carbohydrate at one of the four glycosylation sites (Fan *et al.*, 1993). It is interesting to note that Bjork *et al.* also expressed human AT in BHK cells, but demonstrated two different forms of AT which had properties different from the three forms reported by Fan *et al* (Bjork *et al.*, 1992). These results suggest that difference in growth conditions may influence the degree of carbohydrate processing and thus the forms of AT that are secreted (Goochee and Monica, 1990). The observations indicate that it is essential that the comparison between recombinant AT variants should be made in AT preparations derived from same growth conditions (Fan *et al.*, 1993).

Terminal sialic acid structures of CHO cell–derived AT and rabbit plasma AT were determined by the binding of specific lectins. The results demonstrated that CHO cell-derived AT would bind to MAA, but not to SNA, indicating that it contains terminal α2-3 linked sialic acid. Plasma-derived AT was shown to bind to SNA, but not to MAA indicating the presence of terminal α2-6 linked sialic acid. These findings are consistent with previous studies (Zettlmeissl *et al.*, 1989). The recombinant AT showed no reactivity to GNA, PNA or DSA, which suggested that terminal mannose, O-linked

glycan, or terminal galactose-β-(1-4)-acetylgalactosamine were not present. These results are in agreement with previous reports (Zettlmeissl *et al.*, 1989).

4.5 *In Vivo* Clearance of Plasma-Derived AT and Recombinant AT-WT

It has been reported that foreign AT was more rapidly catabolized than homologous AT. The hypercatabolism of human AT in the rabbit was documented (Regoeczi, 1987). Similarly, mice were also showed to catabolize human AT more rapidly than homologous AT (Shiffman and Pizzo, 1982). Because of these observations, we decided to produce recombinant rabbit AT for *in vivo* study in rabbits, which eliminated the problems of using a heterologous system. Although the recombinant AT was expressed from CHO cells, which impart a different glycosylation pattern from that produced in rabbit hepatocytes, our study provides a partially homologous system in that the *in vivo* studies of recombinant AT were performed in the same species as that from which the cDNA that we used was derived. While a completely homologous analysis would have been desirable, this would have required not only a transformed rabbit hepatoma cell line to be available, but also that it not produce endogenous AT. The partial homology that we achieved is greater than in any other published analysis of recombinant AT *in vivo* behaviour.

To investigate whether the differences in the oligosaccharide portion had an effect on the pharmacokinetic properties of recombinant AT, the plasma clearance profile of CHO-derived AT-WT was compared with that of rabbit plasma-derived AT in the rabbits. The plasma-derived and recombinant AT from CHO cells showed very similar properties. Calculation of the plasma curve components was undertaken by a

curve-peeling technique using linear regression analysis. Curve peeling showed that the plasma curves were best described by three exponents (Carson and Jones, 1979). Therefore, a three-compartment model, proposed previously by Carlson *et al.* was used to describe the behaviour of AT (Carlson *et al.*, 1985). This model has been used previously to explain the clearance of the radiolabeled AT from the rabbit circulation. The three compartments were defined as: compartment 1, intravascular space (plasma compartment); compartment 2, noncirculating vascular wall associated compartment; and compartment 3, extravascular space (Carlson *et al.*, 1985).

Following curve peeling of each exponential from each plasma curve, and calculation of the clearance equations in a three compartment model, it was possible to calculate fractional constants (C1, C2, C3) and the respective rate constants of exchange between these compartments (a1, a2, and a3) (Carlson *et al.*, 1985; Witmer and Hatton, 1991). No statistically significant difference was observed in a1 between plasma-derived AT and CHO-derived AT. The extravascular compartment half-lives which represent the clearance of protein from the circulation showed no statistically significant difference between plasma-derived AT and CHO-derived AT. The result support the suitability of the transfected CHO cell expression system employed in this study.

Two possible types of kinetic models have been proposed by Carlson *et al.* to describe the *in vivo* three exponential distribution of AT in the rabbit (Carlson *et al.*, 1984; 1985) (Shown in Figure 4.1). The first model consists of a central plasma compartment into which radiolabeled AT is injected. The nonvascular associated compartment and extravascular compartment exchange with the central plasma

Figure 4.1 Two models for the three compartment distribution of AT in the rabbits. Model A, the independent compartment model consists of a central plasma compartment into which radiolabeled AT is injected. The nonvascular associated compartment and extravascular compartment exchange with the central plasma compartment independently. Model B, the continuous transport model represents that AT moves from the plasma through nonvascular associated compartment to the extravascular space. This model suggests that AT from a central plasma compartment first passes to the vascular-endothelial compartment, and then moves to the extravascular compartment (Modified from Carlson *et al.* 1984).

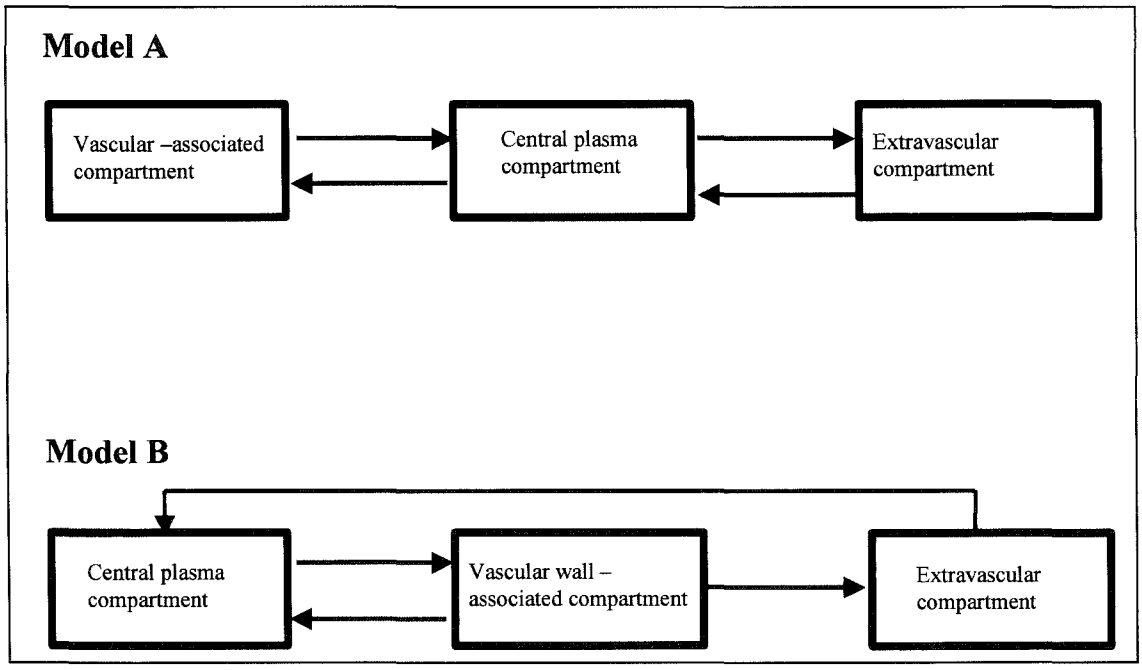
Model A
Vascular –associated compartment
Central plasma compartment
Extravascular compartment
Model B
Central plasma compartment
Vascular wall – associated compartment
Extravascular compartment

compartment independently. The second model considers that AT moves from the plasma through nonvascular associated compartment to the extravascular space. This model suggests that AT from a central plasma compartment first passes to the vascular-endothelial compartment, and then moves to the extravascular compartment (Carlson *et al.* 1984).

It is interesting to note that the rate constant of exchange for the plasma compartment is significant higher in CHO-derived AT than plasma-derived AT. These observations suggest that CHO-derived AT gains access to non-circulating vascular associated compartment and extravascular compartment quicker than plasma derived AT. This difference may be due to the different patterns of glycosylation between plasma and CHO derived AT. It is also possible that the higher rate constant of exchange for the plasma compartment may be due to the degradation of AT in the plasma. To exclude this possibility, plasma samples were obtained from a rabbit injected with ^{125}I-labeled AT and subjected to electrophoresis. The result showed that radiolabeled AT was intact up to 4 days post-injection in the circulation. These results indicate that the higher rate constant is most likely due to rapid distribution of AT to the extravascular compartment and/or non-circulating vascular associated compartment, rather than due to rapid protein degradation.

4.6 *In Vivo* Clearance of Recombinant AT-WT and Underglycosylated AT Variants

Compared to the wild-type AT preparation, all underglycosylated mutant AT proteins showed rapid catabolism as demonstrated by an increased rate of terminal

clearance. The rate constant for protein catabolism is significantly higher for underglycosylated mutant variants than that of wild-type recombinant AT. The *in vivo* catabolic half-lives for the AT-N96Q, AT-N135Q, AT-N155Q, and AT-N192Q decreased by 16%, 25%, 20% and 17% respectively relative to that of AT-WT. A statistically significant difference in the catabolic half-life was identified between the AT-WT and each mutant variant. However, no statistically significant difference was identified among the catabolic half-lives of the underglycosylated mutant variants. These results suggested that, for the most part, and in particular for terminal clearance, the extent of glycosylation is more important than its location for determining AT clearance. Further *in vivo* studies of double and triple underglycosylated forms of AT as well as totally deglycosylated AT are needed before a final conclusion can be made. The findings from the current study are consistent with previous suggestions that AT clearance is most strongly influenced by its degree of sialylation. Removal of terminal NeuAc by sialidase treatment *in vitro* drastically decreases the *in vivo* half-life of both plasma and recombinant AT (Zettlmeissl *et al.*, 1989).

The mechanisms by which AT is cleared from the circulation are not completely understood. Recent investigations suggested that lipoprotein receptor-related protein (LRP) is responsible for removal of thrombin-AT complexes from the circulation (Kounnas *et al.*, 1996). Based on the interaction of AT with the luminal surface of the normal compared to the de-endothelialized rabbit thoracic aorta in conjunction with recent crystal structure studies, a model to explain the *in vivo* behavior of AT has been proposed (Witmer and Hatton, 1991; Wells *et al.*, 1999). The model views the turnover

of AT and thrombin-AT as follows. Plasma AT binds to extracellular heparan sulfate proteoglycan sites in the blood vessel subendothelium where AT is presumably located at a favorable site for inhibiting thrombin. A small amount of thrombin production due to "wear-and-tear" injury can be contained by this endogenous pericellular AT. Thrombin that binds to the heparan sulfate-bound AT cleaves the exposed loop and forms the thrombin-AT complex. This interaction induces conformational changes at the heparin-binding site, with a consequent release of the thrombin-AT complex from the heparan sulfate proteoglycan sites. The thrombin-AT complex is then displaced by active AT at the heparan sulfate-binding sites to maintain the antithrombotic potential of the extracellular space. The displaced thrombin-AT complex then passes into the blood stream or lymph circulation and is cleared by liver mediated through lipoprotein receptor-related protein (LRP) (Kounnas *et al.*, 1996; Wells *et al.*, 1999).

Previous studies have shown that the rapid clearance of radiolabeled β-AT from the plasma compartment was due to a rapid uptake of β-AT by organ capillaries and quick transendothelial passage of β-AT (Carlson *et al.*, 1985). The β-AT isoform was also absorbed preferentially by the aortic subendothelium, and when bound to the subendothelium, β-AT was displaced more readily by thrombin by forming a thrombin-AT complex (Witmer and Hatton, 1991). These observations indicate that β-AT is the more active form of AT and may play a vital role for controlling thrombogenic events caused by injury to the vascular wall. Indeed, β-AT has been shown to be more effective than α-AT in preventing thrombosis on the injured vessel wall after balloon injury of the rabbit aorta (Frebelius *et al.*, 1996).

Our results from the study of the AT-N135Q mutant, which is equivalent to plasma-derived β-AT, is consistent with previous observations of the *in vivo* behavior of plasma-derived α-AT and β-AT. Although no attempt was made to measure their distribution in the aortic wall endothelium and subendothelium, it is deduced, based on the previous study of plasma derived β-AT, that reduced half-life is due to rapid transendothelial passage and higher binding affinity toward subendothelium (Witmer and Hatton, 1991). These properties may lead to more active biological function *in vivo*. In comparison with AT-N135Q, the other three underglycosylated mutants, AT-N96Q, AT-N155Q, and AT-N192Q have very similar *in vivo* behavior. These observations suggest that elimination of any glycan side chain may accelerate transendothelial passage of AT.

4.7 Heparin Binding Affinity of Wild-Type and Underglycosylated AT Variants

The interaction of AT with heparin causes a marked fluorescence enhancement of the intrinsic protein emission intensity (Nordenman *et al.*, 1978b). This fluorescence enhancement is due to a heparin-induced conformational change in AT, which results in change in the local microenvironment around buried tryptophan residues. There are four tryptophan residues in AT. In human AT, these tryptophan residues are located at amino acid position 49, 189, 225, and 307 (Manson *et al.*, 1989). It has been shown that high-affinity heparin gave a fluorescence increase of about 40% when bound to either human or bovine plasma-derived AT (Olson, 1988).

The interaction of the purified recombinant AT proteins with heparin was investigated by monitoring heparin-induced intrinsic fluorescence change on AT. The

identical overall change in intrinsic fluorescence (40%) and similar binding curves between plasma-derived and recombinant rabbit AT were observed. The same held true for three mutagenically underglycosylated AT variants (AT-N96Q, AT-N135Q, and AT-N192Q), with the exception of AT-N155Q, which showed an increase of 16% in intrinsic fluorescence, equivalent to a 2-fold reduction in the overall fluorescence change relative to the AT-WT.

To quantify the differences in affinity of the recombinant AT for heparin, dissociation constants were determined for heparin-AT complexes using the enhancement of endogenous tryptophan fluorescence that accompanies heparin binding. The titrations were fit by nonlinear regression analysis to calculate Kd values (Olson, 1993b). Although the recombinant AT-WT appears to show slightly decreased heparin affinity compared with plasma-derived AT, no statistically significant difference was obtained.

In comparison with AT-WT, AT-N135Q and AT-N192Q appear to have slightly higher heparin affinity. However, there is no statistically significant difference in dissociation constants for heparin amongst the AT-WT and the AT-N135Q or AT-N192Q. The AT-N96Q showed a small (2-fold) increase in Kd. Compared with AT-WT, however, there was significant reduction in heparin affinity for AT-N155Q (6-fold increase in Kd). These results suggest that a failure to glycosylate Asn 155 in recombinant rabbit AT lead to reduction in its ability to bind to heparin.

During the time that the experimental work of this study was being completed, Olson *et al.* published a study in which the effect of individual carbohydrate chains of

recombinant human AT on heparin affinity was investigated (Olson *et al.*, 1997). In this study, each of the four Asn residue sites of glycosylation in human AT molecule was mutated to Gln to block glycosylation. The authors demonstrated a heterogeneous population of recombinant AT produced from BHK cells. Two main forms of AT in each variant were identified with elution profiles at about 0.5M and 1.1 M NaCl respectively (Olson *et al.*, 1997). When the first heparin affinity purified product was applied for rechromatography with heparin-agarose affinity, the authors were able to obtain the AT products with only higher heparin affinity. Using AT preparations with the higher heparin affinity, the authors found that that AT-N96Q and AT-N155Q, and AT-N192Q variants showed approximately two- to threefold higher affinity compared with wild-type AT. AT-N135Q variant showed a sevenfold higher affinity (Olson *et al.*, 1997).

AT-N135Q is equivalent to β-AT in rabbit or human plasma, which has been reported to have an increased heparin affinity (Turk *et al.*, 1997). Although a higher heparin affinity for AT-N135Q is seen in the present study, no statistically significant difference from AT-WT was observed. This is most likely due to the fact that our expression system produced limited quantities of AT. As a result, we were unable to obtain sufficient amounts of AT to further separate lower affinity AT from AT with higher heparin affinity by rechromatography with heparin agarose. Therefore, our AT preparations were more heterogeneous than the AT preparation used by Olson *et al* with regard to heparin affinity (Olson *et al.*, 1997). The presence of AT with lower heparin

affinity in each preparation of AT likely limited our ability to detect the difference in heparin affinity between AT-WT and AT-N135Q.

It has been shown that heparin binding to AT occurs as a two-step process. The first step is association of heparin and AT involving electrostatic interactions and no conformational change. The second step involves conversion of AT to the active conformation (Olson *et al.*, 1993b). The higher affinity of β-AT for heparin arises not from stronger initial binding to heparin but from faster conversion of β-AT to the active protease-binding conformation (Bjork and Olson, 1997). The oligosaccharide side chain does not interfere with the initial weak binding of heparin to AT. Instead, the carbohydrate side-chain at Asn-135 reduces the heparin affinity of α-AT primarily by altering the heparin-induced conformational change (Bjork and Olson, 1997).

It is interesting to note that using AT with higher heparin affinity, Olson *et al.* demonstrated that deletion of Asn 155-linked oligosaccharides enhanced the heparin-affinity of human AT (Olson *et al.*, 1997). However, the authors also showed the presence of a population of nonfunctional AT with lower heparin affinity in the AT-N155Q mutant. This population of nonfunctional AT was not identified in AT-N96Q, AT-N155Q, and AT-N192Q (Olson *et al.*, 1997). The presence of such nonfunctional antithrombin in this variant led the authors to conclude that the elimination of the glycan side chain at Asn155 causes greater propensity of this deglycosylated AT to spontaneously transform to more stable, but inactive conformations with reduced heparin affinity through intra- or intermolecular insertion of their reactive center loops into β-sheet A (Olson *et al.*, 1997). Our results with AT-N155Q showed that the

removal of glycan at 155 reduces AT heparin affinity. The underlying reasons that may be responsible for the difference between our observation and the report from Olson et al. are not clear. There are several possible explanations:

1). While our study used the rabbit AT cDNA and CHO cells as the expression system, Olson *et al.* expressed mutant variants in BHK cells using the human AT cDNA (Olson *et al.*, 1997). It is possible that a significant large proportion of AT-N155Q mutant produced in our system underwent a conformational transformation to an inactive, stable conformation, which only occurred in a small proportion of the AT-N155Q mutant produced in the system using human AT cDNA and BHK cells. This conformational change could reduce heparin affinity, and consequently, reduce the heparin accelerated thrombin inhibitory activity. Olson *et al.* removed this portion of nonfunctional AT by rechromatography when they analyzed their mutant variants (Olson *et al.*, 1997).

The spontaneous conversion of active AT to the inactive (latent form) has been documented in plasma from health individuals (Zhou *et al.*, 1999). This process is slow under physiological condition and is likely to contribute to the natural senescence and turnover of the protein. However, more rapid conversion occurs on incubation of AT at 41°C or 50°C (Wardell *et al.*, 1997). It is possible that elimination of glycan side chain at Asn155 accelerates the conversion of rabbit AT to inactive forms. In addition, the inactive AT can form dimers with active AT and thus interfere the function of active AT (Zhou *et al.*, 1999). Moreover, recent studies have suggested that the latent form of AT preferentially links to the β-isoform of AT to form a dimer complex (Zhou *et al.*, 1999).

This dimer complex could be eliminated from the circulation rapidly. Future study is needed to analyze AT-N155Q recombinant AT using nondenaturing PAGE electrophoresis. The results from such a study would be helpful in identifying the latent form of AT as well as dimer complexes.

2). It is also possible that the results of our study could reflect the fact that Asn155-linked carbohydrate plays an important role in the heparin affinity of rabbit AT, which may not be apparent in human AT. Based on crystallization of intact AT and co-crystallization of AT and heparin pentasaccharide, as well as computer modeling, it has been suggested that the heparin binding sites of AT are formed by the amino-terminal portion of the molecule in conjunction with residues on helices A and D (Carrell, *et al* 1997b). Asn 155 lies at the N-terminal end of helix E on the surface of the molecule. It is possible that the absence of glycan chain at this position allows this region to assume a conformation that impinges on, and constricts the proposed heparin binding site, thus impairing the ability of the AT-N155Q mutant to bind heparin (Huntington, *et al.*, 2000b).

4.8 Thrombin Inhibitory Activity of AT-WT and mutant AT variants

The thrombin inhibitory action of AT depends upon the formation of a stable 1:1 stoichiometric covalent complex through the P1 residue of AT and the active site serine of the thrombin (Bjork, 1982b). This reaction is slow with a inhibition rate constant of 7-11 x 10^3 $M^{-1}sec^{-1}$. However, the rate of inhibition of thrombin by AT is accelerated up to 2000-4000 fold when heparin is added to the reaction (Atha *et al.*, 1984; Bjork *et al.*,

1989). The reported rate of the AT-thrombin reaction is 1.5-4 x 10^7 $M^{-1}sec^{-1}$ in the presence of optimal amount of heparin (Olson *et al.*, 1993b).

The functional properties of recombinant AT-WT and mutant underglycosylated AT variants were examined through their thrombin inhibitory activities. Initial qualitative experiments revealed that the recombinant wild-type and all underglycosylated mutant variants were biologically active as judged by their ability to form SDS-stable complexes with thrombin. Further analysis of the kinetics of thrombin inhibition by AT variants was performed using a discontinuous thrombin inactivation assay. Using pseudo-first order conditions, second order rate constants (K_2) were subsequently calculated for the thrombin inhibitory activity of AT (Olson *et al.*, 1993b). The mean K_2 for the inhibition of human α-thrombin by rabbit plasma-derived AT was found to be 9.32 x 10^3 $M^{-1}sec^{-1}$ a value similar to that published previously by others (Olson *et al.*, 1993b). Use of high-affinity heparin prepared in our laboratory increased this rate constant to 1.63 x 10^6, a value that is 9-fold lower than the published value (Olson *et al.*, 1993b). This difference is most likely due to the fact that the heparin used in the previous publications was a more highly purified fraction subjected to both affinity purification and size-fractionation (Olson *et al.*, 1993b). This highly purified fraction has higher AT affinity than the heparin that we used in the current study, and would therefore be expected to support higher maximal rates of inhibition. In addition, we used a single concentration of our high-affinity heparin, one which may not have supported maximal rates of thrombin inhibition. Thus, there are at least two factors which explain the lower maximal rates of thrombin inhibition observed in our study,

without even considering the possibility that rabbit AT is intrinsically less reactive with human thrombin than its human counterpart.

The recombinant CHO-derived rabbit AT-WT was less active than its plasma-derived counterpart both in the presence and absence of heparin. The decreased thrombin inhibitory activity seen in recombinant AT may be caused by the nature of the carbohydrate content which influences heparin binding and kinetics of thrombin inactivation. Previous studies have showed that the pattern of glycosylation is more heterogeneous in recombinant AT than that in plasma-derived AT (Zettlmeissl *et al.*, 1989; Fan *et al.*, 1993). A small fraction of AT with increased glycosylation has been isolated from recombinant AT and was found to be responsible for decreased heparin affinity (Bjork *et al.*, 1992). In addition, previous reports have indicated that a fraction of heparin affinity purified AT from BHK cell-derived conditioned medium was inactive (Olson *et al.*, 1997). It is possible that a small fraction of inactive recombinant wild-type AT is present in our AT preparation. Therefore, the calculated second order rate constant for recombinant AT-WT is lower than that of plasma-derived AT.

No significant differences were observed between the AT-WT and three underglycosylated mutant variants (AT-N96Q, AT-N135Q, and AT-N192Q), in terms of either heparin uncatalyzed or heparin catalyzed rate constants. However, the rate constant was significantly reduced for the AT-N155Q variant, by 2 and 20 fold in the absence and presence of heparin, respectively. These results suggest that a failure to glycosylate Asn 155 in AT results in a reduction of its ability to inhibit thrombin most notably in its heparin-catalyzed mode, as predicated by its lower affinity for heparin.

This finding could be due to the presence of a significant portion of non-functional AT in the AT-N155Q preparation as it has been proposed that elimination of Asn 155 linked glycan side change may cause spontaneous transformation of AT to its inactive form (discussed in the previous section) (Olson *et al.*, 1997). However, it is also possible that this glycan side chain may play an important role in AT-thrombin interaction, and removal of it decreases thrombin inhibitory activity.

Human AT has been crystallized in a dimeric form in which one molecule is in an intact conformation, and the other in an inactive, latent form (Carrell and Evans, 1992). By comparison to the α1-antitrypsin crystal structure, in which the P1 Met residue faces away from the body of the protein and is available for protease interaction, the AT P1 Arg faces toward the body of the protein (Carrell and Travis, 1985). As a consequence, AT is proposed to circulate in a sub-maximally active state. The structure of pentasaccharide-bound antithrombin has recently been solved by X-ray crystallography (Carrell *et al.* 1997b). This structural study and biochemical studies have indicated that binding of heparin to AT causes a series of conformational changes, involving an interdomain rotation of the bottom half of the molecule in relation to the top half, expulsion of the preinserted proximal hinge of the reactive center loop, and reorientation of the P1 Arg into an outward-facing position, providing an optimal conformation (Carrell *et al.*, 1997b; Belzar *et al.*, 2002). These conformational changes allow AT to bind to the active site of thrombin. The binding of thrombin to the reactive bond of AT is accompanied by conformational changes of both thrombin and AT. The changes include insertion of the cleaved reactive-center loop of the AT into the A β-

sheet of the molecule, with pole to pole displacement of the protease (Huntington and Carrell, 2001; Huntington *et al.*, 2000b). It is possible that deletion of Asn 155-linked oligosaccharide may affect these conformational changes and thus impair AT inhibitory activity.

Our results demonstrate that elimination of the Asn-155 linked oligosaccharide is associated with reduced heparin binding affinity and thrombin inhibitory activity of AT. The exact mechanisms responsible for these findings are not known. More studies are needed to further characterize this molecule.

4.9 Future Studies

1). Previous research has demonstrated that the accelerating effect of heparin on factor Xa inhibition by AT is mainly due to the conformational activation of AT upon binding of the pentasaccharide, while the major contribution to the rate enhancing effect of heparin on thrombin inactivation results from the bridging by heparin of the ternary complex with thrombin and AT (Olson *et al.*, 1992). In the present studies, we investigated the effect of each carbohydrate chain of recombinant AT on its *in vitro* biological function, primarily heparin binding affinity and thrombin inhibitory activity. Future studies should evaluate the effect of each carbohydrate chain of AT on its inhibitory activity on factor Xa. It will be very interesting to study the factor Xa inhibitory activity of AT-N155Q mutant. The results of such a study would provide more information on the biological effects of Asn 155-linked carbohydrate in the AT function.

2). The exact mechanisms for which the absence of Asn155 linked glycan results in a decrease in heparin affinity and thrombin inhibitory activity is not known. One of the explanations is that the absence of Asn155 linked glycan promotes the spontaneous transformation of AT to an inactive form through intra- or intermolecular insertion of their reactive center loops into β-sheet. It will be useful to analyze the wild-type and underglycosylated mutant variants of AT using nondenaturing PAGE electrophoresis. This analysis should be helpful in identifying the latent form of AT, AT dimer complexes, and possible aggregates if they are formed in the AT preparations.

3). The results from the present study indicate that the absence of any glycan side chain is associated with increased rate of catabolism of AT. This may result from the accelerated transendothelial passage of underglycosylated AT variants (Witmer and Hatton, 1991). Further studies in continuation of this investigation should be performed to evaluate the distribution of recombinant wild-type and mutant AT variants in the aortic wall endothelium and subendothelium.

4). Recently, O'Reilly *et al.* demonstrated that cleaved form of AT functions as an antiangiogenic agent. Cleavage of AT by protease induces conformational change, which results in the loss of its heparin affinity. These conformational changes can profoundly alter its activity, from that of an inhibitor of thrombin to an agent that blocks blood vessel formation (angiogenesis) and induces tumor regression (O'Reilly *et al.*, 1999). These findings suggest that cleavage of AT is associated with a change of its binding specificity from heparin to other receptors on cell surfaces or in the extracellular matrix. It would be very interesting to study the antiangiogenetic effect of cleaved forms

of underglycosylated AT, since the *in vivo* study has suggested that these mutant variants pass through the vessel wall more rapidly than AT-WT.

5). The recombinant AT preparations used in the present study show heterogeneity, which is attributed to incomplete glycosylation at Asn 135 and heterogeneity in structure of glycan chains. Recent studies from Picard *et al.*, demonstrated that the preference of the oligosaccharyl transferase for Thr, rather than Ser at the third position of Asn-135 consensus sequence was responsible for the production of partially glycosylated β-isoform of AT (Picard *et al.*, 1995). Future studies should use the rabbit AT expression construct with Thr at the third position of the Asn-135 consensus sequence. The use of such an expression construct will eliminate the production of AT with incomplete glycosylation at Asn 135 position, and thus reduce glycosylation heterogeneity.

REFERENCES

Adamson, S., Charlebois, T., O'Connell, B., Foster, W. (1998) Viral safety of recombinant factor IX. Semin Hematol. 35:22-27.

Alhenc-Gelas, M.L., Aiach, M., Gorenflot, A., Andreaux, J.P. (1985) Antithrombin III antigen in human platelets. Thromb. Haemost. 54:599-602.

Andersson, L.O., Barrowcliffe, T.W., Holemer, E., Johnson, E.A., Sims, G.E.C. (1976) Anticoagulant properties of heparin fractionated by affinity chromatography on matrix-bound antithrombin III and by gel filtration. Thromb Res. 9, 575-583.

Anderson, S., Davis, D.N., Dahlback, E., Jornvall, H., Russell, D.W., (1989) Cloning, structure, and expression of the mitochondrial cytochrome P-450 sterol 26-hydroxylase, a bile acid biosynthetic enzyme. J. Biol. Chem. 264, 8222-8229.

Atha, D.H., Stephens, A.W., Rosenberg, R.D. (1984) Evaluation of critical groups required for the binding of heparin to antithrombin. Proc Natl Acad Sci USA 81, 1030-1034.

Austin, R.C., Rachubinski, R.A., Fernandes-Rachubinski, F., Blajchman, M.A. (1990) Expression in a cell-free system of normal and variant forms of human antithrombin III. Ability to bind heparin and react with α-thrombin. Blood 76, 1521-1529.

Ashwell, G., Harford, J. (1982) Carbohydrate-specific receptors of the liver. Annu Rev Biochem. 51, 531-54.

Austin, R.C., Rachubinski, R.A., Ofosu, F.A., Blajchman, M.A. (1991) Antithormbin-III-Hamilton, Ala 382 to Thr: an antithrombin-III variant that acts as a substrate but not an inhibitor of alpha-thrombin and factor Xa. Blood 77,2185-2189.

Ausubel, F.M., Brent, R., Kingston, R.E., Moore, D.D., Seidman, J.G., Smith, J.A., Struhl, K. (1992) Current protocols in molecular biology. Greene Publishing Associates and Wiley-Interscience, New York/Chichester/Brisbane/Toronto/Singapore.

Bary, B., Lane, D.A., Freyssinet, J.-M., Pejler, G., Lindahl, U. (1989) antithrombin activity of heparin. Effect of saccharide chain length on thrombin inhibition by heparin cofactor II and by antithrombin. Biochem J. 262,225-232

Bauer, K.A., and Rosenberg, R.D. (1991) Role of antithrombin III as a regulator of *in vivo* coagulation. Seminars Hematol. 28, 10-18.

Baumann, U., Bode, W., Huber, R., Travis, J., Potempa, J. (1992) Crystal structure of cleaved equine leucocyte elastase inhibitor determined at 1.95 A resolution. J Mol Biol 218, 595-606.

Bause, E., and legler, G. (1981) The role of the hydroxy amino acid in the triplet sequence Asn-Xaa-Thr(Ser) for the N-glycosylation step during glycoprotein biosynthesis. Biochem J. 195, 639-44.

Bayston, T.A., Tripodi, A., Mannucci, P.E., Thompson, E., Ireland, H., Fitches, A.C., Hananeia, L., Olds, R.J., Lane, D.A. (1999) Familial overexpression of β antithrombin caused by an Asn135Thr substitution. Blood 93, 4242-4247.

Beatty, K., Bieth, J., Travis, J. (1980) Kinetics of association of serpin proteinases with native & oxidized alpha-1-proteinase inhibitor and alpha-1-antichymotrypsin. J Bio Chem 225,3931-3934.

Beck, E.A. (1977) The chemistry of blood coagulation: a summary by Paul Morawitz (1905). Thromb Haemost. 37, 376-9

Belzar, K.J., Dafforn, T.R., Petitou, M., Carrell, R.W., Huntington, J.A. (2000) The effect of a reducing-end extension on pentasaccharide binding by antithrombin. J Biol Chem 275, 8733-8741.

Belzar, K.J., Zhou, A., Carrell, R.W., Gettins, P.W.W., Huntington, J.A. (2002) Helix D elongation and allosteric activation of antithrombin. J Biol Chem 277, 8551-8558.

Bjork, I., and Fish, W.W. (1982a) Production *in vitro* and properties of a modified form of bovine antithrombin, cleaved at the reactive site by thrombin. J Biol Chem 257, 9487-9493.

Bjork, I., Jackson, C.M., Jornvall, H., Lavine, K.K., Nordling, K., Salsgiver, W.J. (1982b) The active site of antithrombin; release of the same proteolytically cleaved form of the inhibitor from complexes with factor IXa, factor Xa, and thrombin. J Biol Chem 257, 2406-2411.

Bjork, I., Olson, S.T., Shore, J.D. (1989) Molecular mechanism of the accelerating effect of heparin on the reaction between antithrombin and clotting proteinase. In: Lane, D.A. and Lindahl, U. (eds) Heparin: chemical and biological properties, clinical applications. Edward Arnold, London. Pp.229-255.

Bjork, I., Ylinenjarvi, K., Olsen, S.T., Hermetin, P., Conradt, H.S. (1992) Decreased affinity of recombinant antithrombin for heparin due to increased glycosylation. Biochem J. 286, 793-800.

Bjork, I., Nordling, K., Olson, S.T. (1993) Immunologic evidence for insertion of the reactive-bond loop of antithrombin into the A β-sheet of the inhibitor during trapping of target proteinases. Biochemistry 32, 6501-6505.

Bjork, I., and Olson, S.T. (1997) Antithrombin: a bloody important serpin. Adv Exp Med Biol. 425:17-33.

Blajchman, M.A., Austin, R.C., Fernandez-Rachubinski, F., Sheffield, W.P. (1992) Molecular basis of inherited human antithrombin deficiency. Blood 80, 2159-2171.

Blomback, M., Abildgaard, U., van den Besselaar, A.M.P.H., Clemetson, K.J., Dahlback, B., Exner, T., Francis, C.W., Gaffney, P.J., Gralnick, H., Hoye,r L.W., Johnson, G.J., Kasper, C., Lane, D.A., Kijnen, H.R., Luscher, J.M., Mannucci, P.M., Poller, L., Rapaport, S.I., Saito, H., Stocker, K., Thomas, D. (1994) Nomenclature of quantities and units in Thrombosis and Haemostasis (ISTH/SSC recommendation 1993). Thromb Haemost 71:375-394.

Bock, S.C., Wion, K.L., Vehar, G.A., Lawn, R.M. (1982) Cloning and expression of the cDNA for human antithrombin III. Nucl Acids Res. 10, 8113-8125.

Borg, J.-Y., Owen, M.C., Soria, C., Soria, J., Caen, J., Carrell, R.W. (1988) Proposed heparin binding site in antithrombin based on arginine 47. A new variant Rouen-II, 47 Arg to Ser. J Clin Invest. 81,1292-1926.

Borg, J.-Y., Brennan, S.O., Carrell, R.W., George, P., Perry, D.J., Shaw, J. (1990) Antithrombin Rouen-IV 24 Arg Cys. The amino-terminal contribution to heparin binding. FEBS Lett. 266, 163-166.

Brennan, S.O., George, P.M., Jordan, R.E. (1987) Physiological variant of antithrombin III lacks carbohydrate side chain at Asn135. FEBS Lett. 219,431-436.

Brennan, S.O., Borg, J-Y., George, P.M., Soria, J., Caen, J., Carrell, R.W. (1988) New carbohydrate site in mutant antithrombin (7Ile-Asn) with decreased heparin affinity. FEBS Lett. 237,118-122.

Brinkhous, K.M., Smith, H.P., Warner, E.D., Seegers, W.H. (1939) The inhibition of blood clotting: an unidentified substance which acts in conjunction with heparin to prevent the conversion of prothrombin into thrombin. Am J Physiol 125, 683-687.

Broker, M., Ragg, H., Karges, H.E. (1987) Expression of human antithrombin III in *saccharmyces cerevisiae* and *Saccharomyces pombe*. Biochem Biophys Res Commun. 908,203-213.

Bruch, M. and Bieth, J.G. (1989) Kinetic evidence for a two-step mechanism for the binding of chymotrypsin to alpha 1-proteinase inhibitor. Biochem. J. 259, 929-930.

Bucur, S.Z., Levy, J.H., Despotis, G.J., Spiess, B.D., Hillyer, C.D. (1998) Uses of antithrombin III concentrate in congenital and acquired deficiency states. Transfusion 39,481-498.

Bulleid, N.J., Freedman, R.B. (1988) The transcription and translation in vitro of individual cereal storage-protein genes from wheat (Triticum aestivum, cv. Chinese Spring). Evidence for translocation of the translation products and disulphide-bond formation. Biochem J. 254, 805-10.

Carlson, A.T., and Atencio, A.C. (1982) Isolation and partial characterization of two distinct types of antithrombin III from rabbit. Thromb Res 27, 23-34.

Carlson, T.H., Atencio, A.C., Simon T.L. (1984) *in vivo* behaviour of radioiodinated rabbit antithrombin III. J Clin Invest. 74,191-199.

Carlson, T.H., Simon T.L., Atencio, A.C. (1985) *in vivo* behaviour of human radioiodinated antithrombin III. Blood 66, 13-19.

Carrell, R.W., and Travis J. (1985) a1-Antitrypsin and the serpins; variation and contervariation. Trends Bio Sci. 10, 20-24.

Carrell, R.W., Evans, D.L.I., Stein, P.E. (1991) Mobile reactive center of serpins and the control of thrombosis. Nature 353,576-578.

Carrell, R.W. and Evans, D.L.I. (1992) Serpins: mobile conformations in a family or proteinase inhibitors. Current Opinion in Structural Biol. 2, 438-446.

Carrell, R.W., Stein, P.E., Fermi, G., Wardell, M.R. (1994) Biological implication of a 3 A structure of dimeric antithrombin. Structure 2, 257-270.

Carrell, R.W., and Lomas, D.A. (1997a) Conformational disease. Lancet 350,134-138.

Carrell, R.W., kinner, R.., Jin, L., Abrahams, J.P. (1997b) Structural mobility of antithrombin and its modulation by heparin. Thromb Haemostas. 78,516-519.

Carson, E.R., and Jones, E.A. (1979) Use of kinetic analysis and mathematical modeling in the study of metabolic pathways in vivo: application to hepatic organic anion metabolism. N Engl J Med. 300:1016-1027.

Caso, R., Lane, D.A., Thompson, Olds, R.J., Thein, S.L., Panico, M., Blench, I., Morris, H.R., Freyssinet, J.M. Aiach, M. (1991) Antithrombin Vicenza, Ala 384 to Pro (GCA to CCA) mutation, transferring the inhibitor into a substrate. Br J Haematol. 77, 87-92.

Chan, T.K., and Chan, V. (1981) Antithrombin III, the major modulator of intravascular coagulation is synthesized by human endothelial cells. Thromb Haemostas. 46, 504-506.

Chandra, T., Stackhouse, R., Kidd, V.J., and Woo, S.L. (1983) Isolation and sequence characterization of a cDNA clone of human antithrombin III. Proc. Natl. Acad. Sci. USA 80, 1845-1848.

Chan, V., and Chan, T.K. (1979) antithrombin III in fresh and cultured human endothelial cell: a natural anticoagulant from the vascular endothelium. Thromb Res. 15, 209-213.

Chang, J.-Y. and Tran, T.H. (1986) Antithrombin-III Basel. Identification of a Pro to Leu substitution in a hereditary abnormal antithrombin with impaired heparin cofactor activity. J Biol Chem 261, 1174-1176.

Chang, J.-Y. (1989) Binding of heparin to human antithrombin III activates selective chemical modification at lysin 236, Lys-107, Lys-125, and Lys-136 are situated within the heparin-binding site of antithrombin III. J Biol Chem 264, 3111-3115.

Choay, J., Lormeau, J.C., Sinay, P., Casu, B., Gatti, G. (1983) Structure-activity relationship in heparin: A synthetic pentasaccharide with high-affinity for antithrombin III and eliciting high anti-factor Xa activity. Biochem Biophys Res Commun. 116, 492-499.

Collen, D., Schezt, J., DeCock, F., Holmer, E., Verstraete, M. (1977) Metabolism of antithrombin III (heparin cofactor) in man: effects of venous thrombosis and heparin administration. Eur J Clin Invest. 7, 27-34.

Conard, J., Brosstad, F., Lie-Larsem, M., Samama, M., Abildgaard, U. (1983) Molar antithrombin concentration in normal human plasma. Haemostasis 13:363

Creighton, T.E. (1992) Protein folding. Up the kinetic pathway. Nature 356,194-195.

Cumming, D.A. (1991) Glycosylation of recombinant protein therapeutics: control and functional implications. Glycobiology 1:115-30.

Danielsson, A., Raub, E., Bjork, I. (1986) Role of ternary complexes, in which heparin binds both antithrombin and proteinase, in the acceleration of the reactions between antithrombin and thrombin or factor Xa. J Biol Chem 261, 15467-15473.

Danishefsky, I., Zweben, A., Slomiany, B.L. (1977) Human antithrombin III: carbohydrate components and associated glycolipid. J Biol Chem 253,32-37.

De Boer, H.C., Preissner, K.T., Bouma, B.N., de Groot, P.G. (1995) Internalization of vitronectin-thrombin-antithrombin complex by endothelial cells leads to deposition of the complex into the subendothelial matrix. J Biol Chem 270,30733-30740.

Dingermann, T., Troidl, E.M., Broker, M., Nerke, K. (1991) Expression of human antithrombin III in the cellular slim mould *dictyostelium discoideum*. Appl Microbiol Biotechnol 35, 496-503.

Djie, M.Z., Le Bonniec, B.F., Hopkins, P.C.R., Hipleer, K., Stone, S.R. (1996) Role of the P_2 residue in determining the specificity of serpins. Biochemistry 35, 11461-11469.

Dorner, A.J., Kaufman, R.J. (1990) Analysis of synthesis, processing, and secretion of proteins expressed in mammalian cells. Methods Enzymol 185, 577-96.

Dube, S., Fisher, J.W. Powell, J.S. (1988) Glycosylation at specific sites of erythropoietin is essential for biosynthesis, secretion, and biological function. J Biol Chem 263,17516-17521.

Dwek, R.A., Ashford, D.A., Edge, C.J., Parekh, R.B., Rademacher, T.W., Wing, D.R., Barclay, A.N., Davis, S.J., Williams, A.F. (1993) Glycosylation of CD4 and Thy-1. Phil. Trans R Soc Lond B 342, 43-50.

Dwek, R.A. (1995) Glycobiology: "Towards understanding the function of sugar". Biochemical Society Transactions 23, 1-26.

Egeberg, O. (1965) Inherited antithrombin deficiency causing thrombophilia. Thromb Diath Haemorrh 13, 516-530.

Einarsson, R. and Andersson, L.O. (1977) Binding of heparin to human antithrombin III as studied by measurements of tryptophan fluorescence. Biochim Biophys Acta 490, 104-111.

Erdjument, H., Lane, D.A., Ireland, H., Panico, M., Dimaizo, V., Blench, I., Morris, H.R. (1987) Formation of a covalent disulfide-linked antithrombin-albumin complex by an antithrombin variant, antithrombin "Northwick Park". J Biol Chem 262, 13381-13384.

Fair, D.S., and Bahnak, B.R. (1984) Human hepatoma cells secrete single chain factor X, prothrombin, and antithrombin III. Blood 64, 194-204.

Fan, B., Crews, B.C., Turko, I.V., Choay, J., Zettlmeissl, G., Gettins, P. (1993) Heterogeneity of recombinant human antithrombin III expressed in baby hamster kidney cells. Effect of glycosylation differences on heparin binding and structure. J Biol Chem 268, 17588-17596.

Fan, B., Turko, I.V., Gettins, P.G.W. (1994a) Lysine-heparin interactions in antithrombin; properties of K125M and K290M, K294M, K297M variants. Biochemistry 33, 14156-14161.

Fan, B., Turko, I.V., Gettins, P.G.W. (1994b) Antithrombin histidine variants 1H NMR resonance assignments and functional properties. FEBS Lett. 354, 84-88.

Feizi, T., and Childs, R.A. (1987) Carbohydrates as antigenic determinants of glycoproteins. Biochem J. 245, 1-11.

Fish. W.W., and Bjork, I. (1979) Release of a two-chain form of the human antithrombin from the antithrombin-thrombin complex. Eur J Biochem 101,31-38.

Fish, W.W., Orre, K., Bjork I (1979a) The production of an inactive form of antithrombin through limited proteolysis by thrombin. FEBS Lett. 98, 103-106.

Fish, W.W., Orre, K., Bjork, I. (1979b) Routes of thrombin action in the production of proteolytically modified, secretary forms of antithrombin-thrombin complex. Eur J Biochem 101, 39-44.

Fitches, A.C., Lewandowski, K., Olds, R.J. (2001) Creation of an additional glycosylation site as a mechanism for type I antithrombin deficiency. Thromb Haemost. 86:1023-1027.

Franzen, L-E., Svensson, S., Larm, O. (1980) Structural studies on the carbohydrate portion of human antithrombin III. J Biol Chem 255, 5090-5098.

Frebelius, S., Isaksson, S., Swedenborg, J. (1996) Thrombin inhibition by antithrombin III on the subendothelium is explained by the isoform ATβ. Ateriosclerosis, Thrombosis, and Vascular Biology 16:1292-1297.

Fuchs, H.E., Shifman, M.A., Pizzo, S.V. (1982) In vivo catabolism of α1-proteinase inhibitor-trypsin, antithrombin III-thrombin and 2-macroglobulin-methylamine. Biochim Biophys Acta 716, 151-157.

Fuchs, H.E., and Pizzo, S.V. (1983) Regulation of factor Xa in vitro in human and mouse plasma and in vivo in mouse; role of the endothelium and plasma proteinase inhibitors. J Clin Invest 72, 2041-2049.

Fuchs, H.E., Trapp, H.G., Griffith, M.J., Roberts, H.R., Pizzo, S.V. (1984) Regulation of factor IXa *in vitro* in human and mouse plasma *in vivo* in the mouse. Role of the endothelium and the plasma proteinase inhibitors. J Clin Invest 73. 1696-1703.

Gallager, P., Henneberry, J., Wilson, I., Sambrook, J., Getting, M.J. (1988) Addition of carbohydrate side chains at novel sites on influenza virus hemagglutinin can modulate the folding, transport, and activity of the molecule. J Cell Biol. 107, 2059-2073.

Garone, L., Edmunds, T., Hanson, E., Bernsaconi, R., Huntington, J.A., Meagher, J.L., Fan, B., Gettins, P.G.W. (1996) Antithrombin-heparin affinity reduced by fucosylation of carbohydrate at asparagine 155. Biochemistry. 35,8881-8889.

Gandrille, S., Ajach, M., Lane, D.A., Vidaud, D., Molho-Sabatier, P., Caso, R., deMoerloose, P., Fiessinger, J.-N., Clauser, E. (1990) Important role of arginine 129 in heparin-binding of antithrombin III. J Biol Chem 265, 18997-19001.

Gavel, Y., and von Heijne, G. (1990) Sequence differences between glycosylated and non-glycosylated Asn-X-Thr/Ser acceptor sites: implications for protein engineering. Protein Eng. 3, 433-442.

Gettins, P. and Wooten, E.S. (1987a) On the domain structure of antithrombin III; localization of the heparin-binding region using ^{1}H NMR spectroscopy. Biochemistry 26, 4403-4408.

Gettins, P. (1987b) Antithrombin III and its interaction with heparin; comparison of the human, bovine, and porcine proteins by ^{1}H NMR spectroscopy. Biochemistry 26, 1391-1398.

Gillespie, L.S., Hillesland, K.K., Knaur, D.J. (1991) Expression of biologically active human antithrombin III by recombinant *baculovirus* in *Spodoptera frugiperda* cells. J Biol Chem. 266, 3995-4001.

Girot, R., Jaubert, F., Leon, M., Bellon, B., Ajach, M., Josso, F. (1983) Albumin, fibrinogen, prothrombin and antithrombin III variations in blood, urines and liver in rat nephrotic syndrome (Heymann nephritis). Thromb Harmostas 49, 13-17.

Gitel, S.N., Medina, V.M., Wessler, S. (1984) Inhibition of human activated factor X by antithrombin III and alpha 1-proteinase inhibitor in human plasma. J Biol Chem 259,6890-6895.

Goochee, C. F., and Monica, T. (1990) Environmental effects on protein glycosylation. Bio/Technology 8, 421-427

Griffith, M.J. (1982) Kinetics of the heparin-enhanced antithrombin III/thrombin reaction. Evidence for a template model for the mechanism of action of heparin. J Biol Chem. 257, 7360-7365

Grinnell, B.W., Walls, J.D., Gerlitz, B. (1991) Glycosylation of human protein C affects its secretion, processing, functional activities, and activation by thrombin. J Biol Chem. 22, 9778-9785.

Hatton, M.W.C., Hoogendoorn, H., Southward, S.M.R., Ross, B., Blajchman, M.A. (1997) Comparative metabolism and distribution of rabbit heparin cofactor-II and rabbit antithrombin in rabbits. Am J Physiol [Endocrine Metab 35] 272, E824-E831.

Higuchi, M., Oh-eda, M., Kuboniwa, H., Tomonoh, K., Shimonaka, Y., Ochi, N. (1992) Role of sugar chains in the expression of the biological activity of human erythropoietin. J Biol Chem 267, 7703-7709.

Holmer, E., Soderstrom, G., Anderson, L.O. (1979) Studies on the mechanism of the rate-enhancing effect of heparin on the thrombin-antithrombin III reaction. Eur J Biochem 93, 1-5.

Holmer, E., Kurachi, K., Soderstrom, G. (1981) The molecular-weight dependence of the rate-enhancing effect of heparin to the inhibition of thrombin, factor Xa, factor IXa, factor VIIa and kallikrein by antithrombin. Biochem J 193,395-400.

Hook, M., Bjork, I., Hopwood, J., Lindahl, U. (1976) Anticoagulant activity of heparin: separation of high and low activity heparin species by affinity chromatography on immobilized antithrombin. FEBS Lett 66, 90-93.

Hopkins, P.C.R., Carrell, R.W., Stone, S.R. (1993) Effects of mutations in the hinge region of serpins. Biochemistry 32, 7650-7657.

Hopkins, P.C.R., Crowther, D.C., Carrell, R.W., Stone, S.R. (1995) Development of a novel recombinant serpin with potential antithrombotic properties. J Biol Chem 270,11866-11871.

Horne, A.P. and Gettins, P. (1992) 1H NMR spectroscopic studies on the interactions between human plasma antithrombin III and defined low molecular weight heparin fragments. Biochemistry 31,2286-2294.

Howard, S.C., Wittwer, A.J., Welply, J.K. (1991) Oligosaccharides at each glycosylation site make structure-dependent contributions to biological properties of human tissue plasminogen activator. Glycobiology 1, 411-417.

Howell, W. H., and Holt, E., (1918) Two new factors in blood coagulation-heparin and pro-antithrombin. Am J Physiol 47: 328-341.

Huber, R. and Carrell, R.W. (1989) Implication of the three-dimensional structure of alpha 1-antitrypsin for structure and function of serpin. Biochemistry. 28, 8951-8966.

Hunt, L.T. and Dayoff, M.O. (1980) A surprising new protein super-family containing ovalbumin, antithrombin III, and alpha 1-proteinase center loop preinsertion with expulsion upon heparin binding. Biochemistry 35, 8495-8503.

Huntington, J.A., Read, R.J., Carrell, R.W. (2000a) Structure of a serpin-protease complex shows inhibition by deformation. Nature 407, 923-926.

Huntington, J.A., McCoy, A., Belzar, K.J., Pei, X.Y., Gettins, P.G.W., Carrell, R.W. (2000b) The conformational activation of antithrombin. J Biol Chem 275,15377-15383.

Huntington J.A., and Carrell R.W. (2001) The serpins: nature's molecular mousetraps Science Progress. 84, 125-136.

Irving, J.A., Pike, R.N., Lesk, A.M., Whisstock J.C. (2000) Phylogeny of the serpin superfamily: Implications of patterns of amino acid conservation for structure and function. Genome Research 10,1845-1864.

Jesty, J. (1979) The kinetics of formation and dissociation of the bovine thrombin-antithrombin III complex. J Biol Chem. 254, 10044-10050.

Jesty, J., (1986) The kinetics of inhibition of alpha-thrombin in human plasma. J Biol Chem. 261, 10313-10318.

Jackson, C.M., and Nemerson, Y. (1980) Blood coagulation. Ann Rev Biochem 49, 765-811.

Jornvall, H., Fish, W.W., Bjork, I. (1979) The thrombin cleavage site in bovine antithrombin. FEBS Lett. 106, 358-362.

Jordan, R.E., Beeler, D., Rosenberg, R.D. (1979) Fractionation of low molecular weight heparin species and their interaction with antithrombin. J Biol Chem 254, 2902-2913.

Jordan, R.E., Oosta, G.M., Gardner, W.T., Rosenberg, R.D. (1980) The kinetics of haemostatic enzyme-antithrombin interaction in the presence of low molecular weight heparin. J Biol Chem 255, 10081-10090.

Kaufman, R. (1990) Vectors used for expression in mammalian cells. Methods Enzymol 185,488-511.

Kobayashi, N. and Takeda, Y. (1977) Effects of a large dose of oestradiol on antithrombin III metabolism in male and female dogs. J Clin Invest 7, 373-381.

Koide, T., Odani, S., Takahashi, K., Ono, T., Sakuragawa, N. (1984) Antithrombin III Toyama: replacement of arginine-47 by cysteine in hereditary abnormal antithrombin III that lacks heparin-binding ability. Proc Natl Acad Sci U.S.A. 81,289-293.

Koj, A., Regoeczi, E., Toews, C.J., Leveille, R., Gauldie, J. (1978) Synthesis of antithrombin III and alpha-1-antitrypsin by the perfused rat liver. Biochim Biophys Acta 539, 496-504.

Kornfeld, R., and Kornfeld, S. (1985) Assembly of asparagine-linked oligosaccharides. Ann Rev Biochem 54,631-664.

Kounnas, M.Z., Church, F.C., Argraves, W.S., Strickland, D.K. (1996) Cellular internalization and degradation of antithrombin III-thrombin, heparin-cofactor II-thrombin, and α1-antitrypsin complexes is mediated by the low density lipoprotein receptor-related protein. J Biol Chem 271, 6523-6529.

Kress, L.F., and Cataness, J.J. (1981) Identification of the cleavage sites resulting from enzymatic inactivation of human antithrombin III by Crotalus adamanteus proteinase II in the presence and absence of heparin. Biochemistry 20, 7432-7438.

Kridel , S.J., Chan, W.W., Knauer, D.J. (1996) Requirement of lysine residues outside of the proposed pentasaccharide binding for high affinity heparin binding and activation of human antithrombin III. J Biol Chem 27, 20935-20941.

Kristensen, T., Moestrup, S.K., Gliemann, J., Bendtsen, L., Sand, O., Sottrup-Jensen, L. (1990) Evidence that the newly cloned low-density-lipoprotein receptor related protein (LRP) is the alpha 2-macroglobulin receptor. FEBS lett 276, 151-155.

Kurachi, K., Schmer, G., Hermodson, M.A., Teller, D.C., Davie, E.W. (1976) Inhibition of bovine factor IXa and Xa by antithrombin III. Biochemistry 15, 373-377.

Lane, D.A., Denton, J., Flynn, A.M., Thunberg, L., Lindahl, U. (1984) Anticoagulant activities of heparin oligosaccharides and their neutralization by platelet factor 4. Biochem J. 218, 725-732.

Lane, D.A., Olds, R.J., Boisclair, M., Chowdhury, V., Thein, S.L., Cooper, D.N., Blajchman, M.A., Perry, D., Emmerich, J., Aiach, M. (1993) Antithrombin III mutation

database: First update. For the thrombin and its inhibitors subcommittee of the scientific and standardization committee of the international society on thrombosis and haemostasis. Thrombos Haemostas. 70,361-369.

Lane, D.A., Bayston, T., Olds, R.J., Fitches, A.C., Cooper, D.N., Millar, D.S., Jochmans, K., Perry, D.J., Okajima, K., Thein, S.L., Emmerich, J. (1997) Antithrombin mutation database: 2nd (1997) update. For the Plasma Coagulation Inhibitors Subcommittee of the Scientific and Standardization Committee of the International Society on Thrombosis and Haemostasis. Thromb Haemost. 77, 197-211.

Larsson, H., Akerud, P., Nordling, K., Raub-Segall, E., Claesson-Welsh, L., Bjork, I. (2001) A novel anti-angiogenic form of antithrombin with retained proteinase binding ability and heparin affinity. J Biol Chem 276: 11996-12002.

Lawrence, D.A., Ginsburg, D., Day, D.E., Berkenpas, M.B., Verhamme, I.M., Kvassman, J.O., Shore, J.D. (1995) Serpin-protease complex are trapped as stable acyl-enzyme intermediates. J Biol Chem 270, 25309-25312.

Lawson, J.H., Butenas, S., Ribarik, N. Mann, K.G. (1993) Complex-dependent inhibition of factor VIIa by antithrombin III and heparin. J Biol Chem 268:767-770.

Lechner, K., Niessner, H., Thaler, E. (1977) Coagulation abnormalities in liver diseases. Semin Thromb Haemostas. 4, 40-56.

Lee, A.K.Y., Chan, V., Chan, T.K. (1979) The identification and localization of antithrombin III in human tissue. Thromb Res. 14, 209-217.

Leon, M., Aiach, M., Coezy, E., Guennec, J.Y., Jarnet, J., Girot, R., Fiessinger, J.N., Jaubert, F. (1982) Antithrombin III in rat hepatocytes. Thromb Res. 28, 115-123.

Leon, M., Aiach, M., Coezy, E., Guennec, I.Y., Fiessinger, J.N. (1983) Antithrombin III synthesis in rat liver parenchymal cells. Thromb Res. 30, 369-375.

Leonard, B., Bies, R., Carlson, T., Reeve, E.B. (1983) Further studies of the turnover of dog antithrombin III. Study of ^{131}I-labelled antithrombin protease complexes. Thromb Res. 30, 165-177.

Liang, O.D., Rosenblatt, S., Chatwal, G.S., Preissner, K. T. (1997) Identification of novel heparin-binding domains of vitronectin. FEBS lett. 407,169-172.

Lis, H., and Sharon, N. (1993) Protein glycosylation structure and functional aspects. Eur J Biochem. 218, 1-27.

Liu, C.S., and Chang, J.Y. (1987) The heparin binding site of human antithrombin III; selective chemical modification at Lys 114, Lys 125, and Lys287 impairs its heparin cofactor activity. J Biol Chem. 262, 17356-17361.

Loeliger, A. and Hers, J.F.Ph. (1957) Chronic antithrombinaemia (antithrombin V) with haemorrhagic diathesis in a case of rheumatoid arthritis with hypergammagloblulinaemia. Thromb Diath Haemorrh. 1, 499-528

Longas, M.O., and Finlay, T.H. (1980) The covalent nature of the human antithrombin III-thrombin bond. Biochem J. 189, 481-489.

Longstaff, C., and Gaffney, P.J. (1991) Serpin-serine protease binding kinetics:α2-antiplasmin as a model inhibitor. Biochemistry. 30, 979-986.

Maniatis, T., Fritsch, E.F., Sambrook, J. (1982) Molecular cloning: A laboratory manual. Cold Spring Harbor, NY, Cold Spring Harbor Laboratory.

Mann, K.G. (1999) Biochemistry and physiology of blood coagulation. Thromb Haemost. 82, 165-174.

Manson, H.E., Austin, R.C., Fernandez-Rachubinski, F., Rachubinski, RA, Blajchman, M.A. (1989) The molecular pathology of inherited human antithrombin III deficiency. Transfus Med Rev. 3, 264-281.

Mast, A.E., Enghild, J.J., Pizzo, S. V., Salvesen, G. (1991) Analysis of the plasma elimination kinetics and conformational stabilities of native, proteinase-complexed, and reactive site cleaved serpins: Comparison of α_1-proteinase inhibitor, α_1-antichymotrypsin, antithrombin III, α_2-antiplasmin, angiotensinogen, and ovalbumin. Biochemistry. 30, 1723-1730.

Miller-Anderson, M., Borg, H., Andersson, L-O. (1974) Purification of antithrombin III by affinity chromatography. Thromb Res 5, 439-452.

Mizuochi, T., Fuji, J., Kurachi, K., Kobata, A. (1980) Structural studies of the carbohydrate moiety of human antithrombin III. Arch Biochem Biophys. 203, 458-465.

Molho-Sabatier, P., Aiach, M., Gaillard, I., Fiessinger, J.N., Fischer, A.M., Chadeuf, G., Clauser, E. (1989) Molecular characterization of antithrombin (ATIII) variants using polymerase chain reaction; identification of the ATIII Charleville as an Ala 384 Pro mutation. J Clin Invest. 84, 1236-1242.

Monkhouse, F.C., France, E.S., Seegers, W.H. (1955) Studies on the antithrombin and heparin cofactor activities of a fraction adsorbed from plasma by aluminium Hydroxide. Circ Res. 3, 397-402.

Montreuil, J. (1984) Spatial conformation of glycans and glycoproteins. Biol Cell 51,115-131.

Morawitz, P. (1905) Die Chemie der Blutgerinnung. Ergebnisse der Physiologie, biologischen Chemie und experimentellen Pharmakologie 4,307.

Mottonen, J., Strand, A., Symersky, J., Sweet, R.M., Danley, D.E., Goeghegan, K.F., Gerard, R.D., Goldsmith, E.J., (1992) Structural basis of latency in plasminogen activator inhibitor 1. Nature 355, 270-273.

Mourey, L., Samama, J.P., Delarue, M., Petitou, M., Choay, J., Moras, D. (1993) Crystal structure of cleaved bovine antithrombin III at 3.2 A resolution. J. Mol Biol 232, 223-241.

Najjam, S., Chadeuf, G., Gandrille, S., Aiach, M. (1994) Arg-129 plays a specific role in the conformation of antithrombin and in the enhancement of factor Xa inhibition by the pentasaccharide sequence of heparin. Biochim Biophys Acta 1225,135-143.

Nesheim, M.E. (1983) A simple rate law that describes the kinetics for the heparin-catalyzed reaction between antithrombin III and thrombin. J Biol Chem 258:14708-14717.

Niewiarowski, S. Kowalski, E. (1958) Un nouvel anticoagulant derive du fibrinogen. Rev. Hematol. 13,320

Nordenman, B., Nystrom, C., Bjork, I. (1977) The size and shape of human and bovine antithrombin III. Eur J Biochem 78, 195-203.

Nordenman, B. and Bjork, I. (1978a) Binding of low-affinity and high-affinity heparin to antithrombin. Ultraviolet difference spectroscopy and circular dichroism studies. Biochem. 17, 3339-3344.

Nordenman, B., Danielsson, A., Bjork, I. (1978b) The binding of low-affinity and high-affinity heparin to antithrombin. Eur J Biochem. 90,1-6.

Norner, A.J., Kaufman, R.J. (1990) Analysis of synthesis, processing, and secretion of proteins expressed in mammalian cells. Methods Enzymol. 185,577-596.

Olds, R.J., Lane, D.A., Boisclair, M., Sas, G., Bock, S.C., Thein, S.L. (1992) Antithrombin Budapest 3. An antithrombin variant with reduced heparin affinity resulting from the substitution L99F. FEBS Lett. 6, 241-246.

Olson, S.T., and Shore, J.D. (1982) Demonstration of a two-step reaction mechanism for inhibition of α–thrombin by antithrombin III and identification of the step affected by heparin. J Biol Chem. 257, 14891-14895.

Olson, S.T. (1988) Transient kinetics of heparin-catalyzed protease inactivation by antithrombin III. J Biol Chem. 263, 1698-1708.

Olson, S.T., and Bjork, I. (1991) Predominant contribution of surface approximation to the mechanism of heparin acceleration of the antithrombin-thrombin reaction; elucidation from salt concentration effects. J Biol Chem. 266, 6353-6364.

Olson, S.T., Bjork, I., Sheffer, R., Craig, P.A., Shore, J.D. Choay, J. (1992) Role of the antithrombin-binding pentasaccharide in heparin acceleration of antithrombin-proteinase reaction; resolution of the antithrombin conformational change contribution to heparin rate enhancement. J Biol Chem 267, 12528-12538.

Olson, S.T., Sheffer, R. Francis, A.M. (1993a) High molecular weight kininogen potentiates the heparin-accelerated inhibition of plasma kallikrein by antithrombin: role for antithrombin in the regulation of Kallikrein. Biochemistry 32,12136-12147.

Olson, S.T., Bjork, I., Shore, J.D. (1993b) Kinetic characterization of heparin-catalyzed and uncatalyzed inhibition of blood coagulation proteinases by antithrombin. Metheds Enzymol. 222, 525-559.

Olson S.T., Stephens, A.W., Hirs, C.H.W., Bock, P.E., Bjork, I. (1995) Kinetic characterization of the proteinase binding defect in a reactive site variant of the serpin, antithrombin; role of the P1' residue in transition-state stabilization of antithrombin-proteinase complex formation. J Biol Chem. 270, 9717-9724.

Olson, S.T., Frances-Chumura, A.M., Swanson, R., Bjork, I., Zettlemeissl, G. (1997) Effect of individual carbohydrate chains of recombinant antithrombin on heparin affinity and on the generation of glycoforms differing in heparin affinity. Arch Biochem Biophys. 341, 212-221.

O'Reilly, M.S., Pirie-Shepherd, S., Lane, W.S., Folkman, J. (1999) Antiangiogenic activity of the cleaved conformation of the serpin antithrombin. Science 285,1926-1928.

Owen, M.C. (1975) Evidence for the formation of an ester between thrombin and heparin cofactor. Biophys Biochim Acta. 405, 380-384.

Owen, M.C., Brennan, S.O., Lewis, J.H., Carrell, R.W. (1983) Mutation of antitrypsin to antithrombin. α_1-antitrypsin Pittsbergh (358 Met→ Arg), a fatal bleeding disorder. N Engl J Med 309, 694-698.

Owens, M.R., and Miller L.L. (1980) Net biosynthesis of antithrombin III by the isolated rat liver perfused for 12-24 hours; compared with rat fibrinogen and α-2 (acute phase) globulin, antithrombin III is not an acute phase protein. Biochim Biophys Acta 627, 30-39.

Parekh, R.B., Tse, A.G.D., Dwek, R.A., Williams, A.F., Rademacher, T.W. (1987) Tissue-specific N-glycosylation, site-specific oligosaccharide patterns and lentil lectin recognition of rat Thy-1. EMBO J. 6, 1233-1244.

Patthy, L. (1985) Evolution of the proteases of blood coagulation and fibrinolysis by assembly from modules. Cell 41,657-663.

Paulson, J.C., (1989) Glycoproteins: what are the sugar chains for? TIBS 14, 272-274.

Perlmutter, D.H., Glover, G.I., Rivetna, M., Schasteen, C. S., Fallon, R.J. (1990) Identification of a serpin-enzyme complex receptor on human hepatoma cells and human monocytes. Proc Natl Acad Sci. U.S.A. 87, 3753-3757.

Peterson, C.B., and Blackburn, M.N. (1985) Isolation and characterization of an antithrombin-III variant with reduced carbohydrate content and enhanced heparin binding. J Biol Chem 260, 1723-1729

Peterson, C.B., Noyes, C.M., Pecon, J.M., Church, F.C., Blackburn, M.N. (1987) Identification of a lysyl residue in antithrombin which is essential for heparin binding. J Biol Chem. 262, 8061-8065.

Peterson, T.E., Dudek-Wojciechowska, G., Sottrup-Jensen, L. (1979) Primary structure of antithrombin III (heparin cofactor); partial homology between α1-antitrypsin and antithrombin III. In: Collen D., Wiman, B., and Verstrate, M. (eds): The physiological inhibitors of coagulation and fibrinolysis. Amsterdam, Elsevier/North-Holland. Pp. 43-54.

Picard, V., Erdsal-Badju, E., Bock, S.C. (1995) Partial glycosylation of antithrombin III asparagine-135 is caused by the serine in the third position of its N-glycosylation consensus sequence and is responsible for production of the β-antithrombin III isoform with enhanced heparin affinity. Biochemistry 34, 8433-8440.

Pittman, D.D., Wang. J.H., Kaufman, R.J. (1992) Identification and functional importance of tyrosine sulfate residues within recombinant factor VIII. Biochemistry. 31: 3315-3325.

Pricer, W. E.., Jr., and Ashwell, G. (1971) The binding of desialylated glycoproteins by plasma membranes of rat liver. J Biol Chem 246, 4825-4833

Pricer W.E. jr., Hudgin, R. L. Ashwell, G., Stockert, R.J., Morell, A.G. (1974) A membrane receptor protein for asialoglycoproteins. Methods Enzymol. 34, 688-691.

Rademacher, R.W., Parekh, R.B., Dwek, R.A. (1988) Glycobiology. Annu Rev Biochem. 57, 785-838.

Ratnoff, O.D. (1982) Disordered hemostasis in hepatic disease. In: Schiff, L. and Schiff, E.R. (eds): Disease of the liver. Philadelphia, J.B. Lippincott. PP. 237-258.

Reeve, E.B., Leonard B., Wentland, S.H., Damus, P. (1980) Studies with ^{131}I-labelled antithrombin III in dogs. Thromb Res 20;375-389.

Regoeczi, E. (1987) Distribution of antithrombin III in rabbits: role of host and protein Am J Physiol 252, R457-461.

Rosenberg, J.S., McKenna, P.W., Rosenberg, R.D., (1975) Inhibition of human factor IXa by human antithrombin. J Biol Chem 250, 8883-8888

Rosenberg, R.D., and Damus, P.S. (1973) The purification and mechanism of action of human antithrombin-heparin cofactor. J Biol Chem 248, 6490-6505.

Rosenberg, R.D. (1975a) Actions and interactions of antithrombin and heparin. N Engl J Med 292,146-151.

Rosenberg, J.S., McKenna, P.W., Rosenberg, R.D., (1975b) Inhibition of human factor IXa by human antithrombin. J Biol Chem 250, 8883-8888

Rosenfeld, L., and Danishefsky, I. (1984) Effects of enzymatic deglycosylation on the biological activities of human thrombin and antithrombin. Arch Biochem Biophys 229, 359-367.

Sairam., M.R. (1989) Role of carbohydrates in glycoprotein hormone signal transduction. FASEB J. 3, 1915-1926

Sambrook, J., Fritsch, E.F., Maniatis, T. (1989a) Quantitation of DNA and RNA. In: Nolan, C. (ed): Molecular cloning: a laboratory manual, 2nd ed. Cold Spring Harbor Laboratory Press, Cold Spring Harbor, New York. Pp. E5.

Sambrook, J., Fritsch, E.F., Maniatis, T. (1989b) Transfer of proteins from SDS-polyacrylamide gels to solid supports: immunological detection of immobilized protein (Western blotting). In: Nolan, C. (ed): Molecular cloning: a laboratory manual, 2nd. Cold Spring Harbor Laboratory Press, Cold Spring Harbor, New York. Pp. 18.60-18.75.

Sanger, F., Nicklen, S., Coulson, A.R. (1977) DNA sequencing with chain terminating inhibitors. Proc Natl Acad Sci USA 74, 5463-6472.

Sasaki, H., Bohtner, B., Dell, A., Fukuda, M. (1989) Carbohydrate structure of erythropoietin expressed in Chinese Hamster Ovary cells by a human erythropoietin cDNA. J Biol Chem 262, 12059-12076.

Schapira, M. Ramus, M.A., Jallat, S., Carvallo, D., Courtney, M. (1986) Recombinant α_1-antitrypsin Pittsburgh (Met358→Arg) is a potent inhibitor of plasma Kallikrein and activated factor XII fragment. J Clin Invest. 77, 645-637

Schengrund, C-L., Jensen, D.S., Rosenberg, A. (1972) Localization of sialidase in the plasma membrane of rat liver cells. J Biol Chem 247, 2742-2476.

Schreuder, H.A., De Boer, B., Dijkema, R., Mulders, J., Theunissen, H.J.M., Grootenhuis, P.D.J., Hol, W.G.J. (1994) The intact and cleaved human antithrombin III complex as a model for serpin-proteinase interactions. Nature Struct Biol 1, 48-54.

Scott, C.F., Carrell, R.W., Glaser, C.B., Kueppers, F., Lewis, J.H., and Colman, R.W. (1986) alpha-1 antitrypsin-Pittsburgh. a potent inhibitor of human plasma factor XIa, Kallikrein, and factor XII. J Clin Invest 77, 631-634.

Scott, C.F. and Colman, R.W. (1989) Factors influencing the acceleration of human factor Xa inactivation by antithrombin III. Blood 73, 1873-1879.

Seegers, W.H., Johnson, J.F., Fall, C. (1954) An antithrombin reaction related to prothrombin activation. Am J Physiol 176, 97-103.

Sharon, N. and Lis, H. (1982) Glycoproteins: research booming on long-ignored ubiquitous compounds. Mol Cell Biochem. 42, 167-187.

Sheffield, W.P., Brothers, A.B., Wells, M.J., Hatton, M.W.C., Clarke B.J., Blajchman, M.B. (1992) Molecular cloning and expression of rabbit antithrombin III. Blood 79,2330-2339.

Shifman, M.A. and Pizzo, S.V. (1982) The *in vivo* metabolism of antithrombin III and antithrombin III complexes. J Biol Chem 257, 3243-3248.

Shore, J.D., Day, D.E., Francis-Chmura, A.M., Verhamme, I., Kvassman, J., Lawrence, D.A., Ginsburg, D. (1995) A fluorescent probe study of plasminogen activator inhibitor-I; evidence for reactive center loop insertion and its role in the inhibitory mechanism. J Biol Chem 270, 5395-5398.

Silverman, G. A., Bird, P.I., Carrell, R.W., Church, F.C., Coughlin, P.B., Gettins P.G.W., Irving, J.A., Lomas, D.A., Luke, C.J., Moyer RR.W., Epemberton P.A., Remold-O'Donnell, E., Salvesen, G.S., Travis, J., Whisstock, J.C. (2001) The serpins are an expanding superfamily of structurally similar but functionally diverse proteins. J Biol Chem 276, 33293-33305.

Skriver, K., Wikoff, W.R., Patston, P.A., Tausk, F., Schapira, M., Kaplan, A.P., Bock, S.C. (1991) Substrate properties of C1 inhibitor Ma (alanine 434-glutamic acid). Genetic and structural evidence suggesting that the P12-region contains critical determinants of serine protease inhibitor/substrate status. J Biol Chem 266, 9216-9221.

Spellman, M.W., Basa, L.J., Leonard, C.K., Chakel, J.A., O'Connor J.V. (1989) Carbohydrate structures of human tissue plasminogen activator expressed in chinese hamster ovary cells. J Biol Chem 264, 14100-14111.

Springer, T.A. (1990) Adhesion receptors of the immune system. Nature 346,425-434.

Stead, N., Kaplan, A.P., Rosenberg, R.D. (1976) Inhibition of activated factor XII by antithrombin-heparin cofactor. J Biol Chem 251,6481-6488.

Stein, P.E., and Carrell, R.W. (1995) What do dysfunctional serpin tell us about molecular mobility and disease. Structural Biology 2, 96-113.

Stephens, A.W., Siddiqui, A., Hirs, C.H.W. (1987) Expression of functionally active human antithrombin III. Proc Acad Sci U.S.A. 84, 3886-3890.

Stephens, A.W., Siddiqui, A., Hirs, C.H.W. (1988) Site-directed mutagenesis of the reactive center (serine 394) of antithrombin III. J Biol Chem 263,15849-15852.

Stockert, R.J., Paietta, E., Racevskis, J., Morell, A.G. (1992) Posttranscriptional regulation of the asialoglycoprotein receptor by cGMP. J Biol Chem 267,56-59.

Stone, S.R., and Hermans, J.M. (1995) Inhibitory mechanism of serpin; interaction of thrombin with antithrombin and protease nexin1. Biochemistry. 34, 5164-5127.

Strickland, D.K., Ashcom, J.D., Williams, S., Burgess W. H., Migliorini, M., Argraves W.S., (1990) Sequence identity between the α_2-macroglobulin receptor and low density lipoprotein receptor-related protein suggests that this molecule is a multifunctional receptor. J Biol Chem 265, 17401-17404.

Sun, X.J., and Change, J.Y. (1990) Evidence that arginine-129 and arginine-145 are located within the heparin binding site of human antithrombin III. Biochemistry. 29, 8957-8962.

Takeuchi, M., Inoue, N., Strickland, T. W., Kubota, M., Wada, M., Shimizu, R., Hoshi, S., Kozutsumi, H., Takasaki, S., Kobata, A. (1989) Relationship between sugar chain structure and biological activity of recombinant human erythropoietin produced in Chinese hamster ovary cells. Proc Natl Acad Sci U.S.A 86, 7819-7822.

Takeuchi, M., and Kobata, A. (1991) Structures and functional roles of the sugar chains of human erythropoietins. Glycobiology 1, 337-346.

Taylor, J.W., Ott, J., Ekstein, F. (1985) The rapid generation of oligonucleotide-directed mutations at high frequency using phosphorothioate-modified DNA. Nucleic Acids Res 13, 8765-8771.

Theunissen, H.J.M., Dijkema, R., Grootenhuis, D.J., Swinkels, J.C., de Poorter, T.L., Carati, P., Visser, A. (1993) Dissociation of heparin-dependent thrombin and factor Xa inhibitory activities of antithrombin-III by mutations in the reactive site. J Biol Chem 268, 9035-9040.

Turk, B., Brieditis, I., Bock, S.C., Olson, S.T., Bjork, I. (1997) The oligosaccharide side chain on Asn-135 of α-antithrombin, absent in β-antithrombin, decreases the heparin affinity of the inhibitor by affecting the heparin-induced conformational change. Biochemistry 36, 6682-6691.

Tulin, J: (1972) Historical background of blood coagulation. In: Clot (eds). Tulin, J., Charles, C. Thomas-Publisher. Springfield/Illinois. Pp.3-31

Villanueva, G.B. and Danishefsky, I. (1977) Evidence for a heparin-induced conformational change on antithrombin III. Biochem Biophys Res Commun 74,803-809.

Vogel, C.N., Kingdon H.S., Lundblad R.L. (1979) Correlation of the *in vivo* and *in vitro* inhibition of thrombin by plasma inhibitors. J Lab Clin Med 93,668-673.

Wachtfogel, Y.T., Bischoff, R., Bauer, R., Hack, C.E., Nuijens, J.H., Kucich, U., Niewiarowski, S., Edmunds, L.H..Jr., Colman, R.V. (1994) α_1-Antitrypsin Pittsburgh

(Met^{358}→ Arg) inhibits the contact pathway of intrinsic coagulation and alters the release of human neutrophil elastase during simulated extracorporeal circulation. Thromb Haemostas. 72, 843-847.

Wardell, M.R., Chang, W-S. W., Bruce, D., Skinner, R., Lesk, A.M., Carrell, R.W. (1997) Preparative induction and characterization of L-antithrombin: a structural homologue of latent plasminogen activator inhibitor-1. Biochemistry. 36, 13133-13142.

Wasley, L.C., Atha, D.H., Bauer, K.A., Kaufamn, R.J. (1987) Expression and characterization of human antithrombin III synthesized in mammalian cells. J Biol Chem 262, 14667-14777.

Wasley, L.C., Timony, G., Murtha, P., Stoudemire, J., Dorner, A.J., Caro, J., Krieger, M., Kaufamn, R.J. (1991) The importance of N- and O-linked oligosaccharides for the biosynthesis and in vitro and in vivo biological activities of erythropoietin. Blood 77, 1614-1632.

Watada, M., Nagakawa, M., Kitani, T., Okajima, Y., Maeda, Y., Urano, S., Ijichi, H. (1981) Identification of the AT III synthesizing hepatocytes by immunofluorescent technique. Thromb Haemostas 46, 284 (abstract).

Wells, M.J., and Blajchman, M.A. (1998) *In vivo* clearance of ternary complexes of vitronectin-thrombin-antithrombin is mediated by hepatic heparan sulfate proteoglycans. J. Biol Chem 273, 23440-23447.

Wells, M. J., Sheffield, W.P., Blajchman, M.A. (1999) The clearance of thrombin-antithrombin and related serpin-enzyme complexes from the circulation: role of various hepatocyte receptors. Thromb Haemost 81,325-337

Whisstock, J.C., Skinner, R., Lesk, A.M. (1998) An atlas of serpin conformations. Trends Biochem Sci. 23,63-67,

Whisstock, J.C., Pike, R.N., Jin, L., Skinner, R., Pei, X.Y., Carrell, R.W., Lesk, A.M. (2000) Conformational changes in serpins: II The mechanism of activation of antithrombin by heparin. J Biol Chem 301, 1287-1305.

Witmer M.R., and Hatton, M.W.C. (1991) Antithrombin III-β associates more readily than antithrombin III-α with uninjured and de-endothelialized aortic wall in vitro and in vivo. Arterioscler Thromb 11,530-539.

Witmer M.R., Hadcock S.J., Peltier S.L., Winocour, P.D., Richardson, M., Hatton, M.W.C. (1992) Altered levels of antithrombin III and fibrinogen in the aortic wall of the

alloxan-induced diabetic rabbit: evidence of a prothrombotic state. J Lab Clin Med. 119, 221-230.

Wittwer, A.J., Howard, S.C., Carr, L.S., Harakas, N.K., Feder, J., Parekh, R.B., Rudd, P.M., Dwek, R.A., Rademacher, T.W. (1989) Effects of N-glycosylation on *in vitro* activity of Bowes melanoma and human colon fibroblast derived tissue plasminogen activator. Biochemistry 28, 7662-7669.

Wittwer, A.J., and Howard, S.C. (1990) Glycosylation at Asn-184 inhibits the conversion of single-chain to two-chain tissue-type plasminogen activator by plasmin. Biochemistry 29, 4175-4180.

Wright, H.T., Qian, H.X., Huber, R. (1990) Crystal structure of plakalbumin, a proteolytically nicked form of ovalbumin; its relationship to the structure of cleaved α-1-proteinase inhibitor. J Mol Biol. 213,513-528.

Wu, Y.I., Sheffield W.P., Blajchman, M.A. (1994) Defining the heparin-binding domain of antithrombin. Blood Coagul Fibrinolysis 5,83-95.

Young, G., Driscoll, M.C. (1999) Coagulation abnormalities in the carbohydrate-deficient glycoprotein syndrome: case report and review of the literature Am. J Hematol 60: 66-69.

Zettlmeissl, G., Conradt, H.S., Nimtz, M., Karges, H.E. (1989) Characterization of recombinant human antithrombin III synthesized in Chinese hamster ovary cells. J Biol Chem 264, 21153-21159.

Zhou, A., Huntington, J.A., Carrell, R.W. (1999) Formation of the antithrombin heterodimer *in vivo* and the onset of thrombosis. Blood 94:3388-3396.

Zhou, A., Carrell, R.W., Huntington, J.A. (2001) The serpin inhibitory mechanism is critically dependent on the length of the reactive center loop. J Biol Chem 276, 27541-27556.

Zhou, C., Yang, Y., Jong, A.Y. (1990) Mini-prep in ten minutes. BioTechniques 8,172-173.

CHAPTER 5 (APPENDIX)

CHARACTERIZATION OF A HIGHLY POLYMORPHIC TRINUCLEOTIDE SHORT TANDEM REPEAT (STR) WITHIN THE HUMAN ANTITHROMBIN (AT) GENE

5.1 Introduction

5.1.1 Antithrombin Gene Structure

The antithrombin (AT) gene consists of seven exons and six intervening sequences distributed over approximately 15 Kbs (Olds *et al.*, 1993). Initially it had been thought that there were only six exons but subsequent studies revealed a 1 kilobase intron within exon 3 (Bock *et al.*, 1988). This discovery has led to the unusual numbering of the exons 1, 2, 3a, 3b, 4, 5, and 6. Subsequently, it was proposed to designate exons 3a and 3b as exons 3 and 4, respectively. Therefore, current common usage refers to AT gene exons as exons 1 to 7 (Figure 5.1) (Blajchman *et al.*, 1992a).

Linkage of the putative antithrombin gene to chromosome 1q was first indicated by the phenotype of antithrombin deficiency in patients with cytogenetically detectable deletions in this region (Lovrien *et al.* 1978). Initial studies linked inherited antithrombin deficiency to the Duffy gene, which encodes an erythrocyte membrane antigen located on chromosome 1 (Lovrien *et al.*, 1978). The localization of the AT gene to chromosome 1q was confirmed by analysis of somatic cell hybrids and by analysis of antithrombin deficient individuals with chromosomal deletions (Bock *et al.*, 1985; Winter *et al.*, 1982; Magenis *et al.*, 1978). In situ hybridization has refined the location of the gene to 1q23 –25 (Bock *et al.*, 1985). Subsequent studies of DNA polymorphisms within the

Figure. 5.1 Structural organization of the antithrombin gene. The black bar represents exons while black line represents introns. (ATT)n indicates two trinucleotide polymorphic sites (Modified from Lane et al., 1997; copyright permission obtained).

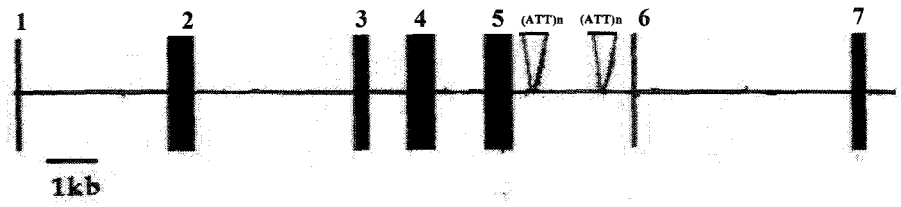
1
2
3
4
5
(ATT)n
(ATT)n
6
7
1kb

antithrombin gene in kindreds with antithrombin deficiency further confirmed that the clinical phenotype was tightly linked to the antithrombin locus on 1q (Bock *et al.*, 1985; Sacks *et al.*, 1988).

Antithrombin cDNA has been cloned and sequenced by three independent groups between 1982 and 1983 (Bock *et al.*, 1982; Prochownik *et al.*, 1983a; Chandra *et al.*, 1983). An open reading frame of 1392 nucleotides was found, which includes 96 nucleotides encode the 32-amino acid signal peptide, and 1,296 nucleotides encode a 432 amino acid mature plasma polypeptide. Subsequent analysis revealed that the transcriptional start site lies 70 nucleotides upstream from the initiator methionine. At the 3' end of the gene, the termination codon and the polyA tail are separated by 87 nucleotides containing a typical polyadenylation signal 54 nucleotides downstream from the termination codon (Bock *et al.*, 1988; Olds *et al.*, 1993).

The entire sequence of the human AT gene was reported (Olds *et al.*, 1993). The gene spans 13,480 bp from the transcriptional start site to last nucleotide of the polyadenylation signal. Analysis of the intron structure of the antithrombin gene reveals the presence of nine complete and one partial Alu repeat elements, with all but one orientated in the reverse direction. The frequency of these repeats is considerably higher in the antithrombin gene (22%) than the overall frequency of such repeats in the human genome (5%), but is consistent with the high frequency of similar repeats observed in other serpin genes. The significance of this observation is unclear, although in at least a few kindreds, it appears that homologous recombination between Alu repeats,

specifically those in intron 4 and 5, is responsible for a gene deletion resulting in inherited AT deficiency (Olds *et al.*, 1993).

5.1.2 Inherited Antithrombin Deficiency

5.1.2.1 Classification of Inherited Antithrombin Deficiency: Antithrombin deficiency can be classified based on the known or presumed site of the molecular pathology in the AT gene and its resulting effect on the circulating molecule. There is no universally accepted nomenclature for the various types of antithrombin deficiency. The classification described in this thesis is that proposed by Lane *et al.* (Lane *et al.* 1997).

5.1.2.1.1 Type I AT Deficiency: Type 1 AT deficiency is inherited as an autosomal dominant trait. Affected heterozygous individuals are characterized by a decrease of both antigenic and functional levels of AT to approximately 50% of those observed in normal individuals (Lane *et al.*, 1993). This condition is caused by a wide variety of heterogeneous molecular mechanisms either through the complete or partial deletion of the gene, or in majority of cases through small insertion or deletions of additional nucleotides within the gene that prevents either transcription, translation, secretion or decreased circulation of the inhibitor (Fernandez-Rachubinski *et al.*, 1992; Olds *et al.*, 1991; Olds *et al.*, 1990; Vidaud *et al.*, 1991). Approximately 80 point mutations and 12 large deletions have been reported to cause type I deficiency. The catabolic rate of infused radiolabeled antithrombin is normal in patients with inherited antithrombin deficiency, suggesting that the deficiency is not exacerbated by accelerated clearance of antithrombin (Knot *et al.* 1986).

5.1.2.1.2 Type II AT Deficiency: Type II AT deficiency is characterized by a low level of antithrombin activity but normal antithrombin antigen. Approximately 35 variants have been identified and can be grouped into three categories:

(1): Type II RS (reactive site) mutations impair the ability of AT to inhibit proteases. These mutations characterized to date have been single nucleotide substitutions altering codons between amino acid residues 382 and 407, the region adjacent to the AT reactive center Arg^{393}-Ser^{394} or at the "hinge region (P10 to P12) (Blajchman, *et al.*, 1992a, 1992b; Stephen *et al* 1987; Lane *et al.*, 1989). Twelve different missense mutations and a total of 55 cases have been reported in cases of type II RS defects (Lane *et al.* 1997).

(2): Type II HBS (heparin binding site) is characterized by the presence of normal plasma progressive AT activity but impaired heparin cofactor activity (Manson *et al.*, 1989). The mutations in this variant have been shown to lie within the first putative heparin-binding region of AT (residues 41 and 47) and second putative heparin-binding region (Lane *et al.* 1997). Heterozygous individuals with this type of AT deficiency do not appear to be at increased risk for thromboembolic events. In contrast, homozygously affected individuals have been reported with clear-cut histories of thromboembolic disease. Such homozygous individuals appear to be at increased risk for thromboembolic events (Finazzi *et al.*, 1987; Borg *et al.*, 1988; Caseo *et al.*, 1990). The Ile-7 to Asn mutation creates a new glycosylation site, and the presence of an oligosaccharide at this site may sterically interfere with heparin binding site. Twelve

distinct mutations and 70 cases have been reported to have type II HBS (Lane *et al.* 1997).

(3): Type II PE (pleiotropic effect) mutations affect both the reactive site and the heparin binding site. Most of these mutations occur in the region P9' to P14', which is thought to be involved in the conformational linkage between the reactive site and the heparin binding site Eleven distinct mutations and 18 cases in total have been grouped into type II deficiency PE (Lane *et al.* 1997).

5.1.2.2 Prevalence: The prevalence of AT deficiency in individuals with symptomatic thrombotic disease is approximately 5% (Hirsh *et al.*, 1989). In the normal population, AT deficiency has been estimated to affect from one per 2,000 to one per 5,000 individuals (Winter *et al.*, 1982; Thaler *et al.*, 1981). A study of almost 4200 healthy blood donors in the west of Scotland estimated the prevalence of Type I deficiency at 1 in 4200; type II RS deficiency at 1 in 22,100, and type II HBS deficiency at 1 in 350 (Tait *et al.*, 1994). In a recent study of normal blood donors, the estimated prevalence of inherited antithrombin deficiency in the general population was approximately one in 500 (Wells *et al.*, 1994). Therefore, inherited antithrombin deficiency may be more common than previously appreciated.

5.1.3 LABORATORY DIAGNOSIS OF ANTITHROMBIN DEFICIENCY

The laboratory diagnosis of antithrombin deficiency is based upon the results of functional and immunological assays.

5.1.3.1 Functional Assays: Antithrombin activity can be measured by either plasma heparin cofactor activity or the progressive antithrombin activity assay performed in the absence of heparin.

The progressive antithrombin activity assay measures the ability of AT to inhibit thrombin or factor Xa both in the absence of heparin. In this assay, inhibition rates are slow and the initial rate of inhibition is usually measured in the presence of excess antithrombin. In the absence of heparin, assays based on thrombin and Xa inhibition may reflect the activity of other plasma inhibition (primarily α_1-antitrypsin and α_2-macroglobulin) as well as that of antithrombin (Abilgaard *et al.*, 1977).

In the plasma heparin cofactor activity assay, inhibition of thrombin or factor Xa by AT is much more specific. Because reaction rates are extremely fast in the presence of heparin, the reaction is usually allowed to proceed to completion in the presence of excess enzyme. Prolonged incubation of test samples at 37° C in the presence of heparin and an excess of thrombin has been shown to result in partial proteolysis of the antithrombin by thrombin leading to an underestimation of its true activity. Assays of antithrombin which involve heparin may also be sensitive to heparin cofactor II concentrations. However, these effects can be minimized by using factor Xa as a substrate instead of thrombin or using bovine rather than human thrombin (Friberger *et al.* 1982; Scully *et al.*, 1977). An important practical point in performing the heparin cofactor assays has been noted by Harper *et al.* who recommend the use of short (<30 seconds) incubation times to increase the sensitivity to antithrombin variants with reduced heparin affinity (Harper *et al.*, 1991).

For initial screening purposes, most laboratories use a synthetic chromogenic substrate to measure residual thrombin activity. In general, an antithrombin activity of lower than 70% of normal pooled plasma represents AT deficiency. In most cases of hereditary AT deficiency, however, AT levels are reduced by approximately 50% of normal (Albildgaard *et al.*, 1977).

5.1.3.2 Immunological Assays: To determine if there is a quantitative AT deficiency, the AT antigen concentration is obtained by an immunochemical method. Both radial immunodiffusion and electroimmunodiffusion can be used to determine antithrombin antigenic levels in plasma using various precipitating antibodies (Laurell, 1972; Mancini *et al.*, 1965). An ELISA assay for determining antithrombin antigen has also been reported. Immunoassays of antithrombin are widely performed and are useful in the diagnosis and the classification of the deficiency states (Edgar *et al.*, 1989). However, normal antigenic levels of antithrombin are commonly found in the presence of a dysfunctional antithrombin variant. Therefore, immunoassays are not recommended as screening tests.

Laurell's technique of 2-dimensional crossed immunoelectrophoresis has been used extensively in the investigation of antithrombin abnormalities. The incorporation of heparin into the agarose for the first electrophoresis is useful in the demonstration of dysfunctional proteins with abnormal heparin affinity. Identification of a slow moving component on crossed immunoelectrophoresis of the plasma in the presence of heparin suggests an abnormal heparin binding affinity (Laurell, 1972).

5.1.4 Molecular Genetic Studies of AT Deficiency

The analysis of genetic polymorphisms within a gene has proved very useful both in the identification of carriers and in the prenatal diagnosis in a number of inherited single gene disorders, including thalassemias and hemophilia A and B (Kleanthous *et al.*, 2001; Goodeve *et al.*, 1998; Prochownik *et al.*, 1983b; Lane *et al.*, 1992). DNA sequencing has been used to identify the mutations in AT deficient individuals, with Southern hybridization of linked restriction fragment length polymorphisms (RFLPs) used to follow the segregation of a specific AT mutation through kindreds (Bock *et al.*, 1983; Daly *et al.*, 1990a). In the AT deficient kindreds where the mutation is unknown, haplotype analysis based on the pattern of linkage of RFLPs within the AT gene can be used to identify the mutant allele. In addition, RFLP analysis has also been applied in the investigation of the genomic basis for antithrombin deficiency in that heterozygosity for any of the RFLPs within the antithrombin locus would exclude a gene deletion affecting that region (Lane *et al.*, 1991). Finally, the analysis of the polymorphisms may allow investigating the origin of mutations, for example, whether apparently unrelated families with the same mutation share a common haplotype suggesting they have a common ancestor (Perry, 1993).

5.1.4.1 Polymorphisms in the Human Antithrombin Gene: Analysis of polymorphism within the antithrombin gene provides a means for following a mutant allele within AT deficient kindreds. Several restriction fragment length polymorphisms (RFLP) have been identified within the human AT gene. This first length polymorphism identified is located 345 base pairs 5' to the initiation codon, consisting of two non-

homologous sequences of DNA (Bock *et al.*, 1983). Sequence analysis has determined that the length of these two alternate sequences contain either 32 base pairs or 108 base pairs. The two alleles thus differ by 76 base pairs and can be detected either on Southern blots or more easily using the polymerase chain reaction to amplify the region of DNA containing the variation. Based on the electrophoretic mobility of shorter and longer fragments, the alleles are identified as either fast (F) or slow (S) respectively. The frequency of the two alleles is F 0.75 and S 0.25 (Bock *et al.*, 1983).

Four polymorphisms involving a single base variation have also been described. The first was within exon 5, resulting from a translationally silent A to G transition at the third position in codon 305. Gln 305 is encoded by either CAA or CAG, the latter sequence creating a recognition site for the restriction enzyme *Pst* 1. Two alleles are found with approximately equal frequency (Prochownik *et al.* 1983b). Three other sequence polymorphisms were identified during the process of characterizing the underlying genetic defects in individuals with antithrombin deficiency. Within exon 4 in codon 295, two alternative sequences GTG/GTA have been found, both of which code for valine. These do not alter any restriction enzyme cutting site, but can be detected by DNA sequencing. The two alleles have almost equal frequencies of 0.43 and 0.57 respectively. An *Nhe* I site polymorphism has been located within intron 4, about 100 base pairs 3' to exon 4. This polymorphic site is associated with the creation of a new recognition site for the restriction enzyme *Nhe*, with the (+) allele representing the presence of the *Nhe* I cutting site, found at a frequency of 0.64 and the (-) allele at 0.36. At position 27 of intron 5, the presence of a G creates a cleavage site for Dde 1 which is

absent when the alternative C is present. The two alleles are found at frequencies of (+) 0.83 and (-) 0.17 (Wu *et al.*, 1989; Bock *et al.*, 1991; Daly *et al.*, 1990a).

In addition to these sequence and length polymorphisms, two single amino acid variations that may represent polymorphisms have also been described. Daly *et al.* have identified a point mutation, GTC to GAG in the signal peptide nucleotide sequence, which leads to a –3 Val to Glu substitution (Daly *et al.*, 1990b). Another possible polymorphism is CCA to CAA in codon 359 in exon 5, leading to the substitution Arg to Gln (Lane *et al.*, 1993).

The ability to use RFLP linkage for genetic diagnosis is dependent upon the availability of informative RFLPs in families. In almost every instance, variability results from restriction site gain/loss by base substitution, microdeletion or insertion. The majority of RFLPs are diallelic polymorphisms, with the maximum heterozygosity being only 50%.

5.1.4.2 Short Tandem Repeat Polymorphism in the Human AT Gene: The analysis of highly polymorphic DNA sequences using the polymerase chain reaction (PCR) provides potentially important polymorphic markers for carrier detection, prenatal diagnosis, and genetic linkage analysis in various genetic disorders (Jeffries 1990). These systems offer several advantages over Southern hybridization analysis of RFLP, including increased speed and sensitivity of detection, and the ability to resolve discrete alleles (Edwards *et al.*, 1991; 1992). Hypervariability at these loci results from changes in the number of repeats, presumably driven either by unequal recombination between misaligned repetitive sequences or by slippage at replication forks leading to

the gain or loss of repeat units (Richard and Paques, 2000). The resulting length variability can be high. In some cases, the frequency of heterozygotes can sometimes approach 100% (Riggins *et al.*, 1992). Furthermore, detection of these STRs is no longer dependent on the restriction endonuclease used. Therefore, these loci provide ideal markers for human genetics.

While analysis of STRs provides a large amount of genetic marker information suitable for linkage analysis, there are several drawbacks to this approach. Firstly, disease diagnosis has to be accurate in the limited number of members of the pedigree. Secondly and more important, linkage between a STR sequence and a disease locus cannot be further tested in other affected families (Riggins *et al.*, 1992).

Two (ATT)n trinucleotide repeat sequences have been identified, both of which are located within intron 5 of human AT gene. The first repeat is located in the tail of Alu 5 and the second repeat is located in the tail of the Alu 8. These repeat sequences are likely to be similar to the previously described short tandem repeats that have been discovered in the human genome (Ni, *et al*, 1994a; 1994b; Waye *et al.*, 1994).

5.1.5 Rationale and Objectives

Dr. Blajchman's laboratory has sequenced the introns of the human AT gene. Two repeat sequences were identified in this region. The first one is located at the tail of Alu 5 and the second one is located at the tail of Alu 8. It is very likely that these repeat sequences are similar to the short tandem repeats that have been discovered in the human genome. If this hypothesis is true, using the polymerase chain reaction method to amplify and sequence this sequence should provide a novel polymorphic marker to

perform genetic analysis of AT deficient kindreds. In addition, this polymorphic marker should also be useful for genetic diagnosis and linkage studies in other chromosome 1 related genetic disorders.

The objective of this research project was to characterize this short tandem repeat sequence and to validate its usefulness by performing genetic linkage studies in previously characterized AT deficient kindreds using this marker.

5.2 Materials and Methods

5.2.1 Materials

5.2.1.1 Source of Chemicals and Reagents: Electrophoresis grade agarose was purchased either from Bethesda Research Laboratories (BRL) (Burlington, ON) or from Pharmacia LKB biotechnology (Baie d'Urfe', QC). Ethidium bromide (EtBr), ampicillin, were purchased from Sigma Chemical Company (St. Louis, MO). Ammonium acetate (NH4Oac), boric acid, ethylene-diamine-tetraacetic acid (EDTA), glycerol, polyethylene glycol (PEG), potassium acetate (KOAc) and sodium acetate (NaOAc) were purchased from BDH Chemicals (Toronto, ON). Acrylamide, ammonium persulfate (APS), N, N'-methylene-bis-acrylamide (BIS), bromophenol blue, glycine, Tris (hydroxymethyl) aminomethane (TRIS) and urea were purchased from Bio-Rad Laboratories (Mississauga, ON). All other chemicals and reagents were of the highest quality available.

5.2.1.2 Plasmid Vector: The pGEM-3Zf (+) vector was purchased from Promega-Biotec. This vector contains sequences coding for the lac Z M15 gene to produce functional β-galactosidase. Bacterial colonies containing recombinant pGEM-3Zf (+) are white in colour due to the disruption of complementation.

5.2.1.3 Radiochemicals: The [^{32}P] dATP (3000 Ci/mmol, 10 μCi/ul) was purchased from Amersham (Oakville, ON).

5.2.1.4 Enzymes: Restriction endonucleases were purchased either from Pharmacia LKB Biotechnology or BRL. T4 DNA ligase, T4 DNA polymerase, T7 DNA sequencing kits were purchased from Pharmacia Biotech (Piscataway, NJ). Taq polymerase was purchased from Perkin-Elmer/Cetus (Toronto, Ontario). The enzymes were used according to the manufacturer's product data sheet.

5.2.1.5 Bacterial Cell Lines: Routine transformations were carried out in competent *E.coli* DH5α cells purchased from BRL (Burlington, ON). Transformed *E.coli* cells were routinely grown at 37° C with shaking in Luria-Broth (LB) medium [1% bacto-tryptone, 0.5% (w/v) bacto-yeast extract, 1% (w/v) NaCl, pH 7.5] supplemented with 100 μg/ml ampicillin. Transformed *E.coli* cells were initially selected on LB plates containing 1.5% (w/v) bacto-agar.

5.2.1.6 Oligodeoxyribonucleotides: The oligonucleotide primers were synthesized by the Institute for Molecular Biology and Biotechnology, McMaster University (Hamilton, Ontario, Canada). The sequences of the three oligonucleotide primers used were as follows:

Primer 1: 5' (TGA AGC CTG AGA ATG AAT TAT CAG) 3';

Primer 2: 5' (AGA GTG GGG AAG GTG TAC TC) 3';

Primer 3: 5' (CCA CTG CAC TCC AGC CTG GG) 3'.

5.2.1.7 DNA Samples: Whole blood samples were from 81 unrelated Caucasian individuals living in the South Ontario region of Canada. These individuals are primarily

of Mediterranean origin (Greek and Italian). Whole blood samples were also obtained from individuals of three diagnosed AT deficient kindreds (AT-Hamilton, AT-Amiens, and AT-Delhi) including total of 65 individuals (Demers *et al.*, 1992; Roussel *et al.*, 1991; Devraj-Kizuk *et al.*, 1988).

5.2.2 Methods

5.2.2.1 Preparation of DNA Samples: Whole blood collected in tubes containing EDTA was centrifuged at 1200 x g for 15 minutes and the buffy coat was collected and stored at -70°C. Genomic DNA was then isolated from these samples using phenol/chloroform extraction method (Poncz *et al.*, 1982).

5.2.2.2 PCR Amplification of the STR: PCR amplification was performed in a total volume of 50 μl using nested primers. Each reaction mixture consisted of 200 ng genomic DNA, 200 pmol of each primer, 200 μM of each dNTP, 50 mM KCl, 10 mM Tris-Cl, pH 8.3, 1.5 mM $MgCl_2$, 0.01% (w/v) gelatin, and 2 units of Taq polymerase (Perkin-Elmer/Cetus). In the initial PCR reaction, primer 1 and primer 2 were used to amplify a DNA segment varying between 622 bp $(ATT)_5$ and 661 bp $(ATT)_{18}$ spanning the AT3-STR in the fifth intron of the AT3 gene. This fragment contained a Sac I restriction enzyme on the 5' tail and a Sph I on the 3' tail of (ATT)n repeat. PCR-amplification was carried out using initial denaturation at 94°C for 7 minutes, followed by 30 cycles of amplification with each consisting of 94°C for 2 minutes, 58°C for 1 minute, and 72°C for 1 minute. An additional extension step was carried out at 72°C for 10 minutes. For the second PCR reaction, 2 μl of the first PCR product was amplified using primers 1 and 3 in the presence of 2 μCi of [α-^{32}P]dATP (3000 Ci/mmol). This PCR

amplification was carried out for 28 cycles, each consisting of 1.5 minutes at 92°C, 45 seconds at 60°C, and 45 seconds at 72°C. The labelled PCR products were then diluted fivefold in formamide loading buffer, and denatured at 100°C for 5 minutes. The samples were then electrophoresed on an 8% DNA-sequencing gel and visualised by autoradiography. Allele sizes were determined relative to both sequencing ladders and the alleles with a known number of repeat units (Edwards *et al.*, 1991; 1992).

5.2.2.3 Subcloning and DNA Sequencing: After initial PCR amplification, the products were phenol extracted, ethanol precipitated and digested with the restriction enzymes Sac I and Sph I. The digested products were then ligated into a pGEM-3Zf(+) plasmid, and the resultant constructs were transformed into DH5α competent host cells. The subcloned PCR products were then sequenced with SP6 universal primer by using the T7 Sequencing Kit. Multiple clones were sequenced for each allele to rule out potential sequence artifacts due to nucleotide base misincorporation during PCR amplification.

5.2.2.4 Linkage Studies: Linkage analysis of AT-STR was performed in three previously described AT-deficient kindreds, AT-Hamilton (Ala382Thr), AT-Amiens(Arg 47 Cys) and AT-Delhi (Arg 47 Cys). The three generations of the AT-Hamilton kindred consists of 81 living family members. A diagnosis of AT deficiency was made in 31 individuals in the AT-Hamilton kindred based initially on functional antithrombin assays. DNA sequencing and restriction enzyme analysis revealed that the affected individuals had the mutant allele exhibiting a point mutation of guanine to adenine in the first base of codon 382, causing an Ala 382 Thr substitution. In the

present study, DNA samples from 53 individuals of the kindred, including 27 affected and 26 non-affected individuals, were examined. The AT-Amiens kindred has eight individuals in three generations, consisting of five affected and three non-affected individuals. Affected members of this kindred have a point mutation, cytosine to thymine, at the first base of codon 47 of the AT gene resulting in an Arg 47 Cys substitution. DNA samples from seven members in this kindred were analyzed. The AT-Delhi kindred has four individuals in two generations, including three affected and one non-affected individuals. Like AT-Amiens, a point mutation causes a substitution of Arg at amino acid 47 to Cys. DNA samples from all four members in this kindred were examined.

5.3 Results

5.3.1 *In vitro* Amplification and Characterization of STR

5.3.1.1 PCR Amplification and Sequencing of STR: An (ATT)n repeat unit was identified within the fifth intron of human antithrombin gene located on chromosome 1q23. Primers flanking this (ATT)n region were designed for PCR amplification of this locus and the resultant products were subcloned and sequenced. The obtained results revealed this (ATT)n STR to be highly polymorphic with repeat units ranging in number from $(ATT)_5$ to $(ATT)_{18}$. The sequencing results for three independent alleles are shown in figure 5.2.

Figure 5.2 DNA sequence analysis of the AT3-STR regions in three different alleles. PCR products were ligated into the pGEM-3Zf(+) plasmid vector and sequenced with the SP6 universal primer. The sequences of the three independent alleles have repeat units of $(ATT)_{18}$, $(ATT)_{16}$, and $(ATT)_5$, respectively.

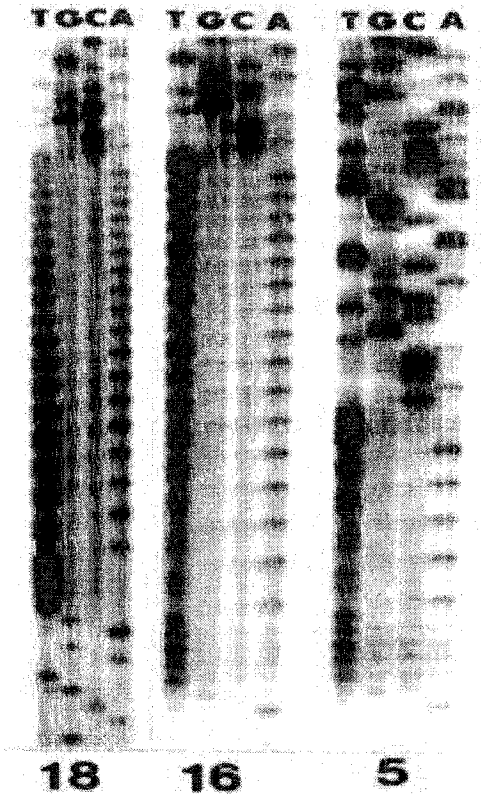
TGCA
TGCA
TGCA
18
16
5

5.3.1.2 Allele Frequency: The allele frequency of this (ATT)n has been evaluated in 81 unrelated Caucasian individuals (162 alleles). The [a-^{32}P]dATP labelled PCR products containing (ATT)n region were analyzed on 8% DNA sequencing gels. Ten distinct alleles were identified with repeat units ranging in number from $(ATT)_5$ to $(ATT)_{18}$. The observed heterozygosity of this locus is 81% (0.81). Allele frequencies are summarized in table 5.1.

5.3.2 Linkage Studies of AT-Deficient Families

To test the applicability of the AT3-STR as a marker for indirect tracking of AT mutations, three previously characterized AT-deficient kindreds, AT-Hamilton, AT-Amiens, and AT-Delhi were analyzed using this (ATT)n polymorphic marker. The data revealed that in each kindred, the inheritance of the various AT3-STR alleles occurred in a Mendelian manner. Consistent with previous studies of trinucleotide and tetranucleotide STRs, electrophoresis of radioactive PCR products showed that each allele had an intense single band with some "shadow" bands below and above (Huang *et al.*, 1991). The shadow bands created during PCR amplification were not eliminated by changes in PCR reaction conditions. These PCR artifacts may be due to 3' base addition by Taq polymerase during PCR amplification. Nevertheless, the shadow band pattern is highly reproducible and does not interfere with allele assignment.

5.3.2.1 Genetic Linkage Study in AT-Hamilton Kindred: The AT-Hamilton kindred consists of eighty-one living family members. A diagnosis of AT deficiency was made in thirty-one individuals based on the functional antithrombin assays. DNA sequencing and restriction enzyme analysis revealed that all affected individuals had the

Table 5.1 Allele Frequency Estimated from 81 Unrelated Caucasian

Allele	Size (bp)	# of repeats	Frequency
A1	115	5	0.117
A2	130	10	0.062
A3	133	11	0.117
A4	136	12	0.012
A5	139	13	0.019
A6	142	14	0.340
A7	145	15	0.025
A8	148	16	0.117
A9	151	17	0.154
A10	154	18	0.037

Observed heterozygosity =0.81

mutant allele possessing of a point mutation of guanine to adenine in the first base of codon 382, causing an Ala 382 Thr substitution. In the present study, DNA samples from fifty-three individuals, including twenty-seven affected and twenty-six non-affected individuals, in this kindred were examined. The results revealed that all of the affected individuals had the $(ATT)_{17}$ allele without an exception, indicating that the AT-Hamilton mutation is strongly associated with the $(ATT)_{17}$ AT3-STR allele. Figure 5.3 illustrates the genetic linkage study results from two subfamilies from the AT-Hamilton kindred.

5.3.2.2 Genetic Linkage Study in AT-Amiens Kindred: Linkage studies were also performed with the AT-Amiens kindred. Affected members of this kindred have a point mutation, C to T, in the first base of codon 47 of the AT gene resulting in an Arg 47 Cys substitution. DNA samples from seven members in this kindred were analyzed. The results are shown in figure 5.4. Clearly the AT-Amiens mutation is associated with an $(ATT)_{18}$ allele as evident by the presence of this allele in all affected individuals.

5.3.2.3 Genetic Linkage Study in AT-Delhi Kindred: Linkage studies were performed with the AT-Delhi kindred. Like the AT-Amiens, a point mutation causes a substitution of Arg at amino acid 47 to Cys. In this family, the mother is normal and is heterozygous. She has alleles with 16 and 14 repeats. The father is affected and has alleles with 18 and 16 repeats. Both daughter and son are affected. They all inherited defective alleles with 18 repeats from their father. The son inherited an additional 14 repeats allele from his mother while the daughter inherited 16 repeat allele. Thus, the mutation in this family is also associated with an allele with 18 repeats as shown in figure 5.5.

Figure 5.3 Linkage studies of AT3-STR in two families (A and B) within the AT-Hamilton (Ala 382 Thr) kindred. Solid symbols represent AT-deficient individuals. The length of the AT3-STR PCR-product is indicated as base pairs (bp), with the number of ATT repeat units for each allele shown in parenthesis. In this kindred, the 151 bp $[(ATT)_{17}$ allele segregates with the AT-Hamilton mutation in all AT-deficient individuals in both the A and B families.

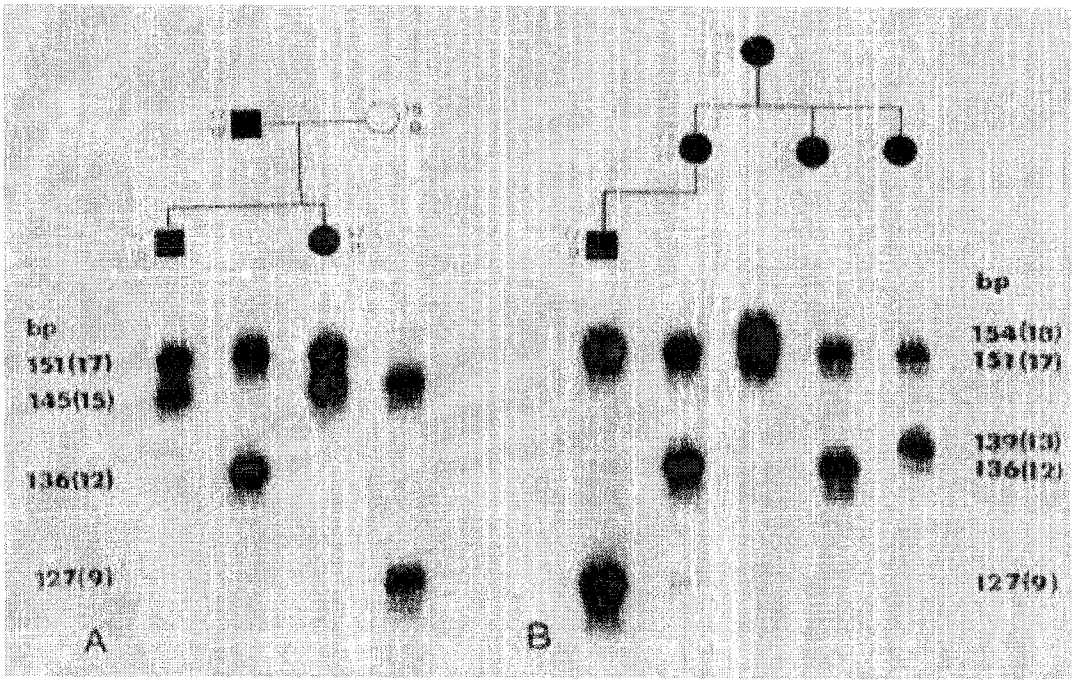
bp
151(17)
145(15)
136(12)
127(9)
A
bp
154(16)
151(17)
139(13)
136(12)
127(9)
B

Figure 5.4 Linkage studies of AT3-STR in the AT-Amiens (Arg 47 Cys) kindred in which the 154 bp [$(ATT)_{18}$] allele segregates with the AT-Amiens mutation in all AT-deficient individuals.

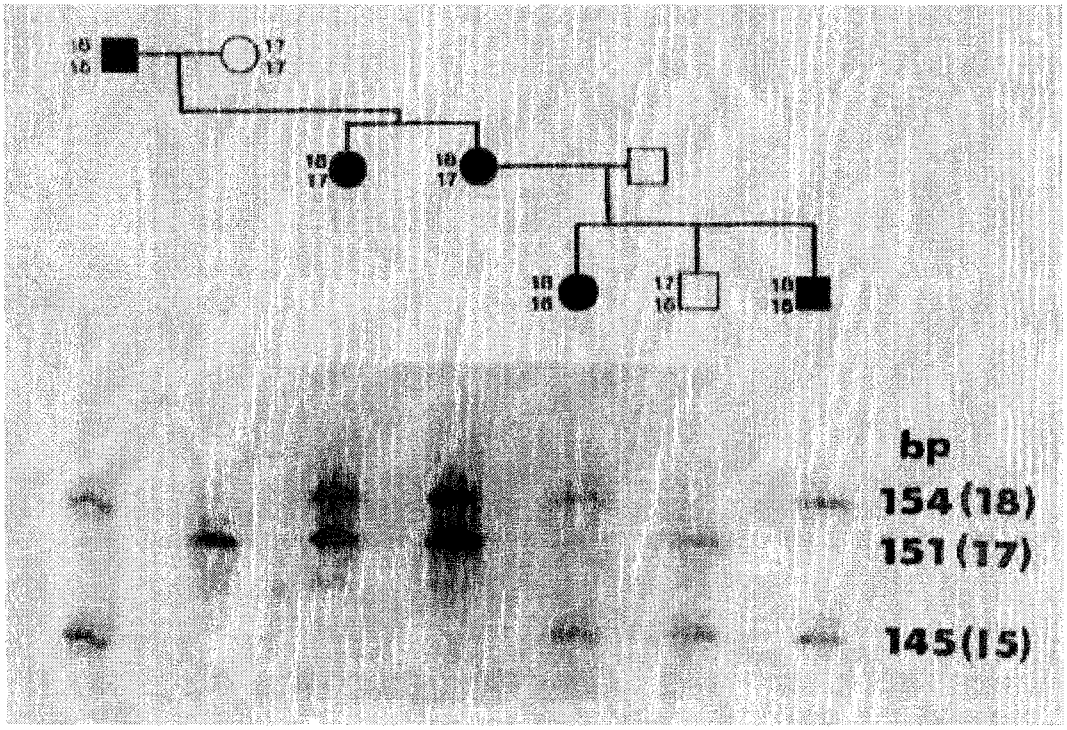
bp
154 (18)
151 (17)
145 (15)

Figure 5.5 Linkage studies of AT3-STR in the AT-Delhi (Arg 47 Cys) kindred in which 154 bp [$(ATT)_{18}$] allele segregates with the AT-Delhi mutation in all AT-deficient individuals.

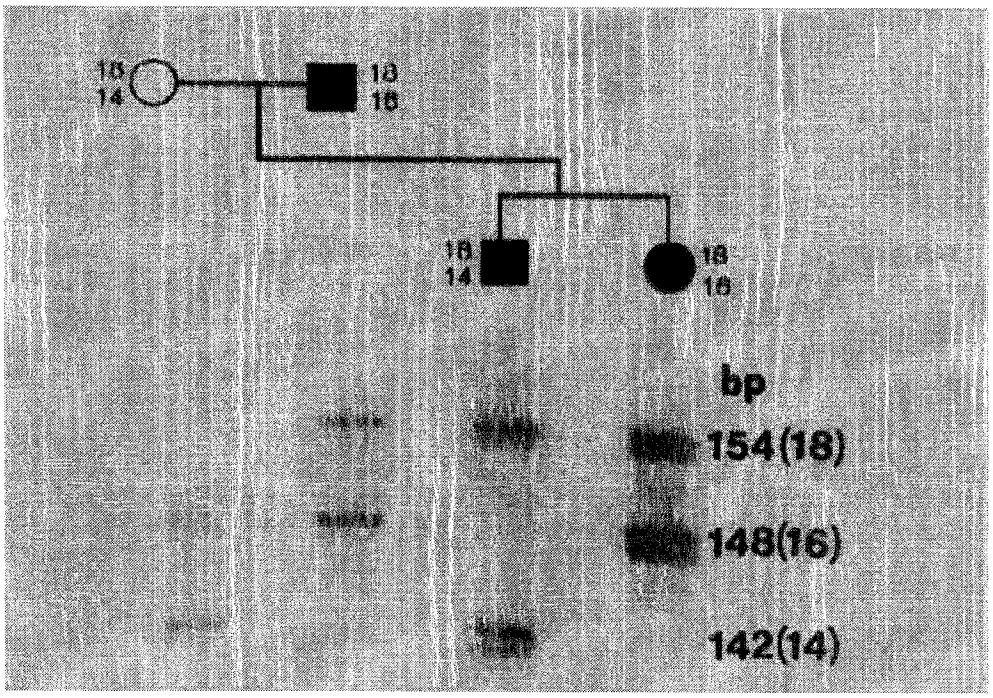
18
14
18
18
18
14
18
18
bp
154(18)
148(16)
142(14)

5.3.2.4 Genetic Linkage Study in Other Kindreds with Arg 47 Cys Mutation:

The linkage studies of AT-Amiens and AT-Delhi have shown that Arg 47 Cys mutation is associated with an $(ATT)_{18}$ allele in both families. It is therefore interesting to investigate whether apparently unrelated families with the Arg 47 Cys mutation have a common allele. To test this hypothesis, we have obtained DNA samples from individuals in two kindreds with Arg 47 Cys mutation. These families were initially diagnosed and characterized in Britain. The genetic linkage studies in these two kindreds showed that the Arg 47 Cys mutation in one family is associated with an $(ATT)_{18}$ allele, while the mutation in other kindreds appeared to be associated with an $(ATT)_{14}$ allele. The summary of the genetic linkage studies in four kindreds with Arg 47 Cys mutation is shown in Table 5.2.

Table 5.2 Summary of (ATT)n STR Analysis in the AT-Deficient Families

Family	Mutation	Allele
1 (Amiens)	Arg47Cys	$(ATT)_{18}$
2 (Delhi, Ont.)	Arg47Cys	$(ATT)_{18}$
3	Arg47Cys	$(ATT)_{18}$
4	Arg47Cys	$(ATT)_{14}$

5.4 Discussion

Many short tandem repeats have been discovered within the human genome, most of which are highly polymorphic due to considerable variation in the number of repeat units (Edwards *et al.*, 1991; 1992; Riggins *et al.*, 1992; NIH/CEPH, 1992; Vergnaud and Denoeud, 2000). PCR amplification and analysis of these STRs have provided an attractive additional tool for carrier detection, prenatal diagnosis, and linkage studies of genetic disorders (Petersen *et al.*, 1991; Clemens *et al.*, 1991; Schichman *et al.*, 2002). In this research project, we have characterized a new (ATT)n STR located within the fifth intron of the human antithrombin gene. We designated this highly polymorphic STR as AT-STR.

5.4.1 Allele Frequency of (ATT)n STR

As with most STR within the human genome, the AT3-STR is highly polymorphic due to variable trinucleotide repeat units ranging from $(ATT)_5$ to $(ATT)_{18}$. This (ATT)n STR compares favourably with the previously described intragenic polymorphic markers within the human antithrombin gene, with a heterozygosity of 81% (Blajchman *et al.*, 1992; Fernandez-Rachubinski *et al.*, 1992). Therefore, PCR-based analysis of this new AT3-STR is genetically informative and should be useful for genetic diagnosis and linkage studies for kindreds with AT-deficiency as well as other chromosome 1 related genetic disorders.

This PCR-based STR analysis has several advantages over the conventional Southern-based RFLP analysis for genetic diagnosis and linkage studies (Edwards *et al.*, 1991; 1992; Peterson *et al.*, 1991; Kaiser *et al.*, 2002).

(1) This PCR-based STR increased speed and sensitivity of detection.

(2) This PCR-based STR has the ability to resolve discrete alleles. The variability at these STR results from changes in the number of repeat units, presumably due to either unequal recombination between misaligned repeats or slippage at replication forks leading to the gain or loss of repeat units (Richard and Paques, 2000). The resulting length variability can be high, with in some cases the frequency of heterozygotes approaching 100% (Tomita *et al.*, 2002).

(3) Furthermore, detection of the STRs is no longer dependent on the restriction endonuclease used.

(4) Finally, this PCR-based STR analysis requires only a small amount of genomic DNA.

While PCR based STR analysis provides a large amount of genetic information suitable for linkage analysis, there are several drawbacks to this approach. First, disease diagnosis has to be accurate in the limited number of members of the pedigree. Second and more important, linkage between a STR repeat fragment and a disease locus cannot be further tested in other affected families, since DNA fragments allelic to that found in the first pedigree tested cannot be clearly identified in other kindreds (Huang *et al.*, 1991; Peake *et al.*, 1990).

5.4.2 Genetic Linkage Studies in AT Deficient Kindreds

Three previously characterized AT-deficient kindreds known as AT-Hamilton (Ala 382 Thr), AT-Amiens (Arg 47 Cys), and AT-Delhi (Arg 47 Cys) were studied in this project by using this AT-STR (Demers *et al.*, 1992; Roussel *et al.*, 1991; Devraj-Kizuk *et al.*, 1988). DNA samples from 27 affected members and 26 non-affected members have been analyzed in AT-Hamilton kindred. The results indicate that the AT-Hamilton

mutation is linked to a 17 repeat allele. The analysis of AT-Amiens and AT-Delhi kindreds revealed that the mutation in both kindreds is associated with allele with 18 repeats. The results showed that these AT deficient kindreds inherit the AT3-STR polymorphic alleles in a Mendelian manner. The results of the genetic linkage studies described here are matched with previous results obtained with both RFLP as well as functional AT3 analyses.

The results indicate that a specific (ATT)n polymorphism is strongly associated with each AT-mutation in the kindreds studied. Therefore, PCR amplification of this AT3-STR should be useful in tracking the mutant allele in families with AT deficiency.

5.4.3 Genetic Linkage Studies in AT Deficient Kindreds With Arg 47 Cys Mutations

Four AT deficient kindreds with Arg 47 Cys mutations are analyzed in this project to investigate whether unrelated kindreds with the same mutation share a common haplotype (Perry and Carrell, 1989). Two kindreds were diagnosed and characterized in Canada, while another two kindreds were initially diagnosed and characterized in Britain (Roussel *et al.*, 1991). The results showed that the mutations in three kindreds are associated with the allele with $(ATT)_{18}$ repeat, while the mutation in fourth kindred is associated with an $(ATT)_{14}$ allele. Therefore, the Arg 47 Cys mutation is associated at least two different haplotypes. Further studies are required to investigation this hypothesis.

5.5 Conclusion and Future Studies

In summary, the AT3-STR locus within the fifth intron of the AT gene is highly polymorphic and therefore is genetically informative. PCR-based analysis of this repeat is well suited for genetic diagnosis and linkage studies for families of AT-deficient as well as other chromosome 1 related genetic disorders.

Since the results presented in this study indicate that a specific (ATT)n polymorphism is strongly associated with particular AT mutations, it is likely that this PCR-based STR system can be used to perform linkage studies in the various kindreds with identical mutations. Future studies in continuation of these investigations may involve using this $(ATT)_n$ AT3-STR combined with other polymorphic markers within AT gene to investigate whether unrelated families with same mutation share a common haplotype. Such studies will provide important information about whether the same mutation has a common origin i.e. a 'founder' effect (Perry and Carrell, 1989).

REFERENCES

Abilgaard, U., Lie, M., Odegard, O.R. (1977) Antithrombin (heparin cofactor) assay with 'new' chromogenic substrates (S-2238 and Chromozym TH). Thromb. Res. 11,549-553.

Blajchman, M.A., Austin, R.C., Fernandez-Rachubinski, F., Sheffield, W.P. (1992a) Molecular basis of inherited human antithrombin deficiency. Blood 80,2159-2171.

Blajchman, M. A., Fernandez-Rachubinski, F., Sheffield, W., Austin, R.C., Schulman, S. (1992b) Antithrombin-III-Stockholm: A codon 392 (Gly→Asp) mutation with normal heparin binding and impaired serine protease reactivity. Blood 79,1428-1432.

Bock, S.C., Wion, K.L., Vehar, G.A., Lawn, R.M. (1982) Cloning and expression of the cDNA for human antithrombin III. Nucl. Acids Res. 10, 8113-8125.

Bock, S.C., and Levitan, D.J. (1983) Characterization of an unusual length polymorphism 5' to the human antithrombin III gene. Nucleic Acids Res. 11, 8569.

Bock, S.C., Harris, F.J., Balazs, I., Trent, J.M. (1985) Assignment of the human antithrombin III structural gene to chromosome 1q23-25. Cytogenet. Cell Genet. 39,67-69.

Bock S.C., Marrinan, J.A., Radziejewska, E. (1988) Antithrombin III Utah: proline-407 to leucine mutation in a highly conserved region near the inhibitor reactive site. Biochemistry 27, 6171-6178.

Bock, S.C., and Radziejewska, E. (1991) A NheI RFLP in the human antithrombin III gene (1q23-q25) (AT3). Nucleic Acid Res. 19, 2519.

Borg, J-Y., Owen, M.C., Soria, C., Soria, J., Caen, J., Carrell, R.W. (1988) Proposed heparin binding site in antithrombin based on arginine 47. A new variant Rouen-II, 47 Arg to Ser. J. Clin. Invest. 81,1292-1296.

Caso, R., Lane, D.A., Thompson, E., Azngouras, D., Panico, M., Morris, H., Olds, R.J. Thein, S.L., Girolami, A. (1990) Antithrombin Padua 1: Impaired heparin binding caused by an Arg47 to His (CGT to CAT) substitution. Thromb. Res. 58, 185-190.

Chandra, T., Stackhouse, R., Kidd, V.J., Woo, S.L. (1983) Isolation and sequence characterization of a cDNA clone of human antithrombin III. Proc. Natl. Acad. Sci. USA 80, 1845-1848

Clemens, P.R., Fenwick, R.G., Chamberlain, J.S., Gibbs, R.A., de Andrade, M., Chakraborty, R., Caskey, C.T. (1991) Carrier detection and prenatal diagnosis in Duchenne and Becker muscular dystrophy families, using dinucleotide repeat polymorphisms. Am. J. Hum. Genet. 49, 951-960.

Daly, M.E., and Perry, D.J. (1990a) Dde1 polymorphism in intron 5 in the antithrombin. Nucleic Acid Res. 18, 5583.

Daly, M., Bruce, D., Perry, D., Price, J., Harper, P.L., O'Meara, A., Carrell, R.W. (1990b) Antithrombin Dublin (-3 Val-Glu): an N-terminal variant which has an aberrant signal peptidase cleavage site. FEBS Lett. 273,87-90.

Demers, C., Ginsberg, J.S., Hirsh, J., Henderson, P., Blajchman, M.A. (1992) Thrombosis in antithrombin-III-deficient persons: Report of a large kindred and literature review. Ann. Intern. Med. 116,754-761.

Devraj-Kizuk, R., Chui, D.H.K., Prochownik, E.V., Carter, C.J., Ofusu, F.A., Blajchman, M.A. (1988) Antithrombin-III-Hamilton: A gene with a point mutation (Guanine to Adenine) in codon 382 causing impaired serine protease reactivity. Blood 72,1518-1523.

Edgar, P., Jennings, I., Harper, P. (1989) Enzyme linked immunosorbent assay for measuring antithrombin III. J. Clin. Pathol. 42,985-987.

Edwards, A, Civitello, A, Hammond, H.A, Caskey, C.T. (1991) DNA typing and genetic mapping with trimeric and tetrameric tandem repeats. Am J Hum Genet 49:746-756

Edwards, A., Hammond, H.A., Jin, L., Caskey, T., Chakraborty, R. (1992) Genetic variation at five trimeric and tetrameric tandem repeat loci in four human population groups. Genomics 12, 241-253.

Fernandez-Rachubinski, F., Rachubinski, R.A., Blajchman, M.A. (1992) Partial deletion of an antithrombin III allele in a kindred with a type 1 deficiency. Blood 80,1476-1481.

Finazzi G., Caccia, R., Barbui, T. (1987) Different prevalence of thromboembolism in the subtypes of congenital antithrombin III deficiency: Review of 404 cases. Thromb. Haemost. 58,1094-1095.

Friberger, F., Egberg, N., Holmer, E., Hellgren, M., Blomback, M. (1982) Antithrombin assay-the use of human or bovine antithrombin and the observation of a second heparin cofactor. Thromb. Res. 25,433-436.

Goodeve, A.,C. (1998) Advances in carrier detection in haemophilia. Haemophilia. 4, 358-64

Harper, P.L., Daly, M., Price, J., Edgar, P.F., Carrell, R.W. (1991) Screening for heparin binding variants of antithrombin. J.Clin. Pathol. 44,477-479.

Hirsh, J., Piovella, F., Pini, M. (1989) Congenital antithrombin III deficiency. Am. J. Med. 87, 34S.

Huang, T.H., Hejtmancik, F., Edwards, A., Pettigrew, A.L., Herrera, C.A., Hammond, H.A., Caskey, C.T., Zoghbi, H.Y., Ledbetter, D.H. (1991) Linkage of the gene for an X-linked mental retardation disorder to a hypervariable (AGAT)n repeat motif within the human hypoxanthine phosphoribosyltransferase (HPRT) locus (Xq26). Am J Hum Genet 49,1312-1319.

Jeffries, A.J., Neumann, R., Wilson, V. (1990) Repeat unit sequence variation in minisatellites: A novel source of DNA polymorphisms for studying variation and mutation by single molecule analysis. Cell 60,473-485.

Kaiser, R., Tremblay, P.-B., Roots I., Brockmoller, J. (2002) Validity of PCR with emphasis on variable number of tandem repeat analysis. Clin. Biochem. 35,49-56.

Kleanthous, M., Kyriacou, K., Kyrri, A., Kalogerou, E., Vassiliades, P., Drousiotou, A., Kallikas, I., Ioannou, P., Angastiniotis, M. (2001) Alpha-thalassaemia prenatal diagnosis by two PCR-based methods. Prenat Diagn. 21, 413-7.

Knot, E.A., de Jone, E., ten Cate, C.W., Iburg, A.H., Henny, C.P., Bruin, T., Stibbe, J. (1986) Purified radiolabeled antithrombin III metabolism in three families with hereditary AT III deficiency: application of a three-compartment model. Blood 67,93-99.

Lane, D.A., Erdjument, H., Thompson, E., Panico, M., DiMarzo, V., Morris, H.R., Leone, G., DeStefano, V., Thein S-L. (1989) A novel amino acid substitution in a congenital variant antithrombin: Antithrombin Pescara, Arg 383 to Pro, caused by a CGT to CCT mutation. J. Biol. Chem. 264,10200-10204.

Lane, D.A., Ireland, H., Olds, R.J., Thein, D., Perry, D., Aiach, M. (1991) Antithrombin III: A database of mutations. Thromb. Haemost. 66,657-661.

Lane, D.A., Olds, R.R., Thein, S-L. (1992) Antithrombin and its deficiency states. Blood Coagulation and Fibrinolysis 3,315-341.

Lane, D.A., Olds, R.J., Boisclair, M., Chowdhury, V., Thein, S.L., Cooper, D.N., Blajchman, M.A., Perry, D., Emmerich, J., Aiach, M. (1993) Antithrombin III mutation database: First update. For the thrombin and its inhibitors subcommittee of the scientific

and standardization committee of the international society on thrombosis and haemostasis. Thromb Haemost 70,361-369.

Lane, D.A., Bayston, T., Olds, R.J., Fitches, A.C., Cooper, D.N., Millar, D.S., Jochmans, K., Perry, D.J., Okajima, K., Thein, S.L., Emmerich, J. (1997) Antithrombin mutation database: 2nd(1997) update. Thromb Haemost 77,197-211.

Laurell, C.B. (1972) Electroimmunoassay. Scand J. Clin Lab. Invest. 125, 21-37.

Lovrien, E.W., Magenis, R.E., Rivas, M.L., Goodnight, S., Moreland, R., Rowe, S., (1978) Linkage study of antithrombin III. Cytogenet Cell Genet 22,319-324.

Magenis, R.E., Donlon, T., Parks, M., Rivas, M.L., Lovrien, E.W. (1978) Linkage relationships of dominant antithrombin III deficiency and the heterochromatic region of chromosome 1. Cytogenet. Cell Genet 22, 327-329.

Mancini, G., Carbonara, A.O., Hermans, J.F. (1965) Immunochemical quantitation of antigens by single radial immunodiffusion. Immunochemistry 2,235-240.

Manson, H.E., Austin, R.C., Fernandez-Rachubiski, F. Rachubinski, R.A., Blajchman, M.A. (1989) The molecular pathology of inherited human antithrombin III deficiency. Transfusion Med. Rev. 3,264-271.

Ni, H., Waye, W.P., Sheffield, B., Eng, B., Blajchman, M.A. (1994a) Genetic linkage studies in antithrombin-deficient kindreds using a highly polymorphic trinucleotide short tandem repeat (STR) within the human antithrombin gene. Am. J. Hematol. 46,107-111.

Ni, H., Waye, J.S., Austin, R.C., Calverley, D., Eng, B., Sheffield, W.P. Blajchman, M.A. (1994b) Characterization of a highly polymorphic trinucleotide short tandem repeat within the human antithrombin gene. Thromb. Res. 74,303-307.

NIH/CEPH collaborative mapping group (1992) A comprehensive genetic linkage map of the human genome. Science 258,148-162.

Olds, R.J., Lane, D.A., Finazzi, G., Barbui, T., Thein S-L. (1990) A framshift mutation leading to type 1 antithrombin deficiency and thrombosis. Blood 76,2182-2185.

Olds, R.J., Lane, D.A., Ireland, H., Leone, G., DeStefano, V., Cazenave, J.P. Wiessel, M.L., Thien, S.L. (1991) Novel point mutations leading to type 1a antithrombin deficiency and thrombosis. Br. J. Haematol. 78,408-411.

Olds, R.J., Lane, D.A., Chowdhury, V., DeStefano, V., Leone, G., Thein, S-L. (1993) Complete nucleotide sequence of the antithrombin gene. Evidence for homologous recombination causing thrombophilia. Biochemistry 32,4216-4224.

Peake, I.R., Bowen, D., Bignell, P., Liddell, M.B., Sadler, J.E., Standen, G., Bloom, A.L. (1990) Family studies and prenatal diagnosis in severe von Willebrand disease by polymerase chain reaction amplification of a variable number tandem repeat region of the von Willebrand factor gene. Blood 76,555-561.

Perry, D.J., and Carrell, R.W. (1989) CpG dinucleotides are "hotspots" for mutation in the antithrombin III gene: Twelve variants identified using the polymerase chain reaction. Mol. Biol. Med. 6,239-243.

Perry, D.J. (1993) Antithrombin and its inherited deficiencies. Blood Rev. 8,37-55

Petersen, M.B., Schinzel, A.A., Binkert, F., Tranebjaerg, L., Mikkelsen, M., Collins, F.A., Economou, E.P., Antonarakis, S.E. (1991) Use of short sequence repeat DNA polymorphisms after PCR amplification to detect the parental origin of the additional chromosome 21 in Down syndrome. Am. J. Hum. Genet. 48, 65-71.

Poncz, M., Solowiejczy, D., Harpel, B., Mary, Y., Schwartz, E., Surrey, S., (1982) Construction of human gene libraries from small amount of peripheral blood: analysis of β-like globin gene. Hemoglobin 6, 27-36.

Prochownik, E.V., Bock, S.C., Orkin, S.H. (1983a) Isolation of a cDNA clone for human antithrombin III. J. Biol. Chem. 258,8389-8394.

Prochownik, E.V., Antonarakis, S., Bauer, K.A., Rosenberg, R.D., Fearon, E.R., Orkin, S.H., (1983b) Molecular heterogeneity of inherited antithrombin III deficiency. N. Eng. J. Med. 308,1549-1552.

Richard, G.-F., and Paques, F. (2000) Mini- and microsatellite expansions: the recombination connection. EMBO Rep. 1,122-126.

Riggins, G.J., Lokey, L.K., Chastain, J.L., Leiner, H.A., Sherman, S.L., Wilkinson, K.D., Warren, S.T. (1992) Human genes containing polymorphic trinucleotide repeats. Nature Genetics 2,185-191.

Roussel, B., Dieval, J., Delobel, J., Fernandez-Rachubinski, F., Eng, B., Rachubinski, R.A., Blajchman, M.A. (1991) Antithrombin III-Amiens: A new family with an Arg47-Cys inherited variant of antithrombin III with impaired heparin cofactor activity. Am. J. Hematol. 36,25-29.

Sacks, S.H., Olds, J.M., Reeders, S.T., Weatherall, D.J., Douglas, A.S., Winter, J.H., Rizza, C.R., (1988) Evidence linking familial thrombosis with a defective antithrombin III gene in two British kindreds. J. Med. Genet 25,20-24.

Sas, G., Pepper, D.S., and Cash, J.D. (1975) Plasma and serum antithrombin-III: differentiation by crossed immunoelectrophoresis. Thromb. Res. 6,87-91.

Schichman, S.A., Suess, P., Vertino, M.A., Gary, P.S. (2002) Comparison of short tandem repeat and variable number tandem repeat genetic markers for quantitative determination of allogeneic bone marrow transplant engraftment. Bone Marrow Transplant 29,243-248.

Scully, M.F., and Kakkar, V.V. (1977) Methods for the determination of thrombin, antithrombin and heparin cofactor using the substrate H-D-Phe-Pip-Arg-p-nitoanilide HCL. Clin. Chim. Acta. 79,595-602.

Stephens, A.W., Thalley, B.S., Hirs, C.H.W. (1987) Antithrombin-III Denver, a reactive site variant. J Biol. Chem. 262, 1044-1048.

Tait, R.C., Walker, I.D., Perry, D.J., Islam, S.I., Daly, M.E., McCall, F., Conkie, J.A., Carrell, R.W. (1994) Prevalence of antithrombin deficiency in the healthy population. Bri. J. Haemat. 87,106-12.

Thaler, E., and Lechner, K. (1981) Antithrombin III deficiency and thromboembolism. Clin. Haematol. 10,369-373.

Tomita, M., Nohno, T., Okuyama, T., Hidaka, K., Xu, W. (2002) Hypervariable locus of the 3'-flanking region of the neurotension receptor gene: an effective region for personal identification in forensic practice. Forensic Science International 127,119-127.

Vergnaud, G., and Denoeud, F. (2000) Minisatellites: mutability and genome architecture. Genome Res. 10, 899-907.

Vidaud, D., Emmerich, J., Sirieix, M.E., Sie, P., Alhenc-Gelas, M., Airch, M. (1991) Molecular basis for antithrombin III type I deficiency: Three novel mutations located in exon IV. Blood 78,2305-2309.

Waye J.S., Eng, B., Ni, H., Blajchman, M.A., Carmody, G. (1994) Trinucleotide repeat polymorphism within the human antithrombin gene (AT3): allele frequency data for three population group. Molecular and Cellular Prober 8,149-154.

Wells, P.S., Blajchman, M.A., Henderson, P., Well, M.J., Demers, C., Bourque, R., McAvoy, A. (1994) Prevalence of antithrombin deficiency in healthy blood donors: a cross-sectional study. Am. J. Haematol. 45,321-324.

Winter, J.H., Bennett, B., Watt, J.L., Brown, T., San Roman, C., Schinzel, A., King, J., Cook, P.J.L. (1982) Confirmation of linkage between antithrombin III and Duffy blood group and assignment of AT3 to 1q22→q25. Ann Hum Genet 46,29-34.

Winter, J.H., Fenech, A., Ridley, W., Benett, B., Cumming, A.M., Mackie, M., Douglas, A.S. (1982) Familial antithrombin III deficiency. Quart J Med 51,373-379.

Wu, S., Seino, S., Bell, G.I. (1989) Human antithrombin III (AT3) gene length polymorphism revealed by the polymerase chain reaction. Nucleic Acids Res. 17,6433.